EUROPA-UNIVERSITÄT FLENSBURG

DOCTORAL THESIS

Combined Optimization of Grid and Storage Expansion in the German Power System

Author:
Ulf Philipp MÜLLER

Supervisors and reviewers:
Prof. Dr. Olav HOHMEYER
Prof. Dr. Jochen WENDIGGENSEN
Prof. Dr. Claudia KEMFERT

A thesis submitted in fulfillment of the requirements
for the degree of Dr. rer. pol.

in the

Department of Energy and Environmental Management
Interdisciplinary Institute for Environmental, Social and Human Sciences

January 2021

storage and grid
time and space
value

complexity and simplicity
numbers and insights
consistency

energy
sustainability
on this here island
generating generations
until the sun falls out.

Acknowledgements

I want to acknowledge the people who have influenced me during the work on this thesis. First of all, I want to thank the supervisors of my thesis. In particular, Olav Hohmeyer for sharing his knowledge, motivating me and reviewing my work. Jochen Wendiggensen for trusting me and providing room for innovation. Finally, Claudia Kemfert for peer reviewing this thesis.

While generating ideas for the topic of this thesis, I developed the research project *open_eGo*. Remembering the beginning of this process, I want to thank Berit Müller, who strongly supported my acquisition ideas and actions. Moreover, David Kleinhans influenced the early ideas about using *OpenStreetMap* for grid modeling and introduced many scientific competences into the process. Appreciating the approval and sponsoring of the project by the *BMWi* and the *PTJ*, the project accelerated and introduced many researcher. Many of these researchers have strongly influenced the outcome of this thesis. In particular, I want to thank the *open_eGo* research group in Flensburg i.e. Ilka Cussmann, Clara Büttner, Wolf-Dieter Bunke and Martin Söthe for creating code out of mental approaches. Furthermore, I appreciate the input, help and the external perspectives, which came from the researchers from the *RLI*, the *OvGU* and *NEXT ENERGY*. Last but not least, I want to thank Lukas Wienholt for being an excellent sparring partner and friend.

George Box wrote in 1987 that "essentially, all models are wrong, but some are useful". In this sense, I want to thank Tom Brown and Jonas Hörsch for developing a very useful open source tool. Speaking of useful tools, I want to mention Malte Scharf, who in the early days of my research reinvented the wheel with me creating *OLF* and later on worked cutting edge when developing *osmTGmod*.

At last, I am grateful for having been part of the inspiring *EEM* bubble. In particular, the Jarplund family of friends created an exceptional base for creativity. Calling out specific names: Clemens and Marion Wingenbach, Samuel Glismann, Simon Hilpert and Frauke Wiese have influenced me to an important extent. Thank you, Franzi Dettner for proof-reading my thesis.

Abstract

The transition of the German power system towards a distributed renewable power supply motivates to determine systematically optimized, yet spatially detailed allocations of grid and storage expansion. In an open source approach, co-optimal grid and storage expansion is allocated to a grid of up to 500 buses and more than a 1000 lines representing in detail the German transmission and sub-transmission grid and in more abstract terms the electrical neighboring countries. Within a multi-period linear optimal power flow approach, the linearized passive flow behavior of the AC components are considered. Grid and storage expansion in Germany are mainly driven by offshore and onshore wind feed-in leading to north-to-south transmission grid expansion, whereas distributed grid and storage expansion play a rather minor role. Instead, distributed biomass power generation is substantially supplying flexibility. Once this technology is less available, curtailment of renewable generation is restricted or specific storage investment costs decrease significantly, distributed storage expansion, mostly as long-term hydrogen storage in the north, becomes a feasible option. Furthermore, the spatially detailed modeling reveals that due to transit flows on the sub-transmission level the transmission level is relieved leading to fewer necessary grid expansion and overall costs.

Executive Summary

Problem

The mitigation of climate change implies a shift from fossil to renewable power production. In Germany, this power system transition has already been partly realized. By law it is planned for the year 2050 that at least 80 % of the power generation shall be supplied by renewable sources. Beyond these goals, many studies have shown that a 100 % renewable power supply is possible, economically feasible and desirable in the context of global warming.

In literature, it has been generally agreed upon that the mentioned transition implies the need for flexibility options such as grid and storage expansion. As these two main options can substitute each other, in order to find cost-optimal solutions, co-optimization approaches have gained significance. These approaches focus on abstract representations of the transmission grid, modeling aggregated regions such as countries in an European system.

In contrast, official grid planning by the transmission and distribution grid operators focuses on line-sharp modeling but does not jointly optimize grid and storage expansion. Instead, solely grid expansion is determined separately for the transmission and distribution grid using closed source data models.

As the transition to a renewable power supply implies a shift from a system dominated by centralized power production on the transmission level to one with a prevailing distributed generation on the distribution level, a joint modeling of transmission and distribution grid becomes increasingly relevant. Thus, grid and storage expansion may be allocated to a power grid of high resolution representing a co-optimal solution, which produces minimal costs for the German system and its European neighbors. Consequently, based on the problem statement and a thorough literature review, the following hypotheses are derived:

- It is possible to model the German power grid down to the 110 kV grid level on the basis of open source and open data to derive cost optimal future grid and storage expansion settings.

- A joint modeling of the transmission and sub-transmission grid (including its passive flow behavior) enables a spatially detailed and possibly diverse allocation of economically co-optimal grid and storage expansion in a future German power system.

- Distributed power flow problems and flexibility investments affect the overall optimum.

Methods

In a multi-period linear optimal power flow problem, the decision variables generation and storage operation ($g_{n,r,t}$ and $h_{n,s,t}$) as well as grid and storage expansion (F_b and $H_{n,s}$) are jointly optimized, such that system costs are minimized over the course of a modeling year (as stated in the following objective function). The variables are component-specifically parameterized by annualized specific investment costs (c_b and $c_{n,s}$) and hourly operational costs ($o_{n,r}$ and $o_{n,s}$).

$$\begin{aligned} \min_{\substack{F_b,H_{n,s} \\ g_{n,r,t},h_{n,s,t}}} & \left[\sum_b c_b \cdot F_b + \sum_{n,r,t} (w_t \cdot \ o_{n,r} \cdot g_{n,r,t}) \right. \\ & \left. + \sum_{n,s} c_{n,s} \cdot \ H_{n,s} + \sum_{n,s,t} w_t \cdot \ o_{n,s} \cdot \ [h_{n,s,t}]^+ \right] \ \forall\, b,n,r,s,t \end{aligned} \tag{1}$$

where

$b \in B$	: branch label
$n \in N$	: bus label
$r \in R$	: generator carrier label
$s \in S$	: storage carrier label
$t \in T$	: snapshot label
c_b	: branch annualized capital cost per capacity
F_b	: branch active power capacity
w_t	: snapshot weighting
$o_{n,r}$	: generator operating (marginal) costs
$g_{n,r,t}$	: generator dispatch
$c_{n,s}$	: storage annualized capital cost per capacity
$H_{n,s}$	: storage nominal active power capacity
$o_{n,s}$	: storage operating (marginal) costs
$h_{n,s,t}$	: storage dispatch

The grid topology (buses and branches) is derived from OpenStreetMap data for the voltage levels of 110kV upwards. Technical parameters such as branch reactances as well as the mentioned annualized capital cost assumptions are based on typical values from literature. Physical power flows have to comply with the first and second Kirchhoff's law. Due to the linearization of the latter mentioned, only the reactances of the passive branches are considered.

AC and DC line expansion is possible on the existing power lines of the status quo grid up to a compromise upper bound. As changes in AC reactances are not considered once grid expansion occurs, the entire optimization is iterated five times ensuring convergence. After each optimization run the reactances are updated according to the calculated grid expansion.

Concerning storage expansion, as a short-term flexibility option, lithium-ion batteries may be projected at any bus of the grid. Long-term flexibility can be supplied by hydrogen storage units at northern grid buses assuming the utilization of existing salt caverns.

The spatial allocation of current and future demand and generation is defined exogenously. For the future development a scenario with 100 % and an intermediate scenario with about 70 % renewable generation capacity are defined according to state-of-the-art studies. Whereas the status quo generation facilities can be allocated in a sufficiently high resolution by using published power plant registers, demand is distributed by an abstract method assuming correlations to the distribution of population and gross value added. In contrast to the future demand, which is assumed to remain at status quo level, expected future renewable energy capacities are allocated linearly related to the status quo distribution.

Hourly demand time series are defined in a bottom-up approach with the help of sector-specific standard load profiles. The weather dependency of potential wind and solar power generation is modeled by using weather data of the year 2011 of high spatial resolution. For the sake of computational tractability, the temporal resolution is reduced calculating only every fifth hour of the year (for sensitivity analysis up to every second hour). Hence, in the objective function, the snapshot weighting is defined as $w_t = 5$.

Besides the temporal resolution, the high spatial complexity of the German transmission and sub-transmission grid with about 4000 substations and 7000 joints is reduced to 300 aggregated buses (for sensitivity analysis up to 500) by a k-means clustering algorithm. Thus, distribution grid topologies remain to be considered, especially in significant rural areas such as the west coast region in Schleswig-Holstein while computational burden is reduced sufficiently. The European countries which are directly interconnected with Germany are modeled as one bus per country including their aggregated demand and generation characteristics.

Results

In Figure 1 the spatial distribution of grid and storage expansion is visualized for the scenario with a 100 % renewable power generation. The main grid expansion in Germany is substantially driven by offshore wind feed-in leading to two north-to-south expansion corridors heading towards load centres in the Ruhr area. In contrast, distributed grid expansion is needed to a comparably low extent. Although the two future scenarios are independent from each other, the grid expansion is consistent. Thus, 85 % of the grid investment is already feasible in the intermediate scenario with a share of 70 % renewable power capacity. The majority of storage expansion becomes feasible when modeling the 100 % renewable power generation setting. The

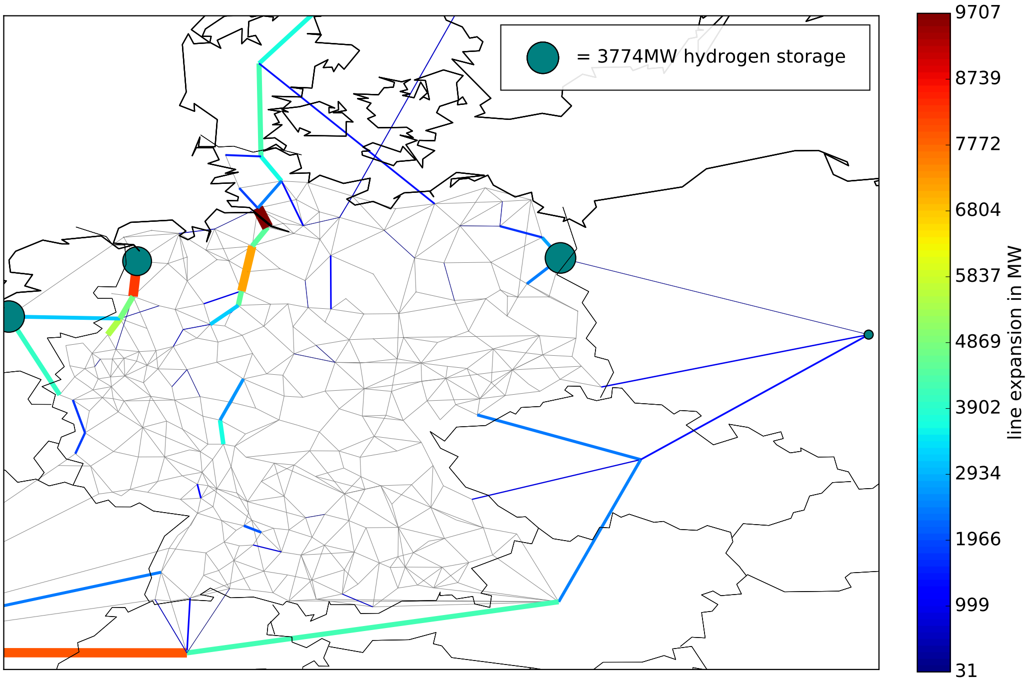

FIGURE 1: Spatial allocation of grid and storage expansion for the scenario *eGo 100*.

German storage expansion of in total about 7 GW is characterized by only two big hydrogen storage units at the northwestern offshore wind feed-in bus and near to the Polish border.

In an extensive sensitivity analysis it is shown that these base results may change significantly when certain assumptions are altered. In Figure 2 the variation of annual endogenous costs is summarized. The most important effects are highlighted in the following.

In the base setting, the potential of grid expansion is not fully exploited. Eliminating the upper bound restriction on grid expansion on the crossborder and inner-German power lines leads to a mayor increase of north-south transmission grid expansion while storage expansion is lowered to a minimum. The northwestern hydrogen storage unit can be completely substituted by higher grid expansion, in particular on the connected corridor southwards. Nevertheless, the entire system costs, loosening the upper bound restriction on the inner-German power lines, are only reduced marginally. In contrast, restrictions on the crossborder line expansion affect the results to a higher extent. Thus, more wind power generation, in particular from Denmark can be imported significantly lowering the need for flexible but expensive biomass dispatch. A similar effect can be observed when considering a future interconnection to Norway, which would introduce additional cost-effective flexible reservoir power generation. Furthermore, avoiding north-to-south loop flows via the Eastern European countries eliminates the need for the storage unit at the Polish border. Instead, this storage expansion can be substituted by northeast-to-southeast grid expansion in Germany.

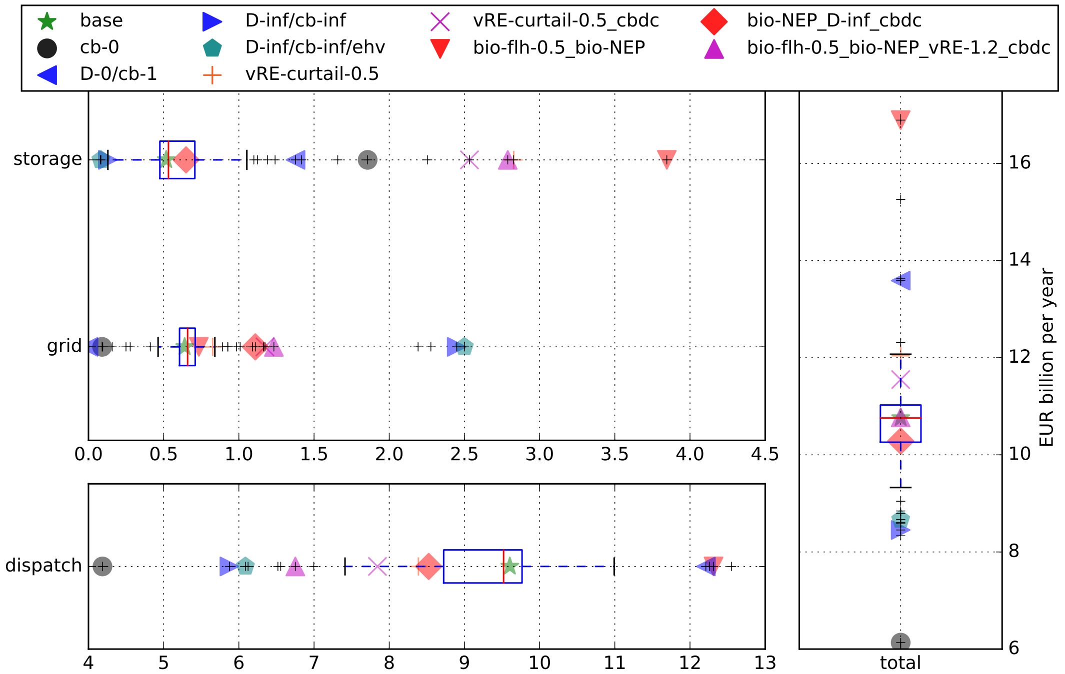

FIGURE 2: Boxplots with median, quartiles, whiskers (1.5 of the interquartile range) and outliers of the annual costs (in EUR billion per year) of the optimization variables grid, storage expansion and dispatch as well as the resulting total endogenous system costs for the *eGo 100 - base* scenario and its 87 sensitivities. A selection of important solutions are explicitly plotted. Note that, the *cb-0* only accounts for the German system costs. Moreover, mind that for some sensitivities, the exogenous costs change.

In contrast, other sensitivities have shown that extensive storage expansion beyond the base results may be a feasible option. Lowering the specific investment costs for storage units showed an immense increase in feasible storage sites. In the most extreme case calculated, with a 95 % decrease in specific costs assumptions, 138 GW storage capacity are installed in Germany. In this case, short-term battery storage play an important role reaching a share of 60 % of the total storage capacity. The storage units are then allocated to many buses, located primarily in Northern Germany and near interconnectors. Furthermore, as local biomass power plants play an important role for supplying local flexibility, in scenarios, which assume lower installed capacities and/or the available resources, more storage expansion occurs. In an interesting setting, in which the installed capacities of biomass are lowered to a status quo level (in combination with an unrestricted inner-German grid expansion and a loop-flow-free approach), although the total storage investment did not significantly increase compared to the base case, storage expansion is highly distributed. At almost all northern grid buses comparably moderately sized hydrogen storage sites of up to 700MW are projected. Moreover, many small storage units with a capacity of about 35MW each reach feasibility in the Ruhr area. Additionally, reducing the available biomass resource to about half of today's consumption but instead increasing solar and wind capacities by 20 %, storage expansion increases to more than 31 GW in Germany, being situated mainly in Schleswig-Holstein, at the offshore wind bus near the Dutch border, in the Ruhr area and near Stuttgart (the latter two as batteries). Moreover, grid expansion is wide-spread and increased by 170 %. A similar change occurs, only without the mentioned battery expansion, if allowed curtailment of solar and wind is restricted.

As in the base scenario results, which showed only minor grid expansion on the distribution level, all other sensitivities also showed a predominant transmission grid expansion. Furthermore, a comparative study has shown that a consideration of the 110 kV grid leads to a positive cost-reducing effect induced by transit flows, which relieve the transmission lines. Negative effects of more local grid restrictions are overcompensated. Consequently, the need for grid expansion in Germany can be reduced by 23 % while reaching slightly lower overall system costs.

Comparing the findings to results from other state-of-the-art studies, it can be stated that the results are plausible. In particular, the base results show rather low investment costs and a dominating effect of wind power driven grid expansion. Considering a wide range of literature results on the one hand while spanning a diverse set of sensitivities on the other hand, shows that the results lie within the range of literature results.

Conclusion

The transformation of the power system towards a distributed renewable power supply calls for models being able to allocate distributed grid and storage expansion while producing minimal costs for the entire system. In an innovative approach, which only uses open data, the German transmission and sub-transmission grid is integrated into a power system model for Germany and its European neighbors. Although computational burden implied the need for spatial complexity reduction, for the first time, co-optimal grid and storage expansion is allocated to a spatially detailed grid with up to 500 buses and more than a 1000 lines. Within the optimization, the passive flow behavior of the AC components is considered by a state-of-the-art linear approximation.

Grid and storage expansion in Germany is mainly driven by offshore and onshore wind feed-in leading to north-to-south transmission grid expansion whereas distributed grid expansion plays only a minor role. In a 100 % renewable power system, significant, but compared to literature, moderate concentrated long-term hydrogen storage capacity may be feasible but can be substituted by grid expansion if the compromise upper bound of grid expansion is ignored and loop flow effects via the Eastern European countries are eliminated. In this setting, distributed flexible biomass power feed-in plays an important balancing role. Once this flexible power is less available, curtailment of fluctuating renewable generation is restricted or specific storage investment costs decrease significantly, distributed storage expansion, mostly as long-term hydrogen storage in Northern Germany, becomes a feasible option.

The consideration of the high voltage level leads to a high spatial distribution and the recognition of relevant grid constraints. The effect of additional grid restrictions are over-compensated by the cost-reducing effect of transit flows which relieve the transmission level. Consequently, the need for grid expansion is lowered moderately while slightly reducing endogenous system cost.

The developed model and its results can help investors and authorities to make local investment decisions, which are in line with a macro-economic optimum. Policy should foster primarily inner-German and cross-border transmission grid expansion and secondarily focus rather on investments into large-scale long-term storage in Northern Germany instead of into small-scale distributed short-term technologies.

Contents

List of Figures

List of Tables

List of Abbreviations

AC	alternating current
ACPF	non-linear power flow, synonym to PF (see below)
ATC	available transfer capacities
BDEW	German Association of Energy and Water Industries
DC	direct current
DCLF	direct current load flow
DSO	distribution grid operator
EEG	German Renewable Energies Act
EEX	European Energy Exchange
EHV	extra high voltage
ENTSO-E	European Network of Transmission System Operators
eTraGo	Electricity Transmission Grid Optimization
EU	European Union
FBMC	flow based market coupling
GENESYS	modeling tool for a genetic optimization of the European electricity system
GEP	generation expansion planning
Green-X	model to derive optimal promotion strategies for increasing the share of renewable energy sources in a dynamic European electricity market
GridKit	a power grid extraction toolkit
HV	high voltage
HVDC	high voltage direct current
IEEE	Institute of Electrical and Electronics Engineers
LCOE	levelized costs of electricity
LOPF	linear optimal power flow
LP	linear programming
MENA	Middle East and Northern Africa
MILP	mixed integer linear programming

MV	medium voltage
NEP	German grid development plan
NGO	non-governmental organization
NOVA	grid planning principle prioritizing grid optimization measures prior to strengthening and expansion measures
NTC	net transfer capacities
oemof-demandlib	Library of the Open Energy Modeling Framework to create power and heat demand profiles
oemof feedin-lib	Library of the Open Energy Modeling Framework to calculate feed-in time series of solar and wind power plants
OEP	OpenEnergyPlatform
OPF	non-linear optimal power flow
OPSD	Open Power System Data
OSM	OpenStreetMap
osmTGmod	Open Source German Transmission Grid Model
PyPSA	Python for Power System Analysis
PF	non-linear power flow
PQ	refers to a specified real power P and reactive power Q generation or load characteristic at a grid bus
PV	refers to a specified real power P and a voltage magnitude V generation or load characteristic at a grid bus
RE	renewable energy
REMix	Renewable Energy Mix for sustainable electricity supply
SLP	standard load profiles
TEP	transmission expansion planning
TEPES	Long-Term Transmission Expansion Planning Model for an Electric System
TSO	transmission grid operator
TYNDP	ten years network development plan
UCTE	Union for the Co-ordination of Transmission of Electricity

Chapter 1

Introduction

1.1 Motivation

The reduction of CO_2 emissions in order to sufficiently limit global warming has been and will be an important and challenging goal for humankind. In this context, the power sector in Germany is in a process of decarbonization. This implies a transition from a conventional to a renewable power supply. The European Union defined the 20/20/20 goals in the year 2009 forcing the member states to supply 20 % of their national energy consumption from renewable energy (RE) sources by the year 2020 (The European Parliament and the council of the European Union, 2009). In line with the European goals, Germany has stated their targets in the German Renewable Energies Act (EEG). In the most recent version of the law (EEG, 2019), in the mid-term future at least 40 % (until 2025) and later 55 % (until 2035) of the electricity consumption shall be supplied by RE sources. In the long-term future (until 2050) this share should further increase to at least 80 %. Beyond these goals there have been published many studies showing that a 100 % renewable power system is possible, economically feasible and desirable in the context of global warming (e.g. Czisch, 2005; e-Highway 2050 project, 2015a; Faulstich et al., 2011; Greenpeace International, Global Wind Energy Council, SolarPowerEurope, 2015; Knorr et al., 2014; Zappa et al., 2019).

It is generally agreed upon that power systems with high shares of fluctuating RE sources require system flexibility, which can be supplied by flexible power plants, storage units, demand response and transmission grid expansions (Huber et al., 2014; Ringkjøb et al., 2018). Bussar et al. (2015) pointed out the different flexibility characteristic of storage and grid, stating that storage units can provide flexibility by shifting load in time whereas grids can shift load in space. Consequently, to some extent, grid and storage capacity can replace each other. As the power transition is supposed to be cost-efficient (see e.g. EEG, 2019; EnWG, 2019), co-optimization of the different flexibility options is a worthwhile task. In a recent literature review about transmission expansion planning (TEP), Gomes and Saraiva (2019) identified this as one major gap in literature since most studies consider only one objective. Nevertheless, in the field of power system planning focusing on abstract representations of countries or continents rather than on particular power lines, a reasonable amount of studies (e.g Brown et al., 2018c; Bussar et al., 2017; Gils et al., 2017; Hagspiel et al., 2014; Hörsch and Brown, 2017; Pleßmann and Blechinger, 2017) have addressed the problem of co-optimization of grid, storage (and generation) expansion.

Another challenge of the RE expansion comes with its spatial distribution. Originally the power grid was designed such that few big power plants were installed to the extra high voltage (EHV) level. On the lower voltage levels only consumers were connected. Hence, the power flowed from the higher voltage levels to the lower ones. In contrast, RE sources are highly distributed and mostly connected to lower voltage levels. Consequently, power flow characteristics change i.e. become more complex implying bidirectional power flows instead of unidirectional ones. Gomes and Saraiva (2019) stated that theses modifications of the power flow patterns, being especially relevant at the transmission-distribution boundary, are scarcely addressed in existing literature. In this context, Palmintier et al. (2017, p. 1525) emphasized that "the growing importance of distributed energy resources will require tearing down the traditional divide between the transmission and distribution systems, while also capturing load dynamics and market interactions." Agricola et al. (2012) similarly, but in the specific context of Germany, stressed that in the future the need for considering the interdependence of the high voltage (HV) and EHV level will increase. In Germany, the HV level is operated mainly at a nominal voltage of 110 kV and is considered to be the highest voltage level of the distribution grid while the EHV level is operated at 220 and 380 kV belonging to the transmission grid. In science, the HV level is often called sub-transmission grid. These terms are used synonymously in this work. Although Agricola et al. (2012) mentioned the increasing interdependence of the transmission and sub-transmission grid (the latter being part of the distribution grid) they did not jointly consider them. Instead, they focus solely on the grid expansion needs of the distribution grid considering the planned development of the transmission grid, being published on a regular basis by the transmission grid operator (TSO) in the so-called German grid development plan (NEP) (see 50Hertz et al., 2019a), as a prerequisite. These NEP do not integrate the distribution grid into their optimization either. This shows, that the status quo of grid planning in Germany still separately plan the different grid levels without considering their interdependencies. Hoffrichter et al. (2018) and van Leeuwen et al. (2014) used an integrated model of the EHV and HV level to show the rising relevance of the HV level for the transmission of power via transit flows. These analyses focused only on dispatch optimizations motivating further research integrating the upper distribution level into the national transmission grid expansion planning.

The idea of integrating the sub-transmission grid planning into the transmission grid planning comes along with the challenge of computational feasibility. Whereas the German transmission grid can be modeled by a grid topology with around 500 buses, the spatial complexity rises by about a factor 9 once the sub-transmission grid is integrated (according to the model used in this work, see Section 4.3.1). In a thorough literature review Pfenninger et al. (2014) pointed out several major challenges in the energy system modeling of the 21st century. The challenges of *resolving details in time and space* and *complexity and optimization across scales* are directly addressed when trying to integrate the lower voltage levels into the planning of the upper ones. In this context, they cited Brummitt et al. (2013) emphasizing the "trade-off between stylized models revealing the big picture but reaching wrong conclusions due to their simplifications, and detailed models revealing insight on only a small subset of a system" (Pfenninger et al., 2014, p. 81).

The problem of complexity increases once more when integrating the idea of co-optimizing power system operation and investment decisions i.e. storage and grid expansion with the approach to jointly consider the transmission and distribution grid. Here, the necessity to "bridge the gap between power system analysis software and general energy system modeling tools" (Brown et al., 2018b, p. 1) becomes highly relevant. On the one hand the physical behavior of the grid and on the other hand a multi-period joint optimization of operation and investment considering grid and storage expansion have to be regarded.

As Pfenninger et al. (2014) pointed out that one major challenge in today's energy modeling is transparency, the use of open data and software has gained importance in energy system modeling. In Pfenninger et al. (2017) four benefits of open models and data were explained. First, quality of science is expected to be improved since "fundamental scientific principles such as transparency, peer review, reproducibility and traceability are almost impossible to implement without access to models and data" (Pfenninger et al., 2017, p. 211). Second, the collaboration between science and policy becomes more effective. Third, it is economically more efficient for society and at last leads to higher societal acceptance for the transition of the energy system. Pfenninger et al. (2017) concluded that the field of energy research is lagging behind other applied fields like climate science. Instead, the vast majority of peer-reviewed energy literature still makes neither code nor data openly available. Although the number of open models and data sets have recently increased, especially the power grid sector lacks of validated data sets including information about the grid topology and its physical characteristics. Medjroubi et al. (2017) showed first approaches to model the German transmission grid by a combined use of OpenStreetMap (OSM) data and literature assumptions motivating a further development of this approach considering also the sub-transmission grid.

1.2 Research questions

In the context of a transition towards a 100% renewable power system in Germany, considering the motivating introduction, the fundamental methodical research question of this work is formulated as follows:

- How is it possible to model the German power grid down to the 110 kV grid level on the basis of open source and open data to derive cost optimal future grid and storage expansion settings?

In particular, decision makers have to bear in mind that cost optimality is only valid with respect to the applied methods and assumptions, which simplify real-world behavior. Theses methods and assumptions are addressed and critically appraised in the course of the thesis. However, if despite some model limitations an adequate method can be developed, specific results for the future power system shall be analyzed focusing on the following research questions:

- How will the spatial distribution of jointly optimized grid and storage expansion be characterized considering a power grid of high spatial resolution?
- How does the integration of the HV level into the optimization problem affects the system design?

1.3 Outline of the thesis

At first, the state of the art in power grid expansion planning is described. Furthermore, literature focusing on the siting and sizing of storage units is considered. Finally, it is explained how the co-optimization of both, storage and grid expansion is addressed so far. Particularly, the representation of real-world transmission and/or sub-transmission grid is a highly relevant aspect. Based on the research questions and the state of the art, the hypotheses are formulated. In Chapter 4, it is presented how to jointly optimize grid and storage expansion considering the linear and non-linear network equations. Moreover, the open data model of the German transmission and sub-transmission grid considering today's power system as well as two future exogenous scenario settings focusing on the mid-term future until 2035 and the long-term perspective of a 100% RE power system is described. In Chapter 5, results are presented with respect to the research questions. Thus, the optimal allocation of grid and storage expansion in the future German power system are presented and furthermore discussed (Chapter 6). As a major part of the discussion, the results are compared to the ones from other studies. At the end of this chapter, very importantly, the hypotheses are evaluated. Finally, the research results are concluded and an outlook on meaningful further research is given.

Chapter 2

State of the Art

2.1 Power grid expansion planning

2.1.1 Transmission grid expansion planning

TEP has been addressed in practice and research for many decades. Relatively new challenges such as deregulation and the energy system transition towards the usage of RE have increased the complexity and relevance of the problem of finding adequate transmission grid expansion measures (Gomes and Saraiva, 2019; Lumbreras and Ramos, 2016). Therefore, a great amount of TEP activities, both academic and in practice have been undertaken recently. The sheer abundance lead to many state-of-the-art reviews (Gomes and Saraiva, 2019; Hemmati et al., 2013a,b; Kishore and Singal, 2014; Krishnan et al., 2016; Latorre et al., 2003; Lumbreras and Ramos, 2016; Mahdavi et al., 2018; Niharika et al., 2016; Lee et al., 2006; Romero et al., 2002). Most of them have focused on academic literature. In contrast, Lumbreras and Ramos (2016) also gave an overview of European projects proposing specific transmission grid development plans. As this work is rather recently published and well elaborated, it is one out of two papers which, out of the mentioned high number of meta studies, are primarily used to describe state-of-the-art TEP in the following. Furthermore, Gomes and Saraiva (2019), being the most recent literature review, is focused on. First, academic approaches are described and secondly, the NEP and the European ten years network development plan (TYNDP) are outlined.

Usually TEP are sub-devided into the problem formulation and solving (e.g. Gomes and Saraiva, 2019; Hemmati et al., 2013b; Lumbreras and Ramos, 2016). The TEP problems are considered to be large-scale highly constrained mixed-integer non-linear programming approaches consisting of objective function and constraints (Hemmati et al., 2013a,b). Nevertheless, the majority of the TEP problems are simplified by linearization (e.g. Gomes and Saraiva, 2019).

Gomes and Saraiva (2019) described six groups of modeling characteristics which categorize different types of problem formulation. These groups are: approach, system costs, contingency criteria, reliability, modeling and planning view. This categorization in similar terms can be found in other meta studies, such as in Lumbreras and Ramos (2016). Moreover Gomes and Saraiva (2019) stated that the following six *recent worries* have been affecting TEP additionally: risk, new changes on the grid, environmental concerns, liberalized power sector, market and computational burden.

Gomes and Saraiva (2019) classified more than 70 scientific papers up until the year 2018 concerning the latter mentioned factors and the different elements of the mentioned groups. By categorizing the articles into the ones published before 2016, in 2017 and 2018 a few modeling trends were analyzed. As older articles focused on deterministic approaches which consider exogenous parameters such as generation or demand to be immutable, newer articles try to reflect recent challenges such as intermittent RE production by probabilistic or robust approaches. Due to similar reasons reliability and security such as (n-1)-contingency are recently addressed more often. These developments lead to more complex models and computational effort. Consequently, modelers tend to deal with this by using the linearized AC network equations respectively linear optimal power flow (LOPF) approaches. In these approaches the dispatch is optimized with respect to network restrictions. Whereas the non-linear optimal power flow (OPF) is a non-linear problem representing Kirchhoff's first and second law leading to the ability to accurately model losses and reactive power flows, these effects are neglected in the case of the LOPF. Here, Kirchhoff's second law is linearized keeping the entire problem linear. Especially due to the relatively low resistances (compared to the reactances) of transmission grids being dominated by overhead lines, the LOPF serves often as an adequate simplification, which lowers the computational burden significantly. Gomes and Saraiva (2019) also mentioned the transshipment model for dealing with line loading as part of the LOPF. In contrast, Lumbreras and Ramos (2016) defined the transshipment or transportation model as a separate category. Here, the second Kirchhoff law is not considered at all. This approach, representing the most simple abstraction of grid restrictions, implies computational advances but due to its simplicity seems to be unsuitable for most real applications (Lumbreras and Ramos, 2016). As OPF approaches consider power plants dispatch, most of the studies, especially in more recent works, consider operational costs. Due to the aim of finding optimal grid expansion, naturally in almost all studies investment costs are dealt with.

Lumbreras and Ramos (2016, p. 24) defined the decision dynamics of TEP as a "multi-stage problem that implements long-term decisions in discrete phases, with clear milestones where it re-evaluates decisions in the light of the revealed uncertainties". Most studies have simplified this complexity. Lumbreras and Ramos (2016) divided these approaches into static, sequential static and dynamic planning. The latter mentioned approach implies no temporal complexity reduction. In contrast, in the static approach, which is used by the vast majority of research studies, only one particular snapshot of the future system is evaluated (Lumbreras and Ramos, 2016). The analysis of Gomes and Saraiva (2019) revealed that almost half of the older studies have used dynamic approaches which in the categorization of Lumbreras and Ramos (2016) would be mostly a sequential static approach modeling several subperiods from the base year to the planning horizon considering the deployment date of investments. Nevertheless, the articles from 2018 have used the static approach more often. Tackling a higher systematic complexity the static approach seems to be more feasible in terms of computational burden which makes static or sequential static approaches more suitable for real problems (Lumbreras and Ramos, 2016).

The general trade-off between spatial and temporal resolution was underlined by Held et al. (2018) stating that previous studies (i.e. Egerer et al., 2015; European Climate Foundation, 2010; Holz and von Hirschhausen, 2013) represented the transmission network in Europe *line-sharp* whereas only considering a reduced set of operating situations. In this context, without analyzing the spatial dimension and evaluating the possibility to abstract the actual grid topology, Lumbreras and Ramos (2016) finally discussed and emphasized the increasing relevance of network reduction methods by referring to Cotilla-Sanchez et al. (2013). Apparently, the field of TEP usually sticks to *line-sharp* analysis. In Section 2.1.3 the more systematic TEP approaches, which aggregate the actual grid topology, will be further analyzed.

Lumbreras and Ramos (2016) outlined similar challenges compared to the *recent worries* described by Gomes and Saraiva (2019). The TEP problem formulation was, as stated, characterized similarly. Anyhow in the following a few characteristics which have not been emphasized so far are described. Lumbreras and Ramos (2016) stressed that in some circumstances it makes sense to jointly plan generation and transmission expansion which has been realized by some researchers. The strong interdependencies between the development of generation and transmission implies a chicken or egg problem which can be overcome by coordinating studies of generation expansion planning (GEP) and TEP (Gomes and Saraiva, 2019). In most studies, the market (although being mostly liberalized generation markets) was approximated by a central cost-based optimization. Lumbreras and Ramos (2016) discussed that the consideration of market designs increases the problem complexity while it is very difficult to assume probable market designs when modeling with long time horizons. Therefore, the practicability does not generally apply. Another interesting finding made by Lumbreras and Ramos (2016) is that although TEP is by nature a mutli-criteria problem mostly only costs are minimized within the objective function. Apart from investment and operational costs, reliability indexes, such as the expected energy not supplied, can be used for penalties. It was concluded that any TEP should include at least investment and operation costs as well as some consideration of reliability. Furthermore there are other relevant objectives i.e. social acceptance, environmental impact, renewable generation integration, congestion cost reduction, impact on system stability and geopolitical risk. Mostly, if considered, these attributes can be integrated in a single objective problem by defining weights and aggregate objectives.

After formulating the planning problem, solving methods are necessary. In Figure 2.1 the different solving approaches are defined. Lumbreras and Ramos (2016) divided the solving approaches into two main families: the interactive and automatic approaches. Traditionally TSOs have used heuristic approaches which imply human intervention. A planning module is iteratively combined with an operational module. The operational module is usually characterized by some sort of power flow analysis (LPF, PF, LOPF or OPF) which may at first identify initial problems. By human intervention afterwards in a planning step possible grid reinforcements are proposed. The performance of these measures are then assessed by another operational step. This procedure is iterated until results are accepted by the planner (see also Choi et al., 2007; Hemmati et al., 2013b). This approach allows to easily consider the planners' experience and to "integrate relatively sophisticated models in their operation module—for instance, a detailed ACPF" (Lumbreras and Ramos, 2016, p. 27).

In contrast, in academic literature mainly fully automatic approaches which do not need any human interaction are utilized (Lumbreras and Ramos, 2016). Therefore Gomes and Saraiva (2019) focusing on academic approaches explicitly described automatic solving approaches. The automatic approaches were further sub-divided into heuristic and optimization methods. In principle heuristics, which predefine specific rules, applying certain planning actions (the automized version of the planning step in the interactive approach) do not guarantee optimality. In contrast, classical optimization methods are deterministic approaches, which always provide a global optimum. Moreover, Lumbreras and Ramos (2016) sub-divided the optimization methods into classical and non-classical approaches. The latter one consists of meta-heuristics which use iterative algorithms often using some sort of random evolution. Although being more sophisticated and, compared to heuristics rather problem-independent, these meta-heuristic also may not find the global optimum but often lead to acceptable results. These methods might lower the computational burden compared to the classical, also called, exact approaches. In academia, the group of exact mathematical and meta-heuristic approaches are used in the majority of the studies (Hemmati et al., 2013b; Gomes and Saraiva, 2019; Lumbreras and Ramos, 2016). Figure 2.1 gives an overview of different classical and non-classical approaches. In terms of TEP, it is important to mention that the often used linear programming (LP) approaches "ignore the discrete nature of investment" (Lumbreras and Ramos, 2016). In contrast, mixed integer linear programming (MILP) can handle discrete grid expansion. Anyhow, for large problems, it is an option to discretize the results afterwards or accept the continuously optimized variables and therefore benefit from the computational advantages of a LP approach.

Finally, Lumbreras and Ramos (2016) concluded that a combination of interactive planning and optimization would be the most suitable solution for obtaining the advantages of both. In the following, the official TEP in Germany and Europe is highlighted, showing high degrees of traditional interactive planning.

In Germany, the four TSO operate the transmission grid as natural monopolist in different control areas within the country. 50Hertz, Amprion, TenneT und TransnetBW together develop a NEP in order to determine the necessary grid expansion in the future. The first plan was published in 2012 (50Hertz et al., 2012).

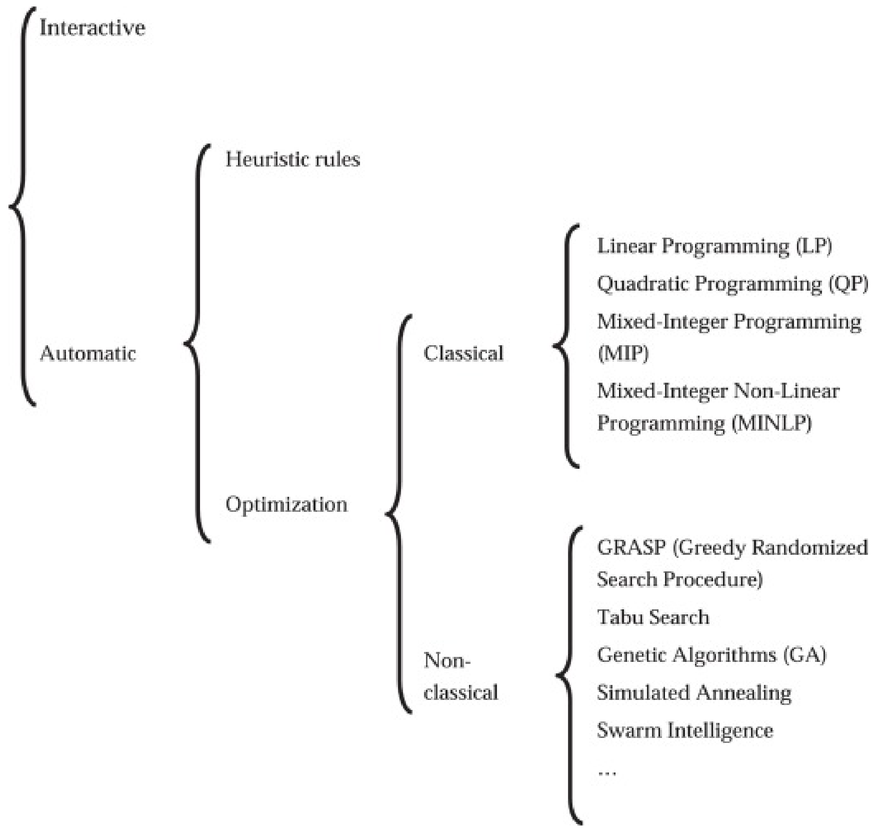

FIGURE 2.1: Solution approaches to TEP (Lumbreras and Ramos, 2016).

At the beginning, new plans were published every year, then every second year. The most recent plan, at the time this work was elaborated, refers to 50Hertz et al. (2019b). Although many approaches utilized have significantly evolved over the years, the main method remained the same throughout the years and will be shortly explained in the following.

As a base, in a scenario framework several scenarios are created which characterize the possible future generation mix for different scenario years up until the year 2035. Based on the scenario framework the actual NEP is developed. The NEP uses a heuristic step-by-step modeling procedure.

First, based on the scenario framework, a market simulation for the market regions in Europe is performed. Within the market regions, the grid was modeled without restrictions as so-called copper plates. Originally, only the net transfer capacities (NTC) between the different market regions constrain the power transmission. The transport of energy from one market region to another is modeled as a transshipment problem where every NTC interconnection could be used up until the assumed maximal capacity at any hour of the year (50Hertz et al., 2019b, p. 59). In contrast, most recently in 50Hertz et al. (2019b) a flow based market coupling (FBMC) approach was used being able to reflect the cross-border capacity allocation in Central Western European day-ahead markets, which is in effect since 2015 (Van den Bergh et al., 2016). FBMC tries to consider the physical behavior of the Western European grid more adequately. Therefore, loop flow characteristics between several countries can be modeled (50Hertz et al., 2019b). Consequently, the demand is met in each hour of the scenario year by the power plant and storage dispatch, such that system costs are as low as possible. Power plants with lower marginal costs are prioritized, thus dispatched with respect to the merit-order. The dispatch optimization was performed in perfect foresight for the entire year in the first years of the NEP until it was changed to a myopic foresight modeling approach (50Hertz et al., 2019b).

The power plant dispatch is then used as an exogenous input for non-linear power flow (PF) simulations considering the existing EHV transmission grid. Consequently, possible overloadings are analyzed. Considering certain best-practice planning principles, the overloading of the lines and transformers are eliminated by iteratively applying certain grid optimization, strengthening and expansion measures. Here the NOVA-principle, which reflects a basic planning principle aiming to prioritize low-cost measures, is applied. The first category, the *grid optimization* (German abbreviation *NO*) includes low-cost measures like topological changes, voltage level (220 kV to 380 kV) upgrades or weather-dependent overhead line monitoring. The second category, the *grid strengthening* (German abbreviation *V*) implies measures like adding new power circuits on existing routes. The last category, the most costly *expansion* (German abbreviation *A*) measures include for example the investment into new power routes, power stations and DC overlay grids. This iterative process is not automated, instead realized by transmission grid planning experts. The iterative process of choosing the NOVA measures is highly intransparent, whereas the planning principles, the input data and results are presented in more detail, although not detailed enough to be directly reproduced and validated by other power system modelers.

In addition to (n-0) PF simulations, (n-1)-contingency analyses are performed in order to comply with security of supply requirements. Furthermore, redispatch simulations are performed but not used for avoiding grid expansion measures as these market based measures are not supposed to be considered for long-term grid planning in order to maintain non-discriminating grid connection for all market participants. As well as redispatch, storage expansion is not used as an optimization variable. Instead, pumped storage units, which are very likely to be built in the future are exogenously considered with respect to the scenario assumptions.

On the European continental scale, the European Network of Transmission System Operators (ENTSO-E) integrates the national grid expansion planning of the TSO (which is consistent with the NEP) on biennial basis by European regulation, whereby "ENTSO-E shall adopt a non-binding Community-wide 10 year network development plan" (Carlini et al., 2019, p. 85). The TYNDP aims to identify European-wide solutions, so called projects of common interest (Carlini et al., 2019; Lumbreras and Ramos, 2016). The common interest is assessed by a complex cost-benefit analysis, hence each project's added valued for society. The possible benefits being evaluated (which are mostly monetized) are socio-economic welfare (increase in cross-market trading grid capacities), sustainability (RE integration and CO_2-emissions mitigation), grid losses and security of supply (Carlini et al., 2019; Lumbreras and Ramos, 2016). Apart from the cost-benefit analysis the modeling procedure is similar to the NEP. Hence, a market and PF simulation are the main methods used. These two models compute the majority of the cost-benefit indicators and are executed in an iterative manner (ENTSO-E, 2018a). Similar to the NEP, this iterative "process is limited in the sense that candidate projects are proposed manually, assessed individually, and no optimization is performed" (Lumbreras and Ramos, 2016, p. 22).

2.1.2 Sub-transmission grid expansion planning

The sub-transmission grid is defined as the intermediate grid between transmission and distribution system (Rad and Moravej, 2017). In Germany (similar in the rest of Europe and e.g. North America) sub-transmission grids are operated at the high voltage level connecting the extra-high voltage level and the medium voltage level. Particularly in Germany, this bridging system is operated at 110 kV. Traditionally, this voltage level is defined to be part of the distribution grid. Therefore, distribution grid operator (DSO) manage the concessions of the sub-transmission grids in Germany. Out of more than 800 different DSO, about 35 mostly larger DSO operate subsystems of the country-wide interconnected 110 kV grid (e.g. the 110 kV grid of the federal state of Schleswig-Holstein is operated by one DSO) .

In the light of the German energy transition towards (distributed) RE, many grid development plans have been elaborated not just for the transmission grid (see previous section) but also for the distribution grid. Consequently, there are many regional distribution grid plans which consider the lower, medium and high voltage level in a particular region. Recent examples for this regional planning practice are the distribution grid plans for the federal states of Hesse (Braun et al., 2018), Baden-Wuerttemberg (Rehtanz et al., 2017) and Rhineland-Palatinate (Ackermann et al., 2014). Moreover, two national distribution grid plans, developing future grid expansion for the entire country, have been published (Agricola et al., 2012; Büchner et al., 2014). The plans consider scenarios of the NEP in order to generate consistent results for all voltage levels.

In contrast to official German and European TEP, in the field of distribution grid planning no dispatch optimization such as a market simulation is used. Instead, two worst cases are defined: The heavy load case, which simulates the worst case of maximal demand and minimal generation and the reverse power flow case which simulates the opposite (maximal generation and minimal demand). The latter one gained importance due to the rise of distributed RE facilities and the shift from uni-directional flows to bi-directional flows (see also Agricola et al., 2012). Nowadays, this case is predominantly deciding on future grid expansion. In order to define the feed-in and demand of these worst cases, statistic simultaneous factors are used for the demand and the different generation technologies. For example according to Agricola et al. (2012) a maximum possible feed-in of wind power generation in the sub-transmission grid is 80 % of its nominal capacity interacting simultaneously with a minimal possible demand of 35 % of the maximal assumed demand. The EHV level is locally modeled in an abstract way. Planned expansion projects on the EHV level are considered as well.

Expansion measures are developed similar to the interactive and iterative process of the NEP. The sub-transmission grid has to be (n-1)-secure in the heavy load case and reverse power flow case (Agricola et al., 2012). Therefore (n-1)-contingency analyses are performed. The maximal loading of the lines and transformers is assumed to be 100 % of the thermal limit current. This constraint has to be valid at normal operating and during (n-1)-contingency. Furthermore a voltage deviation of ± 6 kV is allowed. Line expansion on existing routes and new substations towards the transmission grid, but no other topological changes are considered as possible expansion measures. Similar to the NOVA principle, low cost measures like different switching modes are tried out at first. The planning measures are iteratively checked by (n-1)-contingency analysis until the above mentioned maximal loading and voltage criteria are met. Following this method, Agricola et al. (2012) developed grid expansion measures for HV grids of seven DSO. In order to generate results for entire Germany the results are linearly scaled with respect to the covered area.

In contrast, Büchner et al. (2014) were the first to realize simulations on a line and substation sharp HV model for entire Germany. The sub-transmission model is based on OSM power grid data and the schematic grid maps being to some extent published with respect to regulation (KraftNAV §3 (1)). In addition, the DSO, which were part of the project consortium, reviewed the plausibility of the generated HV grid. Unfortunately Büchner et al. (2014) supplied no information of how the transmission grid is considered or modeled. The same applies for the grid expansion method used.

In international academic literature, according to a state-of-the-art review by Rad and Moravej (2017), most of the articles dealing with sub-transmission expansion planning focused on sub-transmission substations in combination with the medium voltage feeders (e.g. Franco et al., 2016; Jalali et al., 2014; Lavorato et al., 2010; Lotero and Contreras, 2011; Mazhari and Monsef, 2013; Ziari et al., 2012). Two more recent examples with a similar focus are Abedi et al. (2019) and Karimi and Haghifam (2017). Moreover, Hosseini et al. (2010) explained that conventionally, substations and lines are optimized separately in two sub-problems and then motivated their approach by analyzing that although separate expansion has computational advantages, disregarding the interdependence of both sub-problems can lead to suboptimal solutions. Hence, Hosseini et al. (2010) proposed a method of co-optimized sub-transmission substation and line expansion including the consideration of new possible candidate substation sites as well as existing ones. In the modeling the medium voltage (MV) demand and generation is considered and the problem is solved by a genetic algorithm. Shayeghi and Bagheri (2013) additionally integrated distributed generation expansion into the optimization problem minimizing system costs by a hybrid method of LP and genetic algorithm. Karimi and Haghifam (2017) also optimized MV feeder capacities but only considered possible expansion of sub-transmission substations. Kellermann et al. (2018) assessed the impact of RE curtailment on HV grid expansion objected to regional uncertainties in RE supply in the MV and HV level. Borchard and Haubrich (2008) also proposed to integrate the MV and HV grid planning but did not consider the EHV level either. Da Fonseca Manso et al. (2014) optimized the sub-transmission grid and considered a model of the transmission grid. An expansion tree heuristic was used to find near-optimal new branches. The performance of the final solution was tested with a PF. The method was applied on a part of a Brazilian grid which consists of 365 buses including 81 sub-transmission buses.

Rad and Moravej (2017) only presented one paper which generated an optimized solution for integrated transmission, substation and distributed generation expansion problem under various constraints (i.e. Brown et al., 2001). The algorithm was based on the concept of successive backward planning used in traditional transmission network expansion processes. This highly heuristic method immensely depends on the quality of the starting overbuilt system and does not guarantee optimality. It has been applied only on a small urban sub-transmission system in the USA and does not reflect on its scalability. Primarily, it was focused on distributed generation expansion optimization in order to avoid grid expansion on a regional scale. Consequently, Rad and Moravej (2017) motivated their work by highlighting that so far no simultaneous expansion planning of transmission substations, sub-transmission system, and distribution network had been carried out due to the high complexity of the problem. The developed model is highly complex. It optimizes the capacity of existing and candidate HV and EHV substations as well as the connecting MV, HV and EHV power lines. The optimization problem is constrained by the non-linear power flow equations and solved by a genetic algorithm. The work is lacking a consideration of distributed generation and a dispatch (and redispatch) optimization of a marginal cost driven generation mix. Moreover, the problem seems to be applied only on one static snapshot. Finally, while the model was tested on a rather small regional grid in the north-west of Iran consisting of 4 existing and 8 candidate transmission substations (plus the underlying structure), it was not stated whether the model would perform well on an national or continental scale.

Coming from the TEP perspective, Bayatloo and Bozorgi-Amiri (2019) claimed to be the first one combining TEP considering the transmission and sub-transmission grid without mentioning Brown et al. (2001) or Rad and Moravej (2017). Bayatloo and Bozorgi-Amiri (2019, p. 1321) stated "in previous studies, the sub-transmission system, which is one of the essential components of the power grid and is a bridge between transmission and distribution, was neglected. The practicality of the model will increase if we identify the importance of sub-transmission and its impact on the design and expansion of other grid components. Furthermore, it seems critical to consider sub-transmission systems alongside renewable resources due to the fact that renewable-energy power plants directly synchronize with sub-transmission systems rather than transmission network." The uncertainty of RE supply is met by a two-stage stochastic linear programming approach and the linearized AC power flow equations are considered. Similar to Brown et al. (2001) and Rad and Moravej (2017), the method is applied to a, compared to the entire German grid, rather small power grid (60 bus grid in the Iran). Again, the computational burden of solving the problem and its further scalability is not addressed.

In general, the grid expansion planning methods on the sub-transmission level are very similar to the ones on the transmission grid level. Like in TEP there is a discrepancy concerning the degree of automization of the expansion algorithms when comparing the national grid development plans and the state of the art in academic literature. Whereas the presented German development plans focus on rather traditional interactive methods, academic literature focuses on sophisticated automized solution strategies. Besides that, the general modeling approach is similar. In most cases, sub-transmission grid planning is part of the distribution grid planning neglecting the influence of the transmission grid planning whereas its operational behavior is considered slightly more often. Although there are a few sophisticated approaches jointly optimizing the transmission and sub-transmission grid, they do not consider bigger power systems on a national or continental scale. Therefore, the solutions lack in capturing holistic optima for the entire system of a country or even continent.

2.1.3 Aggregated systematic approaches

As described in the previous sections, traditional transmission and sub-transmission grid expansion planning methods consider non-aggregated line and substation sharp grid topologies. Due to this level of spatial detail, the approaches either lack the national or continental holistic perspective (see academic approaches in the previous sections) or miss out on sophisticated automatic solving approaches (NEP or TYNDP). A possibility to address this trade-off is to reduce the complexity of the grid. Lumbreras and Ramos (2016) coming from a traditional TEP perspective highlighted the increasingly relevant role of network reduction techniques. In this context, the advantage of reducing the computational burden comes along with the difficulty to apply the results on the original system (Lumbreras and Ramos, 2016). In the field of large-scale power system modeling reduced grid models have been applied quite often. In the following an overview of theses aggregated approaches is given. None of them considered the sub-transmission grid. Instead, the transmission grid or market-based capacities (i.e. NTC or available transfer capacities (ATC)) were used to generate aggregated abstract grid models representing the original ones.

Brown et al. (2016) pointed out that systematic approaches in literature, which have dealt with European grid expansion in the context of RE integration, either simplify the power flow problem to a transshipment model (Czisch, 2005; Schaber et al., 2012b,a; Schaber, 2013) or strongly aggregate the transmission grid (Czisch, 2005; Becker et al., 2014; Papaemmanouil et al., 2010) for computational efficiency. In contrast to these approaches, they further highlighted the other extreme, the modeling and contingency testing of the TYNDP, which consist of very time consuming detailed simulations difficult to iterate repeatedly with new and innovative technologies. Bridging these two extremes, they presented a modeling approach utilizing a LOPF, hence considering the linearized AC power flows in the European transmission grid. The energynautic in-house grid model, which was derived from openly available data as described in Qiong Zhou and Bialek (2005), contains 200 aggregated buses covering the ENTSO-E area and representing all major demand and generation sites and topologically significant substations. This signifies a grid resolution of about 30 buses being allocated in Germany. In total 400 aggregated lines represent all existing EHV AC and DC links. The AC and DC grid extensions for different scenarios were optimized. In these scenarios, they focused on the advantages of using innovative technologies such as batteries in combinations with solar power plants and a European-wide high voltage direct current (HVDC) overlay grid.

Apart from applying a transshipment model, Schaber et al. (2012b) and Schaber et al. (2012a) used an aggregated grid model, which is less detailed than the one used in Brown et al. (2016). Both applied the same European model in which they defined regions (according to Heide et al. (2010)) consisting of 50 onshore and 33 offshore regions. The transmission capacity between two regions was aggregated on the base of ENTSO-E (2018b). For cross-border capacities, NTC values were used. Apart from the mentioned modeling differences, a similar linear optimization of grid expansion was used as in Brown et al. (2016). Czisch (2005) applied also a linear optimization (considering the linearized network equations) but aggregated the European and North African grid even more, resulting in a model with 19 regions. The 20-node model developed and applied in Papaemmanouil et al. (2010) focused only on the former UCTE area representing most of Europe. Here grid expansion was heuristically optimized within a cost-benefit analysis.

The research project e-Highway 2050 realized by a large consortium of many European TSO, industrial associations, academics, consultants and one NGO (e-Highway 2050 project, 2015a) planned transmission grid expansion for a long-term perspective beyond the temporal scope of the TYNDP. Five scenarios for the power system of the year 2050 were created. The most ambitious one in terms of climate change mitigation was characterized by a 100% renewable power system (except for some gas fueled power plants). The temporal scale was modeled by hourly values of a scenario year. In order to generate robust results concerning weather variations, 99 possible weather years were considered using a Monte-Carlo approach (Couckuyt et al., 2015). In contrast to the approaches of the TYNDP and NEP, the European transmission grid was reduced by a clustering method (e-Highway 2050 project, 2015a; Lumbreras and Ramos, 2016) and grid expansion investments were optimized by an automated iterative process (e-Highway 2050 project, 2015b; Lumbreras and Ramos, 2016). The economic feasibility of possible grid expansion measures were tested by applying a multi-period LOPF of the software tool ANTARES (Couckuyt et al., 2015), assessing annual benefits in terms of less operational costs. Similar to the TYNDP and NEP, only grid expansion measures were considered for optimization. Other flexibility options such as storage investments were not regarded.

There are many more aggregated models, which optimize more than the grid infrastructure (e.g. storage and/or generation expansion). These co-optimization approaches are considered in Section 2.3. In the area of dispatch optimization and (market) simulations similar aggregation methods are used. Becker et al. (2014) and Rodríguez et al. (2014) simulate several scenarios with different interconnection capacities between the different European countries in a continent spreading model. As these approaches do not optimize grid expansion, they will not be further analyzed.

2.2 Modeling of storage expansion

Palmintier and Webster (2016) stated that future systems with larger shares of renewable generation will require a generation mix including flexible power sources. According to them, so far flexibility is rarely fully considered in capacity planning models because of the computational demands of including mixed integer unit commitment within capacity expansion. Although they mentioned the ability of storage units to provide operational flexibility, they only considered the flexibility of conventional power plants in their modeling while disregarding the influence of the power grid.

Flexibility needs in modern and future RE penetrated systems are simulated in several publications. Weitemeyer et al. (2015) simulated different RE shares and different storage sizes for Germany neglecting grid restrictions. Andrey, C. and Fournié, L. and Gabay, M. and de Sevin, H. (2016) simulated scenarios with different RE shares for several European countries in order to analyze the need for flexibility which they defined as “the amount of energy that has to be shifted in order for the residual demand to become constant over a certain period” Andrey, C. and Fournié, L. and Gabay, M. and de Sevin, H. (2016, p. 3). In contrast to Weitemeyer et al. (2015), Denholm and Hand (2011) considered today’s grid restrictions (i.e. for the transmission grid of Texas). Besides this difference they also simulated scenarios with different RE shares and storage sizes. Huber et al. (2014) simulated flexibility needs for different European countries and highlighted the benefits of cooperation when these countries are interconnected. All of these approaches showed the rising need for flexibility in systems with high shares of RE but none of them optimized storage expansion. According to Brijs et al. (2017), literature on storage modeling can be categorized into studies simulating predefined generation and storage portfolios, optimizing storage investments while the generation portfolio is exogenously predefined or co-optimizing storage and generation expansion. In the following, it is only focused on storage optimization approaches, which consider the economic feasibility. Brijs et al. (2017) is lacking an emphasis for studies co-optimizing not only storage (and generation) but also grid expansion. Anyhow, these are not considered in this section, instead will be analyzed in the following one.

Storage expansion planning can be sub-divided into the question of siting and sizing. Many approaches focus on the sizing question only. This can be either due to a very local perspective from an individual distributed generation facility connected to the distribution grid (e.g. Korpaas et al., 2003; Harsha and Dahleh, 2011, 2015) or to a very broad perspective such as in e.g. Schill (2014); Makarov et al. (2012). In Makarov et al. (2012), transmission network constraints were neglected and the system-wide storage capacities were estimated within the Western Electricity Coordinating Council (WECC) system (Fernández-Blanco et al., 2017). Similar in Schill (2014, p. 67), where Germany was "considered to be both an island and a copper plate". In a state-of-the-art review, Lorente et al. (2018) concluded that storage siting is more critical than sizing. The siting decision involves grid modeling, thus more complex models. They affirmed, as a consequence, that research on location decision is still rather scarce. In this context, Fernández-Blanco et al. (2017) stated that co-optimization of siting and sizing has been undertaken relatively often for distribution grids (see Zidar et al., 2016) but is difficult to apply on the transmission grid level because power flows in meshed transmission grids often change direction over the course of the day or as a function of the production from renewable resources. Here, it is crucial to find optimal locations and storage energy and power ratings that are economically feasible at each location (Fernández-Blanco et al., 2017). This work further focuses on approaches which consider larger systems including the transmission grid, hence addressing the co-optimization of storage allocation as well as its nominal power and energy ratings.

Besides the abundant amount of studies conducted on the distribution level, there have been fewer studies published considering the transmission grid, however a variety of studies exists. None of the existing studies consider storage expansion planning in a combined transmission distribution grid planning approach. Consequently, the sub-transmission grid has not been integrated into a storage expansion planning approach at the transmission grid level. In contrast, the vast majority of the studies considering the transmission grid apply their method only on small real or artificial IEEE reference systems (Fernández-Blanco et al., 2017). Wogrin and Gayme (2015) highlighted the importance of considering different storage technologies and optimizing its portfolio as well as siting and sizing these. At the time they claimed to be the first to co-optimize these goals while considering transmission grid restrictions. They used a LOPF approach including storage investment decision variables. Four different technologies i.e. pumped-storage hydro, compressed air energy storage, lithium ion batteries, and flywheel energy storage with their different characteristics (e.g. charging/discharging efficiencies, power-energy ratios and investment costs) potentially supply different types of flexibility. Pumped hydro and compressed air energy storage, due to their great capacities (high energy-power ratios) are rather suitable for long-term (seasonal) energy shifting whereas lithium ion batteries and flywheel storage units supply preferably short-term (hourly, diurnal) flexibility (see also Guney and Tepe, 2017; Child et al., 2018; Groiss et al., 2017). Additionally, Wogrin and Gayme (2015) provided a possibility to reflect local constraints such as pumped hydro or compressed air storage, which can only be built at grid buses where the geological potential is given due to e.g. existing salt-caverns. Ghofrani et al. (2013) also used a LOPF approach, optimally placing and scheduling storage units to minimize social costs. In contrast, probabilistic uncertainties of wind and load behavior were considered and a non-classical genetic solving algorithm was used accepting the possibility of finding local optima. While also considering the linearized network equations, Krishnan and Das (2015) optimized siting and sizing in terms of generating higher profits as a storage operator in a co-optimized energy and ancillary services market. Similarly, Dvorkin et al. (2017) answered the siting and sizing question in a market environment, additionally accounting for up and downtime of conventional generators. Consequently, a computationally demanding bilevel model that scales poorly for larger systems has to be solved (Fernández-Blanco et al., 2017). All of the mentioned complex modeling approaches were applied on small systems and few snapshots. Wogrin and Gayme (2015) tested their method on a 14-bus IEEE system and 288 snapshots. Ghofrani et al. (2013) and Krishnan and Das (2015) both used a 24-bus IEEE reference grid and a timescale of 24 and 48 hours respectively. Finally, Dvorkin et al. (2017) used a real-world example of the ISO New England system but being reduced to a 8-bus model considering 5 representative days on a hourly resolution.

In contrast, Dvijotham et al. (2014) claimed to be the first to co-optimize storage allocation and sizes in a real-world sized transmission grid. Particularly, they considered the 2209 bus-system of the Boneville Power Administration recognizing actual operational data and more than hundred different wind patterns. They integrated a standard LOPF approach for dispatch optimization into a sub-optimal greedy heuristic algorithm iterating over different storage settings determining optimal storage size and location. Starting with storage units at all buses they iteratively reduced the number of storages sites finally reaching results with a small number of storage sites compared to the total number of buses. The temporal resolution appears to be modeled rather scarcely since they optimized the dispatch for only two consecutive hours. For a grid with such a high number of buses the problem was stated to be solved in only 10 minutes, which can be considered relatively fast. They argued that principally the problem could have been modeled directly as a mixed integer linear program but would lead to computational infeasibility when modeling real-world problems with a high number of buses.

Nevertheless, Fernández-Blanco et al. (2017) developed such a mixed-integer problem, which according to them can be applied to large and meshed transmission systems. In a co-optimization approach operational costs of conventional generation and investment costs of storage power and energy ratings were minimized in a central planning approach. In this mixed integer LOPF the standard linearized power flow equations were considered. Furthermore, it was aimed to reflect the stochastic behavior of wind and solar resources. In a particular case study, this is reflected by the usage of five representative days with an one hourly resolution. The storage technologies modeled were expected to have a fixed energy-to-power ratio. Specifically, a rather generic storage technology with an energy-to-power ratio of 6 hours, which could represent a lithium-ion battery technology, was assumed. The case study represents the WECC system by a 240-bus and 448-line model. Although they considered this as a large and meshed transmission system, it is significantly less complex than the model used by Dvijotham et al. (2014). Despite the lower spatial complexity, this deterministic approach reaching a global optimum led to much higher computational burden. On the Hyak supercomputer system at the University of Washington using the commercial solver CPLEX and the modeling language GAMS while accepting a 1% optimality gap, the optimization problems were solved in up to 5.5 hours.

2.3 Co-optimization of grid and storage expansion

Besides the potential positive impact of storage investments on the operation of power systems consequently leading to a higher RE share in the energy production and less system costs, the question of impacts on grid expansion planning arises. Gomes and Saraiva (2019) assessed an increasing importance of this question in recent years considering the grid expansion planning on the transmission grid level. The motivation of co-optimization was well described by Bussar et al. (2015, p. 145) stating "Energy storage systems can provide this flexibility by shifting of load in time while transmission grids provide the shift of load in space. Up to a certain extent, transmission capacity and storage capacity can replace each other, i.e. storage can reduce the load on transmission infrastructure by mitigating local peaks in load and/or generation." This problem implies a need for a combination of long-term and operational planning. In this sense, Després et al. (2015, p. 493) concluded "Even the most accurate long-term energy models still lack a temporal representation of the power sector which is necessary for including inter-temporal constraints associated to the introduction of variable renewable sources." Consequently, the co-optimization of grid and storage expansion makes the problems more complex and computational burden rises (Krishnan et al., 2016). As in grid-only expansion planning, in literature two trends can be noticed. On the one hand line-sharp grid expansion planning focus on computational demanding techno-economically sophisticated mixed-integer approaches which are applied on small (reference or real) grid systems. On the other hand many approaches consider large-scale real-world systems on a national, continental or even global scale being modeled in abstract ways and simplify technical constraints (e.g. using a transshipment model or continuous optimization variables). At first, the state of the art of the first group mentioned, particularly focusing on the transmission grid, will be outlined. Co-optimization approaches applied and developed for the sub-transmission grid (individually or in combination with the transmission grid) were not found in academic literature. Secondly, the aggregated approaches are described.

The literature review by Gomes and Saraiva (2019) referred to two studies (i.e. Li et al., 2015; Zhang et al., 2013), which integrate storage investment optimization into the TEP problem. Actually Li et al. (2015) did not introduce a storage investment optimization. Instead, they proposed a model which can find the optimal trade-off between transmission investment and incentive-based demand response expenses. Certainly, demand response provides flexibility to the system but cannot be considered an energy storage. In contrast, Zhang et al. (2013) really co-optimized storage and grid expansion in a deterministic single-stage mixed-integer linear model. The integrated operational optimization neglected marginal prices of generation facilities and instead minimized line losses which were piecewise linearized.

A few more studies integrating the storage investment optimization into the TEP problem can be found in academic literature (i.e. Gan et al., 2019; Gonzalez-Romero et al., 2019; Hedayati et al., 2014; Konstantelos and Strbac, 2015; Qiu et al., 2017). All of them, like Zhang et al. (2013), used mixed-integer approaches considering discrete storage and grid investments. Moreover, they were all applied on small mostly artificial power systems. In contrast to Zhang et al. (2013), the others solved multi-stage problems. Hence, the optimization problem was divided into sub-problems usually using a Bender's decomposition approach. Furthermore, all approaches have in common that the flow problem was abstracted as a linearized AC power flow problem.

Hedayati et al. (2014) were the first to address the co-optimization problem as a multi-stage mixed integer linear program. They determined the location of a given storage size. Thus, the sizing of the storage units was not considered. Moreover, in the LOPF approach no (n-1)-contingencies were regarded. In contrast, Konstantelos and Strbac (2015) chose a security constrained linear optimal power flow approach. Besides this difference, the methods applied were very similar.

Qiu et al. (2017) considered as well as Hedayati et al. (2014) and Konstantelos and Strbac (2015), apart from the investment optimization, the marginal costs of the generators in an operational optimization. As a novelty, they concentrated on modeling delays of the transmission grid expansion and the degradation of storage capacity considering different RE and load increase scenarios. Five representative days per year were considered while a total planning horizon of 25-years is very long compared to other studies. Furthermore, unlike previous works, they jointly tackled the storage sizing problem. Hedayati et al. (2014); Konstantelos and Strbac

(2015); Qiu et al. (2017); Zhang et al. (2013) tested their methods on the IEEE 24-bus reliability testing system without mentioning possible scalability.

In contrast, in a very recent paper, Gan et al. (2019) applied their model on the 53-bus transmission system of the Gansu provincial power system in China. They used storage units also to provide (n-1)-security avoiding immense over-sizing of the transmission grid due to (n-1)-contingencies. Furthermore, they incorporated the risk of extensive wind curtailment costs. In another recent work Gonzalez-Romero et al. (2019), short and long-term storage constraints were jointly considered (i.e. batteries and hydro) by applying a representative-period framework modeling inter- and intra-periodic constraints. In a bi-level approach the TSO perspective aiming to minimize total system costs was considered on the upper level and the distributed generator company perspective aiming to maximize profits on the lower level were modeled. The generator expansion planning on the the lower level included storage technologies. Theses investment decisions were simulataneously optimized with operation. Finally, the sophisticated agent-based modeling was applied in a case study of only four buses considering four representative days with an one-hourly resolution. Concerning the scarce spatial resolution, whether the method might be computational feasible for larger systems is not discussed.

The application to large-scale problems is challenging in the case of co-optimization (Hagspiel et al., 2014). Nevertheless, a considerable amount of studies have applied joint optimization approaches on countries (Pudjianto et al., 2014; Schaber, 2013), continents i.e. Europe (Alvarez et al., 2013; Bussar et al., 2014, 2015, 2016, 2017; Brown et al., 2018c; Child et al., 2018, 2019; Gils et al., 2017; Haller et al., 2012a,b; Held et al., 2018; Hörsch and Brown, 2017; Pleßmann and Blechinger, 2017; Schaber, 2013; Schlachtberger et al., 2017; Schlott et al., 2018; Scholz, 2012; Scholz et al., 2017; Tranberg et al., 2018; Zappa et al., 2019) or even on the global power system (Aboumahboub, 2012). In the context of this work the articles modeling Germany and Europe will be focused on. In Schaber (2013), Germany was modeled considering 20 regions. The spatial resolution of the European power grid ranges from 15 (Gils et al., 2017; Scholz et al., 2017) to 362 buses (Hörsch and Brown, 2017). All of the mentioned approaches co-optimized grid, storage and generation expansion. This represents a difference to the line-sharp transmission expansion in which, when storage expansion is considered, generation expansion is often disregarded. Another difference is that most of the aggregated approaches (except Pudjianto et al. (2014) and Zappa et al. (2019)) did not consider the discrete nature of grid expansion and/or unit commitment. Hence, they avoided a mixed integer problem in order to simplify the problem. Furthermore many aggregated approaches simplified the modeling of the power flow problem by using a transshipment model.

In this context, two models i.e. GENESYS and REMix, being used in many articles, can be highlighted. The model GENESYS was described and used by Alvarez et al. (2013); Bussar et al. (2014, 2015, 2016, 2017); Thien et al. (2013) in order to co-optimize European grid, storage and generation investments. The model was first presented by Alvarez et al. (2013). They focused on the model description but also generated results for the 21-region model of the European and MENA power system in the year 2050. In simple terms, by applying a genetic algorithm for different power system candidate settings of RE generation, storage and grid installed capacities heuristic dispatch optimizations were performed. The evolution-process including mutation, evaluation and recombination was iteratively carried out until the total system costs (annuity of investment costs, annual maintenance and operating costs) converged to a minimal value. The genetic algorithm enabled to model certain unlinearities of e.g. storage components while reaching a higher computational performance compared to deterministic solving approaches. The other mentioned GENESYS-related articles basically used the same modeling approach. Thien et al. (2013) modeled six different scenarios evaluating different exogenously defined ratios of solar and wind installed capacities comparing the cost differences between the sub-optimal solutions with the optimal one. Bussar et al. (2014) focused on the optimal setting but modeled three years (instead of one) for the operational optimization. Bussar et al. (2015) and Bussar et al. (2016) focused on several sensitivities i.e. limiting the NTC between the regions, restricting the availability of different storage technology options or varying the specific investment costs of the different technology options. In Bussar et al. (2017) the functionality of modeling multiple evolution paths from 2015 to 2050 was introduced.

In contrast to GENESYS, although following basically the same goals, in REMix a linear optimization problem written in GAMS is solved by CPLEX (Scholz, 2012). This implies that unlinear effects are not considered. On the other hand the solutions obtained are proven to be optimal. Scholz (2012) developed the model considering a 36-region model of Europe and the MENA countries. Besides some exception (e.g. Estonia, Lithuania and Latvia were aggregated to one region) mostly the regions were congruent with the considered countries. Several following dissertations added new functionalities to the model. Luca de Tena (2014) studied the feasibility and system impact of electric mobility. Stetter (2014) extended the model by a representation of the global power system, an optimized power plant siting approach and introduced the possibility of considering the linearized AC network equations modeling the power flow between region centers more accurate as in a transshipment model. Finally, Gils (2015) studied the potential role of flexible electric loads and power-controlled operation of combined heat and power plants. Although Stetter (2014) implemented an AC power flow problem, in three more recent journal publications (i.e. Cebulla et al., 2017; Gils et al., 2017; Scholz et al., 2017) apparently it was not used since only active elements i.e. HVDC lines were modeled and optimized. The existing grid infrastructure including passive AC elements and their reactances was not considered. In both articles, in contrast to Scholz (2012), only Europe, hence a 15-region model was applied.

Apart from GENESYS and REMix related works, a few additional articles using a transshipment model are worth mentioning. Pleßmann and Blechinger (2017,

p. 20) argued that a "transition pathway for the entire European power system has been lacking". In this sense the model shall be realistic and detailed, reflecting all relevant power generation and storage technologies and transmission lines connecting several supply regions, and at the same time ensure fast computing. In a linear optimization approach annualized investment costs and operational costs were minimized in 5-years steps, called decision years. Installed capacities were transferred from one decision year to the next considering components' lifetimes. A central constraint to the cost minimization were European greenhouse gas emission targets within the power sector until the year 2050. Europe was modeled as 18 regions mostly representing countries, whereas some are aggregated similar to the approach in Scholz (2012).

In a similar approach Child et al. (2018) also modeled a pathway towards 2050 considering detailed optimization runs in 5 years steps. Moreover, the spatial resolution is comparable, modeling 20 European regions. One central difference is the consideration of a certain amount of prosuming demand. Aiming to quantify the effect of European interconnection, they modeled two opponing scenarios: one with European interconnection assuming potentials up to 2030 considering the TYNDP and beyond that possible HVDC expansion and another one where all regions are self-supplied neglecting any interconnection. In a later, very similar publication (i.e. Child et al., 2019), the role of flexible generation, energy storage and the European transmission grid was stressed and discussed more in detail enabling recommendations for policy. For example, it was highlighted that an increase of the transmission capacities by a factor of four is economically feasible.

Zappa et al. (2019) addressed doubts about the (technical) feasibility of a 100% RE European power system which were elaborated by Heard et al. (2017) and critically discussed by Brown et al. (2018a). In a mixed-integer linear optimization approach they considered flexibility limitations of dispatchable generators. Moreover, the upper limits of possible investment and dispatch were restricted regarding land availability for RE and their spatially consistent temporal resource potentials. In this context, long-term weather data in a hourly resolution was utilized. Moreover, in several scenarios assumptions about the future demand and technology development were varied. Consequently, the sensitivity of these parameters was evaluated. Although addressing doubts about the technical feasibility, the study lacks some key aspects of sophisticated power system modeling. The study did not model seasonal storage, therefore neglected a central flexibility option in a 100% RE system. Moreover, the power flow model was only represented by a transshipment problem. Consequently, the passive impedance-related behavior of the power flows, hence e.g. the effect of loop flows was disregarded. Furthermore, the spatial resolution of the grid is with 30 buses rather coarse.

In comparison, according to Held et al. (2018), while considering an adequate temporal resolution, the representation of the grid infrastructure used in Pleßmann and Blechinger (2017) (18 regions) remained sketchy. In contrast, Held et al. (2018,

p. 113) motivated their work by achieving "an appropriate balance between the level of detail considered in the representation of both the grid and the variability in system operating conditions." Thus, they proposed a much more detailed abstract grid model consisting of 118 buses. The temporal resolution was modeled by about 80 snapshots representing the entire target year. Three different models were combined. Green-X defined the RE development considering resource availability and policy instruments. Enertile co-optimized investment and dispatch decisions in a linear problem serving as a first estimate for a more detailed grid expansion planning with the TEPES model (e.g. considering expert knowledge for choosing candidate power lines). Grid expansion and line losses were taken from TEPES model results whereas operational results were based on the modeling with Enertile. In order to minimize computational burden, iterations between Enertile and TEPES were not realized which may lead to inconsistencies. Although they used TEPES as a separate grid expansion planning tool and a rather detailed grid model, the power flow problem was solved as a simple transshipment problem, which implies already mentioned drawbacks. The decision variable of storage investment was characterized by a simplified representative storage option with similar characteristics as the pumped storage technology. They justified this simplifications by their results, which showed few investment into this technology. Instead, although also modeling the year 2050, they considered conventional power plants like hard coal and lignite with carbon capture and storage technology, which supply flexibility. Furthermore, it is not addressed whether the applied snapshot clustering is able to capture intertemporal constraints adequately especially in the case of seasonal storage units.

The so far described work focusing on co-optimization on large-scale systems used transshipment models. In this context, Hagspiel et al. (2014, p. 654) stated "a joint optimization of generation and transmission is difficult, mainly due to the fact that commercial trades do not directly translate into power flows on a specific line in meshed networks. Instead, according to Kirchhoff's circuit law, loop flows occur and potentially impact the entire transmission system. This is specifically true when dealing with a highly intermeshed alternating current (AC) transmission network like the European power system." This difficulty has been addressed by Hagspiel et al. (2014) and a few others (Haller et al., 2012b; Hörsch and Brown, 2017; Schlachtberger et al., 2017; Brown et al., 2018c).

Hagspiel et al. (2014) developed a linear co-optimization approach considering the linearized physical power flow equations using power transfer distribution factors. Due to the linearization the changing reactances, which occur due to grid expansion were not considered in the linear problem. This problem was solved by an iteration process updating the reactances after an optimization run leading to another optimization afterwards. The method showed good robust results after five of such iterations. The method was applied on a 200 bus-model of Europe. For the dispatch optimization eight typical days per year (addressing each combination of the following situations: summer/winter; workday/weekend; high/low feed-in from wind and solar) on an hourly basis were considered. Possible storage investments were characterized by the compressed air energy storage technology.

A similar method was developed by Haller et al. (2012a) without considering the change of reactances due to grid extension. They emphasized the combination of the following two problems: long-term investment planning and short-term operational planning. In a subsequent work (Haller et al., 2012b), this approach was applied on a 20-regions model of Europe and the MENA countries. In this work, they refrained from using the linearized AC power flow model since Haller et al. (2012a, p. 2694) concluded that “although DCLF constraints certainly do affect actual power flow distributions at certain points in time – their effect on long-term developments of system costs may be rather small.”

In contrast, the recently published open source co-optimization tool Python for Power System Analysis (PyPSA) has been used in several publications principally following the method described in Hagspiel et al. (2014). The functionalities of PyPSA were described in Brown et al. (2018b) in detail, following the idea to “bridge the gap between power system analysis software and general energy system modeling tools.” Brown et al. (2018b, p. 2). In a single linear problem, the multi-period linear optimal power flow approach was applied to co-optimize grid, storage and generation investments and dispatch in the European energy system by Brown et al. (2018c); Hörsch and Brown (2017); Schlachtberger et al. (2017); Schlott et al. (2018); Tranberg et al. (2018). In Hörsch and Brown (2017); Schlott et al. (2018); Tranberg et al. (2018) the linearized AC network equations were considered whereas in Brown et al. (2018c) and Schlachtberger et al. (2017) only HVDC links between regions were modeled as a transshipment problem. In Schlachtberger et al. (2017) the benefits of cooperation in a highly renewable European electricity network was focused on in a 30-bus model. In order to quantify these benefits, possible transmission capacities were restricted from the optimum level to zero. The remaining flexibility had to be covered by investments into storage units. Brown et al. (2018c), using the same 30-bus power model as Schlachtberger et al. (2017) in addition to the power sector integrated the transport, heat and gas sector. In both, a full weather year with hourly resolution was considered. This high temporal resolution reflects the intermittent behavior of RE and most importantly the intertemporal behavior of storage units in a very accurate way. However, the spatial scale and the grid’s physical flow behavior (using a transshipment model) was represented rather coarsely. In contrast, Hörsch and Brown (2017) focused on the impact of spatial scale in co-optimization approaches. With the help of a k-means algorithm they cluster the actual European transmission grid into a model between 37 to 362 buses. Here, due to the high computational burden, only every third hour of the year is considered. By this, the consecutiveness of time is principally reflected (which is usually disregarded in snapshot clustering approaches (see also Kotzur et al., 2018)). The same temporal resolution was used by Schlott et al. (2018) and Tranberg et al. (2018). Schlott et al. (2018)

considered 30 and Tranberg et al. (2018) 64 buses for their representation of the European grid. Both, without considering geographic constraints, consider hydrogen and battery storage as flexibility options.

Chapter 3

Hypotheses

Based on the research questions and the described state of the art the following hypotheses were derived and shall be tested in the subsequent chapters.

- It is possible to model the German power grid down to the 110 kV grid level on the basis of open source and open data to derive cost optimal future grid and storage expansion settings.

- A joint modeling of the transmission and sub-transmission grid (including its passive flow behavior) enables a spatially detailed and possibly diverse allocation of economically co-optimal grid and storage expansion in a future German power system.

- Distributed power flow problems and flexibility investments affect the overall optimum.

Chapter 4

Methods

In the first section of this chapter, the linear optimization problem is formulated. Besides presenting the abstract math of the problem, it is focused on the parameterization of the endogenous decision variables. After that, the ex-post non-linear power flow simulation is shorty described. Furthermore, as a very important base of the work, the status quo grid model including today's and future generation and demand characteristics is explained. Here, it is focused on the parameterization of the exogenous part of the optimization model. Whereas the status quo scenario is used for developing a realistic plausible model serving as a base for the future development, in the following chapter, results will only be presented for the, in the context of this work, more relevant future scenarios (i.e. *NEP 2035* and *eGo 100*). The entire chapter describes the base case assumptions, which lead to results for the base scenarios, as presented in Section 5.1.

4.1 Combined optimization of grid and storage expansion

With respect to the research questions a method is needed which is able to co-optimize grid and storage expansion as well as operational costs. This optimization has to take into account technical restrictions of all components including the grid down to the HV level. Consequently, the open source software PyPSA offering a multi-period optimization of operation and investment considering linear power flow equations (Brown et al., 2018b) is used and customized within the software tool Electricity Transmission Grid Optimization (eTraGo) (see Centre for Sustainable Energy Systems Flensburg and DLR Institute for Networked Energy Systems, 2019). In the following, the functionality of the LOPF will be explained including all constraints and assumptions. In previous works (Müller et al., 2018b,a, 2019b,a; Wienholt et al., 2018) eTraGo and PyPSA's underlying LOPF were used as well but with respect to the research questions parameterized differently.

4.1.1 Linear optimization of system costs

Assuming a linear problem (for the linearization of the non-linear network equations see Subsection 4.1.2) endogenous system costs can be minimized with respect to the following objective function (see Equation 4.1). All variables are continuously optimized avoiding a mixed integer problem and significantly higher computing times.

$$\min_{\substack{F_b, H_{n,s} \\ g_{n,r,t}, h_{n,s,t}}} \left[\sum_b c_b \cdot F_b + \sum_{n,r,t} (w_t \cdot \ o_{n,r} \cdot g_{n,r,t}) \right. \\ \left. + \sum_{n,s} c_{n,s} \cdot \ H_{n,s} + \sum_{n,s,t} w_t \cdot \ o_{n,s} \cdot \ [h_{n,s,t}]^+ \right] \ \forall\, b, n, r, s, t \tag{4.1}$$

where

$b \in B$: branch label
$n \in N$: bus label
$r \in R$: generator carrier label
$s \in S$: storage carrier label
$t \in T$: snapshot label
c_b : branch annualized capital cost per capacity
F_b : branch active power capacity
w_t : snapshot weighting
$o_{n,r}$: generator operating (marginal) costs
$g_{n,r,t}$: generator dispatch
$c_{n,s}$: storage annualized capital cost per capacity
$H_{n,s}$: storage nominal active power capacity
$o_{n,s}$: storage operating (marginal) costs
$h_{n,s,t}$: storage dispatch

Operational (also called marginal) costs of generators and storage units as well as annualized investment costs of the grid components and storage units are part of the objective function and are therefore endogenously defined. In contrast, due to the scope of the work and to reduce computational burden, generator capacities are exogenously defined by assuming probable future developments with respect to well-known state-of-the-art scenarios. Thus, $F_b, H_{n,s}, g_{n,r,t}$ and $h_{n,s,t}$ are the variables of the optimization. The marginal cost assumptions including operating, fuel and CO_2 emission costs ($o_{n,r}$ and $o_{n,s}$) for the different technologies and scenarios can be observed in Table 4.1. Furthermore, for the sake of computational burden and preventing optima plateaus, the marginal costs are changed randomly with a small standard deviation of 0.01 EUR.

The overnight capital cost assumptions for grid and storage components are displayed in Table 4.2 and 4.3. The capital cost assumption of a a new AC power line considers that additional systems can be attached to the existing poles. In contrast, a complete reconstruction is assumed to be approximately four times higher (see also Agricola et al., 2012; 50Hertz et al., 2015b). Consequently, as a conservative assumption, four times higher costs (compared to the ones in Table 4.2) are considered.

The co-optimization of operating and investment costs requires comparable cost assumptions. Therefore the overnight investment costs are annualized by applying

Carrier type	Marginal costs in EUR_{2014}/MWh		
	Scenario		
	Status Quo	**NEP 2035**	**eGo 100**
Uranium (Nuclear)	4.68	5.48	–
Lignite	10.78	17.64	–
Hard coal	14.95	24.79	–
Gas	32.30	41.93	56.05
Oil	41.02	68.86	–
Waste	31.65	39.93	–
Other conventional	31.65	39.93	–
Biomass	23.96	31.11	31.63
Other renewable (e.g. solar, wind)	0	0	0
Storage	0	0	0

TABLE 4.1: Marginal costs per carrier and scenario in EUR_{2014}/MWh (see also Müller et al., 2018b; Bunke et al., 2017). Operating, fuel and CO_2 emission costs are included. The CO_2 costs are assumed to be 5.91 EUR/t_{CO_2} for the *Status Quo* scenario (EEX Germany mean value 2014), 31.00 EUR/t_{CO_2} for the *NEP 2035* scenario (based on 50Hertz et al., 2015b) and 62.05 EUR/t_{CO_2} for the *eGo 100* scenario (based on Nitsch, J. and Pregger, T. and et al., 2012).

Equation 4.2, thus deriving c_b and $c_{n,s}$. The expected lifetimes of each storage technology are assumed as in Table 4.3 according to Erlach et al. (2015). In case of the grid components, 40 years are expected (based on Bundesministerium der Justiz und für Verbraucherschutz, 2005). Moreover, a discount rate of 5 % is considered (as in e.g. Kaldemeyer et al., 2016). Finally, annualized capital costs are displayed in Table 4.2 and 4.3.

$$c_a = c_o \cdot \frac{(1+i)^{\lambda} \cdot i}{(1+i)^{\lambda} - 1} \tag{4.2}$$

where

c_a : annualized capital cost of each extendable storage or grid component
c_o : overnight capital cost of each extendable storage or grid component
i : discount rate
λ : expected component lifetime

Component	**Overnight Costs**		**Annualized Costs**	
		EUR/		EUR/
Overhead Line, 380 kV	85	MVA*km	4.95	MVA*km*a
Overhead Line, 220 kV	290	MVA*km	16.9	MVA*km*a
Overhead Line, 110 kV	230	MVA*km	13.4	MVA*km*a
EHV DC-Link (underground)	375	MVA*km	21.9	MVA*km*a
DC-Converter	200,000	MVA	11,655.6	MVA*a
Transformer, 380-220 kV	14,166	MVA	825.6	MVA*a
Transformer, 380-110 kV	17,333	MVA	1,010.1	MVA*a
Transformer, 220-110 kV	7,500	MVA	437.1	MVA*a

TABLE 4.2: Specific grid expansion costs (overnight and annualized) for all scenarios based on Agricola et al. (2012) (HV grid) and 50Hertz et al. (2015b) (EHV grid). The expected lifetime is assumed to be 40 years for all components (based on Bundesministerium der Justiz und für Verbraucherschutz, 2005)

4.1.2 Constraints

Generators

Generators are optimized concerning their hourly dispatch. For each hour, generators can dispatch power according to Equation 4.3. For the fluctuating technologies wind and solar, the $\bar{g}_{n,r,t}$ varies hourly with respect to the available resources. The resource restriction is explained in detail in Subsection 4.3.4. All other generation facilities are able to dispatch their full nominal power at each hour of the year.

$$0 \leq g_{n,r,t} \leq \bar{g}_{n,r,t} \cdot \bar{g}_{n,r} \; \forall \; n, r, t \tag{4.3}$$

where

$g_{n,r,t}$: dispatch of generator

$\bar{g}_{n,r,t}$: potential generation of a generator per unit of nominal power

$\bar{g}_{n,r}$: nominal power of a generator

Storage units

Wienholt et al. (2018) already described the specific assumptions concerning the constraints of the storage optimization. In the following, the key aspects are recapped.

The possible nominal power of the optimized storage units is assumed to be unlimited (cf. Equation 4.4). Hence, the theoretic cost-optimal need for flexibility can be determined whereas the technical feasibility is discussed ex-post. Nevertheless, local and technological restrictions and characteristics are directly modeled. Two different technologies, a lithium-ion battery with a fixed power-to-energy ratio of 1/6 and a hydrogen cavern storage with a ratio of 1/168 are considered (see Table 4.3). Therefore, hydrogen storage units have a much higher capacity compared

Parameter	Scenario and technology					
	Status Quo		NEP 2035		eGo 100	
	batt	H_2	batt	H_2	batt	H_2
Overnight Costs in TEUR/MW	2,830	1,291	919	891	678	651
Annualized Costs[1] in TEUR/MW*a	229	95	66	65	45	48
Power-to-energy ratio ($r_{n,s}^{-1}$) in $1/h$	$1/6$	$1/168$	$1/6$	$1/168$	$1/6$	$1/168$
Lifetime in a	20	25	25	25	30	25
Standing losses in %	0.97	0.07	0.69	0.07	0.42	0.07
Charging efficiency in %	93	68	93	73	95	79
Discharging efficiency in %	93	38	93	43	95	57

TABLE 4.3: Parameters for extendable battery (batt) and hydrogen (H_2) storage units for the scenarios *Status Quo*, *NEP 2035* and *eGo 100* based on Erlach et al. (2015). [1] including annual operational costs

to the nominal power and are consequently rather utilized for the provision of long-term flexibility (weekly to seasonal). On the other hand, battery storage units supply short-term flexibility on a hourly or daily basis. It is assumed that it is possible to built battery storage units at all buses. In contrast, in this work it is assumed that hydrogen storage units can only be built where salt caverns are situated. Consequently, this technology option is only available in Northern Germany.

$$0 \leq H_{n,s} \leq \infty \; \forall \; n, s \tag{4.4}$$

where

$H_{n,s}$: storage extended nominal active power capacity

Moreover, the dispatch (discharging and charging) of the already existing and the potentially built storage units is optimized. The corresponding constraints for the minimal and maximal discharging, charging and state of charge are displayed in Equations 4.5 to 4.7. Equation 4.8 relates the charging, discharging and state of charge and introduces hourly standing losses and charging and discharging efficiencies. These efficiency parameters can be observed in Table 4.3. Finally, it is assumed that the initial state of charge equals the final state of charge. This, so called cyclic condition, which keeps the energy balanced over the total modeling period, is stated in Equation 4.9.

$$0 \leq h_{n,s,t} \leq \bar{h}_{n,s} \; \forall \; n, s, t \tag{4.5}$$

$$0 \leq f_{n,s,t} \leq \bar{h}_{n,s} \; \forall \; n, s, t \tag{4.6}$$

$$0 \leq soc_{n,s,t} \leq r_{n,s}\bar{h}_{n,s} \; \forall \; n, s, t \tag{4.7}$$

$$soc_{n,s,t} = \eta^{w_t}_{\text{stand};n,s} soc_{n,s,t-1} + \eta_{\text{store};n,s} w_t f_{n,s,t} - \eta^{-1}_{\text{dispatch};n,s} w_t h_{n,s,t} \; \forall \; n,s,t \tag{4.8}$$

$$soc_{n,s,t=0} = soc_{n,s,t=T} \; \forall \; n,s,t \tag{4.9}$$

where

$h_{n,s,t}$: discharging dispatch of storage
$\bar{h}_{n,s}$: nominal power of storage
$f_{n,s,t}$: charging dispatch of storage
$soc_{n,s,t}$: state of charge of storage
$r_{n,s}$: hours to fully charge an empty storage at nominal power
$\eta^{w_t}_{\text{stand};n,s}$: standing losses per hour
$\eta_{\text{store};n,s}$: charging efficiency
$\eta^{-1}_{\text{dispatch};n,s}$: discharging efficiency

Kirchhoff's current law

Most importantly the demand at each bus $d_{n,t}$ has to be met at all times. This constraint is part of the Kirchhoffs's current law displayed in Equation 4.10. Moreover, the equation states that each bus has to be balanced by the attached components' energy feeding in and out of it.

$$\sum_r g_{n,r,t} + \sum_s h_{n,s,t} - \sum_s f_{n,s,t} - \sum_b K_{n,b} f_{b,t} = d_{n,t} \; \forall \; n,t \tag{4.10}$$

where

$g_{n,r,t}$: feed-in of generator
$h_{n,s,t}$: discharging of storage
$f_{n,s,t}$: charging of storage
$f_{b,t}$: power flow of a branch component (line, link or transformer)
$K_{n,b}$: defines whether n is a starting ($K_{n,b} = 1$) or ending ($K_{n,b} = -1$) bus of the attached branch
$d_{n,t}$: inelastic demand

Passive and controllable branches

The power flows on the passive branches (i.e. AC lines and transformers) are determined by the linear network equations. The linearization of the non-linear network equation supplies a good approximation (Brown et al., 2016; Purchala et al., 2005; Stott et al., 2009) as long as the following preconditions apply.

- The voltage angle differences from one end of a line to the other are sufficiently small so that one can approximate $\sin \phi_b \cong \phi_b$.

- The resistances of the lines have to be considerably smaller than the reactances. Purchala et al. (2005) concluded that a minimal reactance-to-resistance ratio of four should apply. In the model used in this work (see also Section 4.3), the AC lines of the EHV level have a ratio of 7.65 whereas the HV lines have a ratio of 3.52. Consequently, the condition for the EHV level is met by far, in contrast the mean ratio in the HV level is slightly lower than the given threshold. Anyhow, Purchala et al. (2005) showed that the deviations are still acceptably low near the threshold.
- Reactive power flows decouple from active power flows.
- Voltage deviations are low.

Consequently, active power flows are calculated on the basis of line or transformer reactances and voltage angle differences as stated in Equation 4.11. This implies that neither reactive power demand and flows nor any grid losses are modeled. Moreover, the passive branches can be loaded at maximum at their optimized active power capacity (see Equation 4.12). Only the latter mentioned constraint applies for DC links which therefore are modeled as controllable branches.

$$f_{b,t} = \frac{\theta_{n,t} - \theta_{m,t}}{x_b} \;\forall\, b, t \tag{4.11}$$

$$|f_{b,t}| \leq F_b \;\forall\, b, t \tag{4.12}$$

where
$f_{b,t}$: branch power flow
$\theta_{n,t}$: voltage angle at the bus where the branch starts
$\theta_{m,t}$: voltage angle at the bus where the branch ends
x_b : branch reactance
F_b : branch optimized active power capacity

The expansion of branch capacities, hence the optimized F_b is restricted as stated in Equation 4.13. The lower bound $\tilde{F}_b \cdot \sigma_{n-1,b}$ of a link, line or transformer is equivalent to the capacity which is available in the *Status Quo* considering generalized (n-1)-security assumptions. All AC lines and transformers in the EHV level are assumed to be loaded at a maximum of 70 % of their nominal capacity (Wiese et al., 2014). Concerning fewer redundancy in the HV level (in average 1.9 parallel HV lines according to the Open Source German Transmission Grid Model (osmTGmod) model, cf. Section 4.3.1), a $\sigma_{n-1,b}$ of 50 % is chosen. For DC links, $\sigma_{n-1,b}$ is set to 1, assuming no additional (n-1)-security margins (50Hertz et al., 2020). This lower bound reflects the idea of not realizing any net decommissioning of existing capacities.

The upper bound of storage expansion is intended to be unrestricted in order to find cost-optimal solutions without biasing its determination. Nevertheless, the cross-border capacities can only be extended at a maximum of four times of today's capacity (Brown et al., 2018c). This reflects the planning of ENTSO-E (2016) for the year 2030 and represents a cautious assumption (which by Brown et al. (2018c) was labelled a *compromise*) in order to not overestimate the European interconnection, especially in the light of not modeling the entire European grid. In contrast, the upper bound of inner-German grid expansion is not defined relative to the status quo capacity. Instead, for each voltage-specific line corridor an absolute upper bound is specified. For the transmission level, according to the so far permitted largest expansion projects in the process of the NEP (e.g. in Amprion, 2011), four three-phase systems of an overhead line type of Al/St 550/70 with each four wires represent the maximal setting (in 50Hertz et al. (2015b), 4 systems are assumed as the upper limit for one pole). For the HV level, the same type and number of wires but only two systems are assumed (see also Agricola et al., 2012). The net grid expansion $F_b - (\tilde{F}_b \cdot \sigma_{n-1,b})$ does not include the (n-1)-security margin. Nevertheless, in order to consider additional investment costs for the (n-1)-security margin, the specific investment costs of potential line expansions (as defined in Table 4.2) are increased by $\sigma_{n-1,b}^{-1}$. Moreover, the (n-1)-security margins can be applied to the optimized capacity ex-post, avoiding an underestimation of grid expansion.

$$\tilde{F}_b \cdot \sigma_{n-1,b} \leq F_b \leq \hat{F}_b \; \forall \; b \tag{4.13}$$

where

$\tilde{F}_b$: *Status Quo* thermal limit active power capacity of branch
$\sigma_{n-1,b}$: (n-1)-security factor of branch
F_b : branch optimized active power capacity
$\hat{F}_b$: branch maximal thermal limit active power capacity

In case of passive branch expansion, the reactance usually decreases. For the sake of maintaining a linear problem, thus keeping computing time comparably low, the reactances are kept constant during optimization. Therefore, the x_b is adjusted afterwards performing several LOPF iteratively. As Hagspiel et al. (2014) showed that after five LOPF iterations the results have converged, which is underlined by modeling tests realized in context of this work, five iterations are performed. Assuming a shunt connection, the x_b changes from one iteration to the other inversely proportional to the change of F_b.

4.2 Non-linear power flow simulation

The optimal system design is defined by the LOPF formulation, as described in the previous section. In order to ensure that this optimal solution, which only has to comply with the linearly approximated power flow equations, is able to meet the non-linear power flow equations, a state-of-the-art PF (using the software PyPSA (see Brown et al., 2018b)) is applied ex-post.

The ex-post PF implies the need for additional model assumptions, which are summarized as follows. The control strategies for the buses are based on Rendel (2015). Thus, larger power plants with a nominal power of more than 50 MW are defined as PV generators. In contrast, smaller generators are considered to be PQ generators with a $\cos\phi = 1$. The slack bus is the bus with the highest annual generation attached to. All aggregated loads at the HV substation are assumed to have a power factor $\cos\phi$ of 0.95 (inductive) (Knorr et al., 2014) (see Section 4.3.3).

All other necessary parameters (e.g. the resistances of the grid components) are defined in the following Section 4.3. For a more detailed description consider reading Müller et al. (2019a,b); Brown et al. (2018b).

The ex-post check is successfully realized for all LOPF-based results presented in Chapter 5. Therefore, the linearization justification in Section 4.1.2 is plausible and can be confirmed. In this work, this ex-post check is only applied for testing validity. Consequently, the non-linear results will not be analyzed in Chapter 5.

Nevertheless, to get an impression of the non-linear behavior, for the *eGo 100* base scenario (LOPF-based results are presented in Section 5.1.2) exemplary PF results are briefly presented in Figure 4.1.

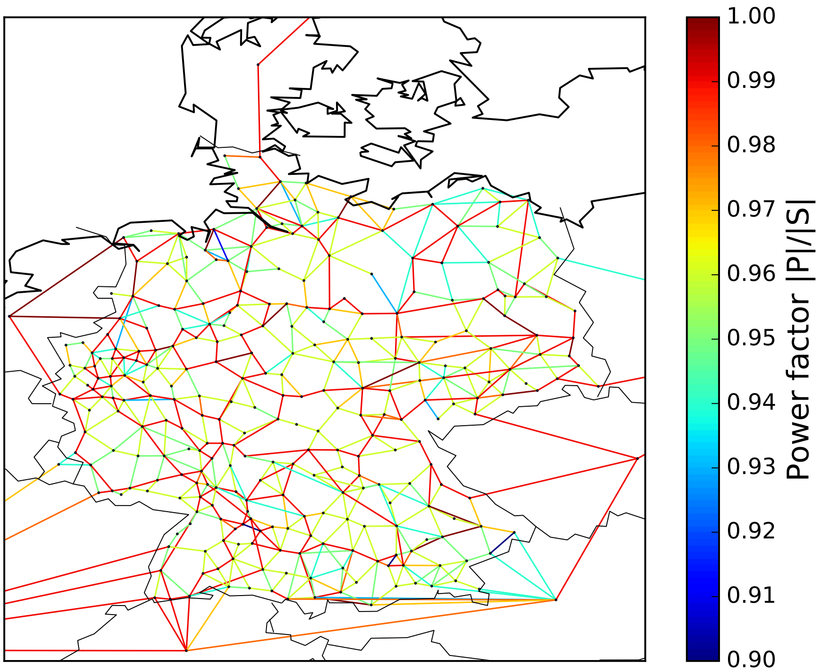

FIGURE 4.1: Annual mean power factor (active power divided by the apparent power) of each line for the *eGo 100* base scenario after performing an ex-post PF.

In this case, the Newton-Raphson algorithm of the PF converged in all snapshots after three or four iterations. Applying the PF the grid experiences reactive power demands, in this example driven by the behavior of the lines and loads. At the PV buses the reactive power is supplied rather locally mostly avoiding lossy reactive power flows and higher grid loadings. Figure 4.1 demonstrates that although significant amounts of reactive power have to be transported, the power lines are mainly used for active power flows. Throughout the year the majority (75 % of the lines) have a power factor of 0.96 or higher and more than 99% of the lines have a power factor above 0.93.

4.3 An open data model of the German transmission and distribution grid

An elementary base for the optimization is an open power grid model of the German EHV and HV level, which had to be developed in the context of this thesis. The model was described for the first time as a whole by Müller et al. (2018b). Prior to that the spatial allocation of generation and demand and the grid connection was described in Hülk et al. (2017). The investigations within the articles Müller et al. (2018a); Wienholt et al. (2018); Müller et al. (2019b) were based on the same grid model. Müller et al. (2019a) provided the most up-to-date and complete model description. Consequently, the following content of this section is directly based on Müller et al. (2018b) and Müller et al. (2019a). These sources being cited here are not explicitly referred to in the following course of this section.

In the first four sections, the general modeling approach of how to generate an open power grid system based on status quo or historical data is presented. The modeled grid, its electric parametrization, and the connected demand and generation are addressed in this context. Based on the *Status Quo* model, two scenarios for the mid- and long-term future are developed (*NEP 2035* and *eGo 100*). These are described in Section 4.3.5.

The implementation of the data creation code is realized within the *data processing* (Centre for Sustainable Energy Systems, DLR Institute for Networked Energy Systems, Reiner Lemoine Institut, 2018). The tool *osmTGmod*, which was forked in order to implement changes mainly considering the representation of the HV level (Wuppertal Institute and DLR Institute of Networked Energy Systems, 2018), provides the grid topology and its electric properties. Within the *preprocessing* of the *data processing*, various data inputs such as power plant lists are structured and initially manipulated. The data model used in this thesis is entirely based on the *data processing* version 0.4.6 (September 2019) including a few small bug fixes compared to the previous version 0.4.5 (August 2018), which was the result of an entire so-called clean-run of the script-based procedural tool, which is mainly coded in pgsql. The relevant tables of the resulting grid model are stored in the OpenEnergyPlatform (OEP) in the schema *grid* (IKS OvGU Mageburg, DLRVE Oldenburg, ZNES Flensburg and RLI Berlin, 2020). All relevant tables are labeled by the tag eTraGo and their content can be filtered by the relevant data version *v0.4.6*.

4.3.1 The grid topology based on OpenStreetMap

The knowledge of the grid topology is essential for the creation of a complete grid model suitable for power flow simulations. As described in Medjroubi et al. (2017), open data approaches are usually based on crowd-sourced OSM data. Accordingly, the open source tool *osmTGmod* is used for this purpose. This tool was originally developed and described by Scharf (2015) being supervised (in cooperation with the Wuppertal Institute) by the author of this thesis. *osmTGmod* uses deterministic as well as heuristic approaches. Most importantly this means that apart from OSM *relations*, *ways* are also considered.

Power lines are mapped as *ways*. *nodes* represent e.g. poles on a power line. In particular, *ways* are tagged with important information such as the number of cables and wires being used for the electric parametrization (see following Section 4.3.2). For instance the information tag *frequency* and *operator* are used to filter out the grid of the German railway system, which is not operated publicly and being one-phased at a frequency of $16\frac{2}{3}$ Hz. Consequently, it is exclusively focused on the public grid.

relations, if they are correctly mapped, provide very valuable information in the context of power flow analysis. They contain a logic combination of the more basic OSM data types *ways* and *nodes*. This more complex data type enables to supply information of the topology considering accurately the electric circuits. If for instance a multiple number of power lines (mapped as *ways*) meet at one pole (mapped as a *node*), *relations* can supply information about which lines are electrically connected and which are not.

Unfortunately, the coverage of relations decreases substantially in the HV level. Therefore it was very important to also consider *ways* which are not part of any *relation*. In this sense, *osmTGmod* supplies heuristics in order to abstract the most probable electric arrangement of the *ways*. Although *osmTGmod* was originally developed for the EHV level only, in order to get a higher coverage, this combined usage of *relations* and *ways* was implemented from the beginning (Medjroubi et al., 2017). This original approach enabled the adequate consideration of the HV level. For instance, applying the *SciGRID* model to the HV level resulted in a total power circuit length of 13,256 km, whereas the number provided by the German Federal Network Agency accounts for 96,658 km (Bundesnetzagentur and Bundeskartellamt, 2016). In contrast *osmTGmod* is able to model 70,742 km. Although being significantly higher, the coverage remains to be rather low comparing to a coverage of more than 95 % in the EHV level. In particular, underground cables are often not mapped and their existence increases in the HV level, especially in urban areas. Since grid expansion within urban areas is less important concerning this work's research questions, this effect can be partly neglected.

Nevertheless, the lower coverage with relations at the HV level and a generally lower data quality has to be addressed by including additional approaches for an automatic correction of minor mapping issues. The developed correction method ensures the connection of isolated HV-MV substations and subgrids to the main grid.

Whenever a subgrid or a single bus is isolated, it is connected to the nearest point on the main grid. A new power line is attached to an existing bus or power line. In the latter case, a new bus is introduced at this point and the existing line is divided into two. In case a subgrid is connected, the bus which is nearest to an existing grid element is chosen for connection. No additional connections of other buses of that subgrid are applied. This generalized process entails an increasing degree of interconnection and enlarges the number of power lines and buses.

Apart from the automatic correction method, some manual modifications are performed on a post processing level. In context of his thesis, Kähler (2018) added topological information mainly within the cities Stuttgart and Munich by utilizing grid maps of the local DSO. Moreover the EHV topology is manually fixed by comparing it to the ENTSO-E map (ENTSO-E, 2018b) in order to get one completely interconnected EHV grid without any subgrids.

Being relevant for a comprehensive connection of generation and demand, the buses are differentiated into substation buses and joints. Only at substation buses, transformer, demand and/or generation can be attached. Substation buses are the ones which lie within an osm substation polygon. Theses polygons are not longer used. Instead, all power lines which are connected within substation polygons are simply interconnected by one bus per voltage level. Furthermore transformers are created to interconnect these substation buses. All of these HV substation buses are assumed to have a connection to the MV level. Substations that are situated within a distance of 75 m from their boundary are aggregated in order to obtain more realistic MV grids (Hülk et al., 2017). This measure slightly decreases the number of substations.

The model of the German grid is extended by an abstraction of its electrical neighbors considering the interconnections with the European transmission grid. Each country being electrically directly connected with the German grid is considered as such an electrical neighbor. The cross-border lines are prolonged as abstract power lines to artificial buses being placed at the centroid of each country. For each nominal voltage of the cross-border lines a corresponding bus is defined. Consequently, transformers are installed interconnecting the voltage levels. Moreover, these foreign buses are interconnected according to ENTSO-E (2018b) using an abstraction produced by the tool *GridKit* (Wiegmans, 2016).

Applying an OSM data set from October 1st, 2016, the abstraction leads to a topology model with 11,305 buses and 19,695 branches. 4,197 of the buses display substation buses of which 3,617 belong to the HV and 580 to the EHV level. More key figures can be observed in Table 4.4. Spatially, the resulting grid topology is displayed in Figure 4.2.

Parameter	**Quantity**
Buses	11,305
thereof	
Substations	4,197
Joints	7,108
Branches	19,695
thereof	
Overhead lines	18,296
Underground cables	871
Transformers	526
DC links	2

TABLE 4.4: Key figures of the resulting topology model of the EHV and HV level.

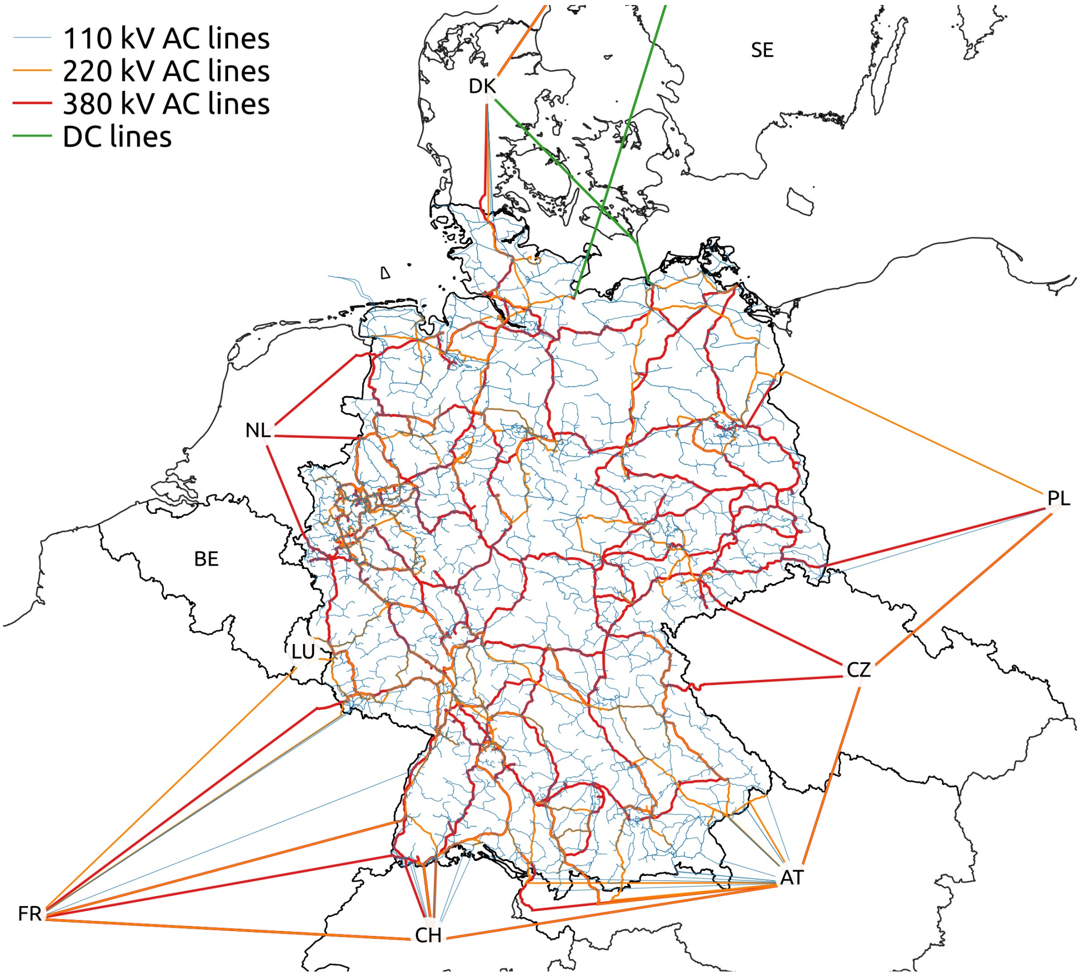

FIGURE 4.2: The status quo grid topology of the EHV and HV level including the electrical neighboring countries.

4.3.2 Electric parametrization of lines and transformers

OSM does not provide PF-ready information. Hence, the grid topology model has to be complemented by assumptions on the electric properties of the grid components. In particular, the lines and transformers need to be parameterized. The general approach is to utilize component specific OSM information in order to realize most adequate assumptions based on literature.

For each power line the OSM information of the voltage level V_{nom} (OSM-key *voltage*), the $type$ (OSM-key *power*, overhead line or underground cable), length l (implicitly derived from the geometry) and number of conductors $cables$ (OSM-key *cables*) are used (see also Scharf, 2015; Müller et al., 2016; Medjroubi et al., 2017). From literature, for each voltage level one standard overhead line and one underground cable is defined representing typically used assets in Germany (see Table 4.5). For these standard components the relevant parameters are the thermal limit apparent power S_{nom} , the resistance R', the capacitance C' and inductance L'. The last three parameters are length specific. All four parameters are given for one three-phase system. The number of systems (or circuits) n of a route between two grid buses (Index ℓ) is calculated by dividing the OSM-key *cables* by three (see Equation 4.14) assuming the exclusive existence of a three-phase AC system in the public grid of Germany and Europe (Schwab, 2012).:

$$n_\ell = \frac{cables_\ell}{3} \; \forall \; \ell \tag{4.14}$$

where

$\ell \in L$: line label

n_ℓ : amount of circuits of line

$cables_\ell$: amount of OSM *cables* of line

Consequently, the resistance R, the reactance X, the capacitance C and the thermal limit apparent power S_{nom} for each line ℓ are then calculated as stated in Equations 4.15 - 4.18 (see Medjroubi et al. (2017)). Mind that the angular frequency ($\omega = 2 \cdot \pi \cdot f$) corresponding to a grid frequency of $f = 50Hz$ has to be considered in Equation 4.16 and 4.17.

V_{nom} in kV	type	S_{nom} in MVA	R' in Ω/km	L' in mH/km	C' in nF/km
110	line	260	0.109	1.2	9.5
110	cable	280	0.0177	0.3	250
220	line	520	0.109	1	11
220	cable	550	0.0176	0.3	210
380	line	1790	0.028	0.8	14
380	cable	925	0.0175	0.3	180

TABLE 4.5: Electrical parameters of standard overhead lines and underground cables for the extra-high and high voltage level. Source: based on Brakelmann (2004)

$$R_\ell = \frac{l_\ell \cdot R'_{V_{nom,\ell},type_\ell}}{n_\ell} \;\forall\; \ell \tag{4.15}$$

$$X_\ell = \frac{l_\ell \cdot L'_{V_{nom,\ell},type_\ell} \cdot \omega}{n_\ell} \;\forall\; \ell \tag{4.16}$$

$$C_\ell = l_\ell \cdot C'_{V_{nom,\ell},type_\ell} \cdot \omega \cdot n_\ell \;\forall\; \ell \tag{4.17}$$

$$S_{nom,\ell} = S_{nom,V_{nom,\ell},type_\ell} \cdot n_\ell \;\forall\; \ell \tag{4.18}$$

where

R_ℓ	: line resistance
l_ℓ	: line length
$R'_{V_{nom,\ell},type_\ell}$	: length, voltage, and type specific resistance of a standard line
n_ℓ	: amount of circuits of line
X_ℓ	: line reactance
$L'_{V_{nom,\ell},type_\ell}$	: length, voltage, and type specific inductance of a standard line
ω	: angular frequency
C_ℓ	: line capacitance
$C'_{V_{nom,\ell},type_\ell}$	: voltage and type specific capacitance of a standard line
$S_{nom,\ell}$	: line thermal limit apparent power
$S_{nom,V_{nom,\ell},type_\ell}$	: voltage and type specific thermal limit apparent power of a standard line

Three representative transformers are defined in order to model all possible interconnections between the voltage levels (see Table 4.6). The transformer is not assumed to be the bottleneck in the power grid (Scharf, 2015). Therefore a transformer is dimensioned such that its nominal capacity equals at least the minimal sum of $S_{nom,\ell}$ of all power lines of the same nominal voltage, which are connected to it. The calculated nominal capacity defines the number of transformers installed with respect to the specific S_{nom} in Table 4.6. The impedance Z of each transformer τ which can be assumed to be equal to the reactance X (Flosdorff and Hilgarth, 2005) is calculated as defined in Equation 4.19. The utilized standard values for the relative short circuit voltage (v_{sc}) change with respect to the higher (V_a) and lower nominal voltage (V_b) side of the transformer (see Table 4.6).

S_{nom} in MVA	V_a in kV	V_b in kV	v_{sc} in %
1,000	380	220	13.5
300	380	110	14
200	220	110	12

TABLE 4.6: Electrical parameters of standard transformers within the extra-high and high voltage level. Source: based on Oeding and Oswald (2011)

$$Z_\tau = X_\tau = v_{sc,V_{a,\tau},V_{b,\tau}} \cdot \frac{V_{a,\tau}^2}{S_{nom,,V_{a,\tau},V_{b,\tau}}} \; \forall \; \tau \tag{4.19}$$

where

$\tau \in T$	: transformer label
Z_τ	: transformer impedance
X_τ	: transformer reactance
$v_{sc,V_{a,\tau},V_{b,\tau}}$	: relative short circuit voltage change of a standard transformer considering the higher and lower voltage side
$V_{a,\tau}$	: higher nominal voltage side of transformer
$S_{nom,,V_{a,\tau},V_{b,\tau}}$	: nominal capacity of a standard transformer considering the higher and lower voltage side

The cross-border lines are parameterized almost in the same way as the inner-German power lines. The OSM-specific information is taken from the cross-border line. The length is prolonged considering the topological approach as described in the previous section. In order to model the more restrictive market driven behavior, the nominal capacities are adjusted with respect to ACER/CEER (2016), assuming the NTC. The aggregated NTC are linearly distributed over all systems of one country-specific set of cross-border lines.

The DC cross-border lines to Sweden and Denmark are defined manually. The voltage level, capacity and length are taken from the manufacturer's data (ABB, 2018a,b). The efficiencies of the lines and the converters are defined according to Forschungsstelle für Energiewirtschaft e.V. (2014).

The interconnections between the foreign buses are parameterized by using the ENTSO-E (2018b) information about the number of systems per voltage level. Consequently, the electric parameters are derived as stated above.

4.3.3 Demand

The primary goal in a power system is to meet the electricity demand. Hence, the modeling of the spatial allocation, the grid connection and the temporal behavior is essential for power grid modeling.

Spatial allocation and grid connection

The requirement for the spatial resolution is defined by the resolution of the grid topology. The aim is to obtain a realistic demand at all substation buses. The lowest grid level considered is represented by the HV-MV substations. Therefore the minimal resolution is characterized by the size of the MV grids. Due to the lack of such detailed data the available sectoral specific electricity consumption data on the level of the federal states (Länderarbeitskreis Energiebilanzen, 2015) is further distributed to smaller geographical entities, which meet the mentioned minimal requirements.

Information about the spatial distribution of population (Statistisches Bundesamt (Destatis), 2016) (resolution 1 ha), the gross value added (Statistisches Bundesamt, 2016) (sectoral on NUTS-3 level) and the OSM-based industrial and retail area (OpenStreetMap, 2017) is used for a spatial allocation of the electricity demand. According to the sectors *residential*, *retail*, *industrial* and *agricultural* the distribution methods vary. Once the demand of the different sectors is distributed in a sufficient resolution (which even meets the spatial resolution requirement to create synthetic MV grids (see also Amme et al., 2018)) it is connected to the substations. First, it is defined to which voltage level each load shall be connected. Industrial large scale consumers (OSM-based industrial load areas, which exceed an annual consumption of 130 GWh/a (derived from Table 4.7)) are directly assigned to the nearest HV substation via Voronoi cells (a well-known method used in several publications, e.g. van Leeuwen et al. (2014); Singh et al. (2014)). All other distributed loads are assigned to their HV-MV substation using catchment areas, so called MV grid districts, which model the areas of MV grids. In short, MV grid districts are created by a combined usage of nearest neighboring municipality areas (Bundesamt für Kartographie und Geodäsie, 2016) and Voronoi cells.

The resulting annual demand per HV-MV substation can be observed in Figure 4.6. Hence, a share of the overall annual German electricity consumption of 501 TWh (based on Länderarbeitskreis Energiebilanzen, 2015) is assigned to each of these grid buses being represented by corresponding grid districts.

A more in-depth description of the allocation and connection procedure and a further analysis and discussion of the resulting model was accomplished in Hülk et al. (2017).

Due to the high level of aggregation, the demand of the foreign countries can be directly taken from ENTSO-E (2015) (The first version of the Open Power System Data (OPSD) time series data set (Muehlenpfordt, 2016), which reproduces the ENTSO-E data, is used.) without applying any distribution method.

Temporal resolution

The one-hourly behavior of the demand at each bus over an entire year corresponds to the desired resolution. In a bottom-up approach standard load profiles (SLP) (EWE Netz, 2013) are used to convert the annual sector specific and nodal demand accordingly. SLP of the German Association of Energy and Water Industries (BDEW) generally describe the temporal demand behavior of German consumers for the sectors *residential*, *retail* and *agricultural* in a resolution of 15-minutes over the year (Meier et al., 1999). These representative profiles are based on measurements of 332 residential, 617 retail and 260 agricultural entities and are valid as a cumulative load for a number of customers with similar characteristics (Meier et al., 1999). In Germany theses profiles are commonly used especially by grid operators to estimate the temporal behavior of customers which are not measured in such a high resolution. According to Willis and Scott (2000, p. 49), already the cumulative demand curve of 100 households "looks smooth and 'well-behaved.'". Therefore, it can be assumed that aggregates at the HV buses are significantly large enough for statistic generalization. In addition to these three standard profiles, a stairs function for the industry sector developed by Schachler (2014) is used. In Figure 4.3 all four sector specific profiles are displayed. The load profiles apply for the year 2011 (being coherent with the choice of the weather year, see Section 4.3.4). The quarter hourly normalized time series have to be aggregated to hourly ones.

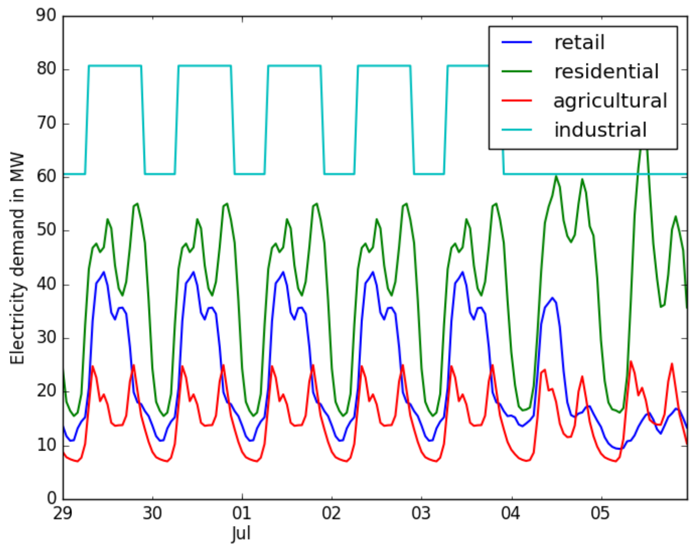

FIGURE 4.3: BDEW SLP and the industrial profile for one exemplary week aggregated for one HV-MV substation, based on oemof developer group (2016) i.e. EWE Netz (2013) and Schachler (2014)

Consequently, the aggregated demand P_{demand} at each bus n and at each hour t (out of $T = 8760\,h$) is calculated according to Equation 4.20 where $P_{SLP,q,t}$ is the normalized SLP output per sector q and hour t and $C_{n,q}$ the sector specific annual consumption at each bus. The python package *oemof-demandlib* (oemof developer group, 2016) is used for implementation. The package provides the four mentioned standard profiles and the described methods to scale the data.

$$P_{demand,n,t} = \sum_{q} P_{SLP,q,t} \cdot C_{n,q} \ \forall \ n, t \tag{4.20}$$

where

$P_{demand,n,t}$: aggregated demand per bus and hour
$P_{SLP,q,t}$: hourly and sectoral SLP output
$C_{n,q}$: sector and bus specific annual consumption

A power factor $\cos \phi$ of 0.95 (inductive) for aggregated loads at the HV substation is assumed (Knorr et al., 2014) to model the reactive power demand as a function of the P_{demand} from Equation 4.20.

Overall, the above mentioned 501 TWh annual consumption for Germany is temporarily dissolved resulting in an aggregated peak load of 78 GW (cf. Figure 4.5). The aggregated temporal behavior is similar to the ENTSO-E vertical load of the same year (ENTSO-E, 2015). The similarity of the load patterns can be observed in Figure 4.4 for the 43rd week of the year 2011. Besides the similarity, the bottom-up SLP-based approach creates a more extreme curve. The peaks are higher and the troughs are lower. This characteristic can be observed throughout the entire year as Figure 4.5 underlines.

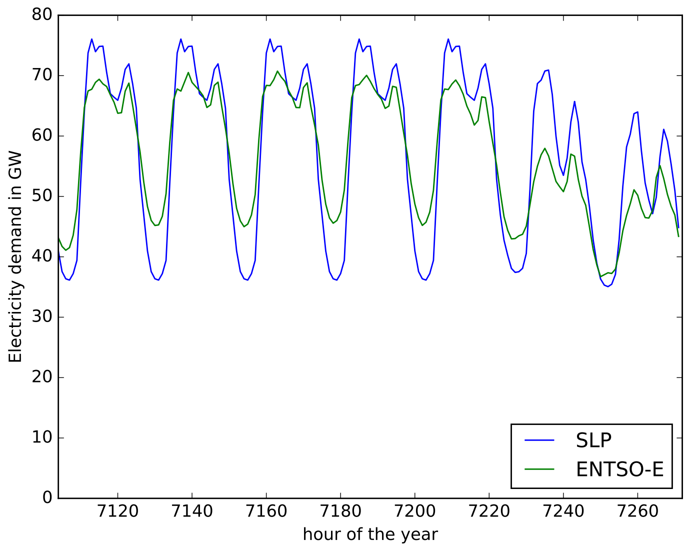

FIGURE 4.4: Comparison of the SLP-based demand profile aggregated for Germany and the ENTSO-E vertical load (ENTSO-E, 2015) for the 43rd week of 2011

A more extreme demand curve may induce higher line loads. Consequently, in particular grid expansion needs are expected to be rather overestimated. Thus, the utilized demand curve can be considered a quite cautious estimate. Gotzens et al. (2020) compared the aggregated demand curve of their bottom-up SLP based approach with the ENTSO-E demand curve and determined the same tendency to higher peaks and lower troughs. In contrast to the findings in Gotzens et al. (2020), in which the times of overestimation and underestimation are rather evenly divided, Figure 4.5 depicts, that the overestimation occurs two thirds of the time throughout the year.

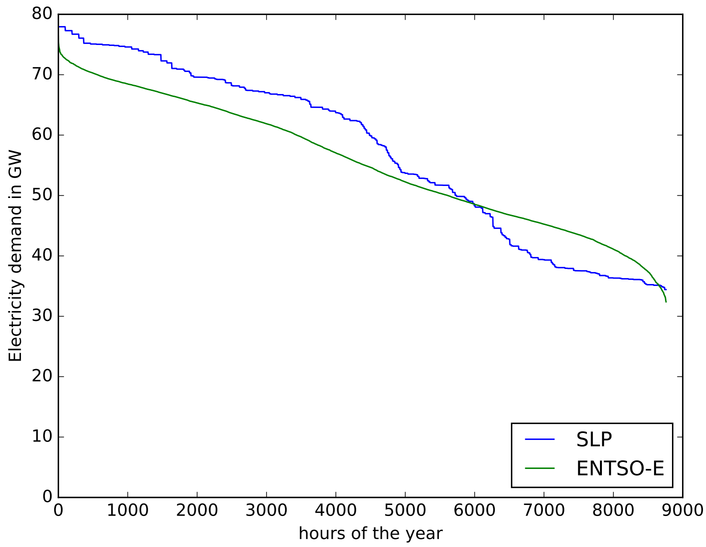

FIGURE 4.5: Annual duration curve for the SLP-based demand curve aggregated for Germany as well as for the ENTSO-E vertical load (ENTSO-E, 2015) for the year 2011

The tendency for overestimation corresponds to the fact that the total annual consumption of 501 TWh lies 3 % above the total consumption of the ENTSO-E demand. Both approaches do not cover the entire electrical demand. On the one hand, the ENTSO-E demand curve only has a so-called *representativity factor* of 91 % for Germany. Hence, 9 % of the total German electricity load is not represented by the data. Unfortunately, the drivers for this low ratio are not clearly documented by ENTSO-E Data Expert Group (2016). Moreover, Schumacher and Hirth (2015) concluded that the *representativity factor* is not an appropriate scaling factor. On the other hand, in the context of this work, the demand of the railway system (about 12 TWh per year (Knörr et al., 2016)) is excluded.

4.3.4 Generation

In order to meet the demand, generation facilities which generate electricity, have to be modeled. In the next two subsections the spatial allocation, grid connection and temporal modeling of power plants including storage units is described.

Spatial allocation

Information about power plants including their geographic position is much easier to obtain than spatially detailed information about the demand. Two different registries, one for the conventional power plants (Gerbaulet and Kunz, 2016) containing large, mainly fossil power plants (also storage units) with nominal capacities above 10 MW and one for renewable power plants (Bunke, 2016) are used. The used registers include all power plants being listed until the end of 2015. All entries are georeferenced. Concerning the conventional power plants, postal addresses are utilized to geolocate every single plant. Regarding the renewable power plants, the minimal accuracy is defined by the post code area. This level of spatial detail is assumed to be acceptable with respect to the nodal resolution of the HV grid.

For the connection of the power plants to the grid buses the general approach is similar to the connection of the demand (cf. Section 4.3.3) and was also described in Hülk et al. (2017). The power plants are first filtered by the voltage level they belong to. Mostly this information is provided by the mentioned registries. Data gaps are filled by applying the classification of Table 4.7. Consequently, the generators are attached to their grid bus by using the MV grid districts (cf. Section 4.3.3) or by a simple voronoi partition of the EHV substations. An exception are offshore wind parks which are manually connected to realistic EHV buses, based on (50Hertz et al., 2015c; Bundesamt für Seeschifffahrt und Hydrographie, 2017b,a). The resulting distribution of generators connected to the HV buses can be observed in Figure 4.6; those assigned to the EHV buses in Figure 4.7. In order to reduce complexity without losing relevant information all generators are aggregated considering their connected bus and their generation type (e.g. solar, onshore wind).

grid level connection	**nominal capacity in MW**
EHV	> 120
HV	17.5 - 120
$\leq$HV-MV	< 17.5

TABLE 4.7: Grid level connection of power plants considering their nominal capacities based on Konstantin (2009) and Agricola et al. (2012).

For the neighboring countries the aggregated capacities are based on ENTSO-E (2014) considering the year 2015. The capacities per generation type are directly connected to the corresponding foreign buses without any need for a complex connection method. The total installed *Status Quo* capacities per technology for Germany and the entire grid model can be observed in Table 4.9. Thus, for Germany the share of RE in terms of installed capacities is at 47% for the *Status Quo* scenario.

Temporal resolution

According to the temporal resolution of the demand, the generation necessarily is dispatched one-hourly over the period of a year. This dispatch is optimized in the LOPF. The marginal costs of the generators substantially impact the resulting feed-in (see Section 4.1). In contrast to the endogenous dispatch, the potential feed-in of

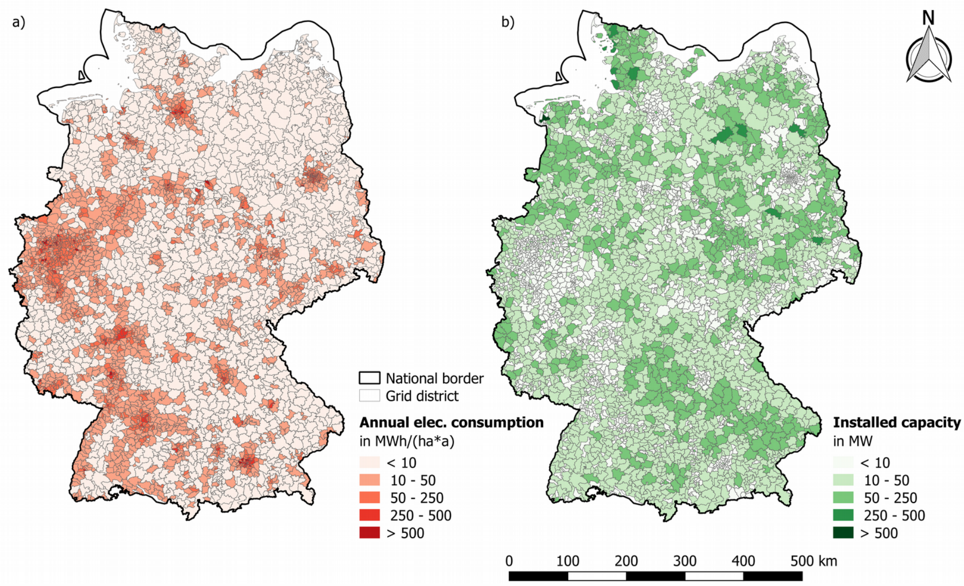

FIGURE 4.6: Demand (a)) and installed generation capacity (b)) per MV grid district (resp. HV-MV-substation) in the status quo scenario (Hülk et al., 2017)

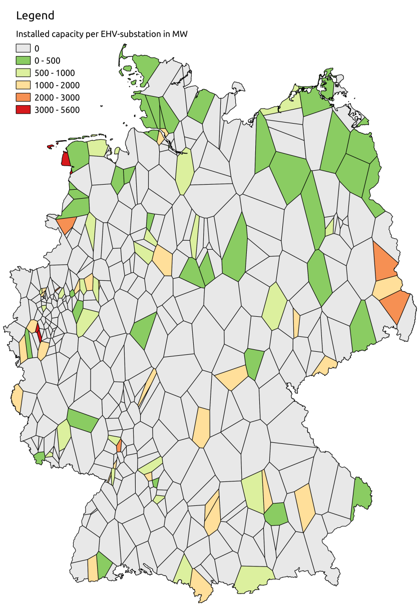

FIGURE 4.7: Installed generation capacity per EHV catchment area resp. grid bus (Hülk et al., 2017).

each power plant at each hour of the year is an exogenic constraint, which shall be described in this section.

All conventional and renewable power plants (except reservoir, run-of-river, wind and solar) can be dispatched freely up until their individual nominal capacity. In case of reservoir and run-of-river power plants, the resource availability is restricted by a simple approach as realized and discussed in Wingenbach (2018). Hence, the annual full load hours of the reservoir power plants are defined as a country-specific upper bound with respect to the simulation results in e-Highway 2050 project (2015b). All run-of-river power plants can only be dispatched up to 65% of their nominal power ratings at all times. In contrast, a more sophisticated approach to model resource scarcity applies for solar and wind power plants assuming certain weather conditions.

The *oemof feedin-lib* (Krien and oemof developing group, 2016) in combination with the *CoastDat-2* (Geyer and Rockel, 2013) weather data is used to generate normalized potential feed-in time series per *CoastDat-2* weather cell. The weather cells with a horizontal grid size of 0.22° in rotated coordinates (Geyer, 2014) measure approximately 22 km at each edge. For the generators of the neighboring countries, the weather data of the raster at the corresponding grid bus is used. From the reanalysis data, most importantly, wind speed time series, corresponding surface roughness length and solar irradiation are used. The chosen weather year is 2011 (in coherence with the demand data) because it has been used in 50Hertz et al. (2015b) being described by average wind characteristics (50Hertz et al., 2015a).

Moreover, generic reference power plants are used to generate the normalized potential feed-in time series. The solar reference module is the *Yingli YL210 2008 E*, which is assumed to have an azimuth of 180° and a slope of 30°. The offshore reference power plant is a *SIEMENS SWT 3.6 120* with a rotor diameter of 120 m, a nominal power of 3.6 MW and a hub height of 90 m. This type is assumed to be very representative having a substantial global market share of 60 % in the year 2016 (Fraunhofer IEE, 2018), which was even higher in Germany. In case of onshore wind power plants, seven different representative types and power classes are defined (Schlemminger, 2018). These power plants are the most commonly used ones of their power class with respect to information in the registry of Bunke (2016). According to the nominal power one of the seven representative power plants respectively its power curve is chosen to calculate the normalized potential feed-in.

The resulting potential feed-in time series of fluctuating RE are then compared to historic average full load hours (Wirth, 2018; Schlemminger, 2018). Consequently, a well-known overestimation of the potential feed-in when using the *CoastDat-2* weather data is revealed. Besides the weather data, the assumptions on the performance of the power plant technology are crucial in this context. The comparison to historic data does not reflect any possible future technological improvements which are especially interesting in the light of future scenarios (as described in Section 4.3.5). Therefore the full load hours of 50Hertz et al. (2015b) (considering the same weather year) are utilized for further validation. In case of wind power production, the higher full load hours of 50Hertz et al. (2015b) for Germany are used. Consequently, based on the comparison to historic and literature data (50Hertz et al., 2015b) correction factors (see Table 4.8) are developed, which linearly downscale the potential feed-in meeting the annual potential energy production for Germany. The same correction factor is assumed for the other countries. The general procedure was already applied by others such as Wiese et al. (2014); Wingenbach (2018).

Technology	**correction factor**	**full load hours**	
		Germany	overall
Wind Onshore	0.75	2006	1773
Wind Offshore	0.95	4377	4680
Solar	0.8	968	988

TABLE 4.8: Correction factor and full load hours of the potential feed-in of fluctuating RE for the future scenarios

4.3.5 Future scenarios

Based on the *Status Quo* model, two future scenarios are created, which are most relevant for addressing the research questions. The mid-term future is represented by the *NEP 2035* scenario, which models the electricity system for the year 2035. The basis of this scenario is the official NEP (50Hertz et al., 2015b). Besides enabling a perspective for the year 2035, by choosing this well-known study, results can be compared and critically discussed in a very specific way. The long-term future is exogenously set by the *eGo 100* scenario which is mainly based on e-Highway 2050 project (2015b). Here, Germany is modeled as a 100% RE system. In both scenarios demand, weather year and grid are the same as in the *Status Quo* scenario. Concerning the demand, according to 50Hertz et al. (2015b), the effect of additional loads due to innovative applications is compensated by higher efficiencies. Furthermore, since the grid is subject to optimization, by default no grid expansion is exogenously defined. Thus, the *Status Quo* grid serves as an existing, exogenous base for optional future grid investment. In the following, the two future scenarios are described in more detail.

NEP 2035

This scenario sketches an electricity system for the year 2035. The goal is to reproduce one of the official NEP scenarios (50Hertz et al., 2015b). The *B2-2035* scenario, which is the most progressive (in context of the energy transition) scenario for the year 2035, is chosen. A high share of RE (74 % of installed generation) and natural gas (17 %) for Germany outline this scenario. Instead of a standard 10 years, a 20 years perspective of the year 2035 is given. An explicit open data reproduction is not possible due to the fact that not all methods and data are open and accessible. In particular, the grid model, the spatial distribution respectively the grid connection as well as temporal characteristics of generation and demand are not identical.

The conventional power plants are modeled by using a NEP specific register (50Hertz et al., 2014). The entries of individual power plants have to be explicitly georeferenced based on the given information. In case of RE (except offshore wind parks) only aggregated capacities per federal states are accessible. These are then spatially allocated proportional to the status quo distribution. Consequently, the individual and aggregated power plants are connected to the *Status Quo* grid using the same method as described in the previous Section 4.3.4. As well as in the *Status Quo* scenario, future offshore wind parks are connected manually to the grid according to 50Hertz et al. (2015c). In case, wind parks are planned to be connected to substations, which do not exist in the *Status Quo* grid, they are allocated to its nearest existing neighbor considering only the EHV level.

Consistently to 50Hertz et al. (2015b), the planned conventional and RE capacities of the neighboring countries are defined according to ENTSO-E (2014). Here the *Vision 3* is used considering the long-term goals of the European Union (EU) (50Hertz et al., 2015b). The resulting overall installed capacities for Germany and the entire model can be observed in Table 4.9.

In contrast to the official NEP *B2-2035* scenario, the planned pumped storage units are disregarded. This assumption originates from the same unbiased approach applied for grid expansion. Hence, storage expansion shall be endogenously optimized and therefore no exogenous increase is assumed. In particular, this means that instead of 12.7 GW only 9.3 GW are exogenously defined (cf. Table 4.10). The disregarded capacity increase, assumed by 50Hertz et al. (2015b), yet rather small can be assessed to be quite ambitious as e.g. Gimeno-Gutierrez and Lacal-Arantegui (2013) merely model realistic additional pumped storage potentials in Germany. However, in the model, batteries are assumed to have the same power-to-energy ratio as pumped storage units, thus they can supply the same short-term flexibility. Consequently, if this kind of flexibility is needed, batteries can be installed anyhwere in the system although potentially with different investment costs. Finally, in an ex-post analysis it can be investigated if projected batteries could be substituted by pumped storage units.

Instead, for the neighboring countries the planned pumped storage units are considered assuming a given development which cannot be influenced in the optimization.

As stated before, in line with the optimization approach, the NEP planned grid expansion measures are not taken into account. Nevertheless, for validation and sensitivity analysis these officially suggested future measures are considered. In particular for the sensitivity analysis, the planned projects which convert Belgium and Norway into a electric neighbors can be modeled based on 50Hertz et al. (2015b). Consequently, the demand and generation characteristics of these two countries are included.

eGo 100

The e-Highway 2050 project (2015b) defines a mostly renewable scenario for the year 2050. This scenario represents the base for the *eGo 100* scenario. The goal is to create a 100% RE scenario. Therefore, the planned gas fired power plants for Germany of 13 GW are disregarded (Wingenbach, 2018; Bunke et al., 2017). Instead, in the neighboring countries, the planned gas fired power plants are considered. Hence, for the overall system, the RE share in terms of installed capacities is 97%. The installed capacities per technology are displayed in Table 4.9.

Technology	**Installed capacities** in GW					
	Status Quo		**NEP 2035**		**eGo 100**	
	DE	total	DE	total	DE	total
Nuclear energy	12.0	92.5	0.0	57.5	0.0	0.0
Lignite	21.2	46.0	9.1	25.7	0.0	0.0
Hard coal	27.8	62.3	11.0	27.3	0.0	0.0
Natural gas	27.5	59.4	40.7	96.2	0.0	28.5
Oil	4.4	15.8	0.8	5.6	0.0	0.0
Waste	1.7	8.0	1.6	1.6	0.0	0.0
Other conventional	2.5	2.5	1.0	1.0	0.0	0.0
Total conventional	**97.1**	**286.5**	**64.2**	**214.9**	**0.0**	**28.5**
Wind onshore	41.3	66.1	88.9	153.6	98.9	382.1
Wind offshore	3.4	5.0	18.5	44.9	27.0	71.5
Solar	38.5	48.3	60.1	113.8	98.5	300.1
Biomass	7.2	15.2	8.3	36.0	27.8	93.3
Hydro	5.3	69.7	5.8	70.7	3.2	84.5
Total RE	**95.7**	**204.3**	**181.6**	**419.0**	**255.4**	**931.5**
Total	**192.8**	**490.8**	**245.8**	**633.9**	**255.4**	**960.0**

TABLE 4.9: Installed generation capacities for Germany (DE) and the entire model region per scenario and technology/fuel (Bunke et al., 2017).

In contrast to the *NEP 2035* scenario, the future generation capacities are available for Germany as a whole. Nevertheless, the spatial allocation procedure is then the same assuming a linear future development proportional to today's spatial distribution.

In e-Highway 2050 project (2015b) substantial pumped storage expansion is assumed for some of the neighboring countries (especially France, Austria and Poland) whereas for Germany no expansion is expected. Following the same approach as in the other future scenario, initially no storage expansion is defined for Germany. For the neighboring countries, additional battery and hydrogen storage units are considered such that the planned figures utilized in Wingenbach (2018) serve as an upper bound restriction for the optimization. In contrast, presuming economic feasibility, pumped storage capacities (as in e-Highway 2050 project, 2015b) are directly exogenously defined. (cf. Table 4.10).

Technology	**Installed capacities** in GW					
	Status Quo		**NEP 2035**		**eGo 100**	
	DE	total	DE	total	DE	total
pumped storage	9.3	19.7	9.3	33.9	9.3	51.4
battery storage	0.0	0.0	0.0	0.0	0.0	16.7[1]
hydrogen storage	0.0	0.0	0.0	0.0	0.0	39.7[1]
Total	**9.3**	**19.7**	**9.3**	**33.9**	**9.3**	**107.8**

TABLE 4.10: Exogenous installed storage capacities for Germany (DE) and the entire model region per scenario and technology, based on (Bunke et al., 2017). [1] planned capacities serve as upper bound in the optimization.

4.4 Complexity reduction

The combination of the high spatial and temporal resolution of the developed model leads to very complex LOPF problems when co-optimizing dispatch, grid and storage expansion. This implies such high needs for computing performance, which is not feasible with state-of-the-art computing technology. Staying with the already very time-efficient LOPF approach, the data model's complexity has to be reduced. In the following, the utilized spatial and temporal reduction methods are explained.

4.4.1 Spatial resolution

K-means clustering

The particular k-means clustering method used is adapted from Hörsch and Brown (2017). The underlying k-means algorithm is state of the art and widely used. The Python package for machine learning *scikit learn* (cf. Pedregosa et al. (2011)) supplies a relevant function, which minimizes the weighted squared euclidean distances of k centroid to its clustered members iteratively. The iterative *expectation–maximization* (E–M) algorithm initially guesses random k clusters centroids, then all candidates are assigned to the nearest k clusters centroids (E-step). In a subsequent M-step the k cluster centroids are actually situated to the centroid of each cluster of member candidates. These E and M steps are repeated until convergence (VanderPlas, 2016). This iterative process is exemplarily visualized in Figure 4.8).

The *Status Quo* grid was originally built for supplying demand by conventional generation. Therefore, the original buses are proportionally weighted according to the *Status Quo* conventional generation capacities and demand connected. Consequently, candidate buses with high weighting tend to be located near their original location. Moreover, regions with higher demand and/or conventional generation densities are represented by more buses than less relevant areas. The *Status Quo* bus weighting is used for all three scenarios. Any possible k value up until the total number of original buses with a bus weighting greater than 0 can be chosen. The challenge is to chose a k value, which on the one hand leads to a good approximation

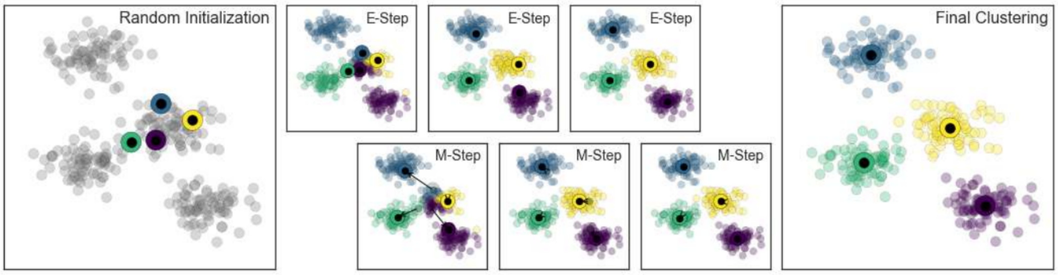

FIGURE 4.8: Exemplary visualization of the E–M algorithm for k-means clustering (VanderPlas, 2016).

with a sufficient degree of spatial detail and on the other hand reduces the problem size significantly in order to reach feasible computing times. After numerous testing runs, a setting with $k = 300$ is chosen as a good trade-off solution.

The results of the algorithm are not reproducible due to the initial random guess. In contrast, the entire method after the initial guess is reproducible. Hence, in order to compare the results of several optimization runs, the initial guess is reused. Consequently, for the same k cluster and scenario setting the same abstracted grid model can be used. Moreover, the robustness of the clustering algorithm is enhanced by using a parametrization far beyond standard values. An amount of initial guesses of 2500, a 1000 of iterations per initial guess and a convergence tolerance of 10^{-20} lead to rather robust results (Müller et al., 2019a).

Before clustering, the entire system has to be modeled homogeneously at a nominal voltage of 380 kV. Therefore, the 220 and 110 kV buses and branches are substituted by 380 kV ones. As stated in Equation 4.21 the reactances and resistances are increased based on their original nominal voltage ($v_{nom,b}$, in kV). As a result, all transformers are modeled as lines.

$$r, x_{b,380} = r, x_b \cdot \left(\frac{380}{v_{nom,b}} \right)^2 \quad \forall\, b \tag{4.21}$$

where

$r, x_{b,380}$: 380 kV equivalent resistance and reactance of branch
r, x_b : original resistance and reactance of branch
$v_{nom,b}$: original nominal voltage (in kV) of branch

For further simplification, after the E-M algorithm converges all lines between two clusters are abstracted as one. According to Kirchhoff's voltage law the admittances and nominal capacities of the original lines are added up. The reduced grid topology is visualized in Figure 4.9.

FIGURE 4.9: The abstract grid topology with 300 buses and 701 aggregated lines (and two DC links) after applying k-means clustering. For better geographic orientation, an osm map is plotted in the background. In addition, important buses (especially relevant for some explanation in Section 5) are marked. a and d represent the north-sea wind offshore feed-in buses Dörpen West and Büttel. The other marker are defined as follows. b: Niebüll, c: Husum, e: Flensburg, f: Rendsburg, g: Neubrandenburg, h: Stuttgart

Furthermore, components (i.e. generators and storage units) of the same carrier type and in the same cluster are aggregated. The normalized maximal possible power outputs of the weather-dependent resources (i.e. wind and solar) which depend on the spatially differing weather conditions, are aggregated considering their weights corresponding to the nominal capacities. The aggregation of storage units, additionally uses the power-to-energy ratio for differentiation.

EHV clustering

The EHV-clustering is a straight-forward approach in order to neglect the HV level and exclusively focus on the EHV level considering all demand and generation in a more aggregated way. All components (e.g. generator, demand) connected to 110 kV buses are assigned to the nearest EHV bus considering the HV topology by using a Dijkstra algorithm. For aggregation of the generators and storage units, the same rules as in the above described k-means clustering are applied. Therefore, the carrier type and power-to-energy ratio distinctions are kept as in the original model.

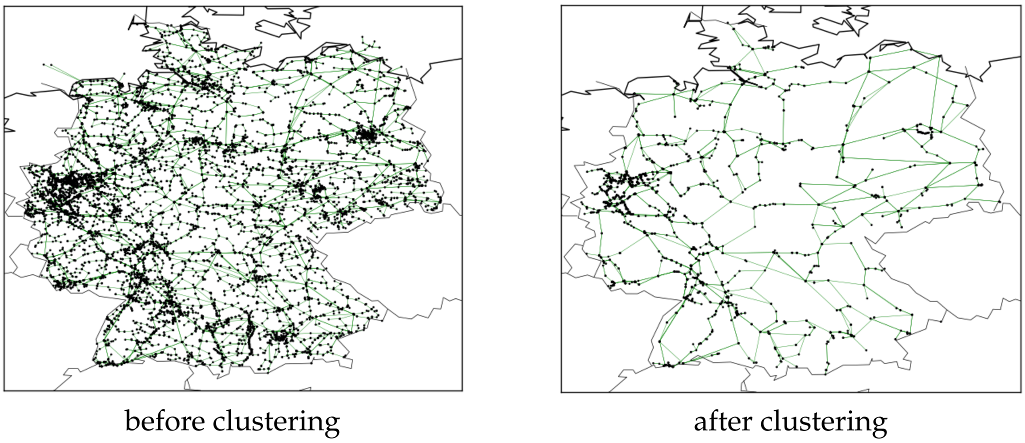

FIGURE 4.10: German grid model before and after EHV clustering.

4.4.2 Temporal resolution

The modeling of storage units implies a strong necessity for considering intertemporal dependencies. Hence, many state-of-the-art clustering methods cannot be used adequately. In contrast, a very simple approach to periodically leave out snapshots applied by Hörsch and Brown (2017) shows considerably good performance and approximization results. In the base setting, only every fifth hour is calculated reducing the computing time immensely. Consequently, every snapshot calculated represents a period of five hours leading to a snapshot weighting $w_t = 5$ (as defined in Equation 4.1). The possible full load hours of the fluctuating RE, as shown in Table 4.8 as well as the annual demand, only change marginally by less than 0.2 %.

Chapter 5

Results

In the following, first, the results for the future scenarios *NEP 2035* and *eGo 100* considering the base assumptions (as defined in the previous section) are described. After having focused on the base scenarios, a detailed sensitivity analysis, concentrating on the *eGo 100* scenario, is presented (starting with Section 5.2). The motivation and methodic approach for each sensitivity is explained shortly at the beginning of each section. Mostly, the sensitivities are designed by changing a certain parameter of the model while all other assumptions remain the same (ceteris paribus). In particular cases, variations are combined.

The analysis of the optimization results clearly focuses on the endogenous variables, thus endogenous system costs induced by investments into grid and storage expansion as well as generation dispatch (see the description of the optimization problem in Section 4.1.1). In order to derive results for the entire system including the exogenous costs for generation and pumped storage investments, systematic levelized costs of electricity (LCOE) (as defined in Ueckerdt et al., 2013) is evaluated as well. Generator investment costs and their expected lifetimes are taken from Schröder et al. (2013). The assumptions for pumped storage are defined as in Wingenbach (2018). The annual system costs are normalized by the annual demand.

The spatial allocation of grid and storage expansion is of high significance. The clipping of the corresponding figures changes according to the results. Hence, for better visualization, distant country buses like Sweden, Poland and France are only displayed if necessary e.g. if storage units are projected. At times, the results are spatially analyzed by mentioning certain cities in Germany. In Figure 4.9 (Chapter 4) all mentioned locations are visualized. For the sake of better visualization, in this section the figures displaying spatial allocations do not include any detailed political background map.

5.1 Base scenarios

5.1.1 NEP 2035

In this scenario system LCOE of 56.9 EUR/MWh are reached (see Table 5.1). The share of exogenous costs i.e. the generation and pump storage investment costs play a predominant role for the system costs. Only 13% of the system LCOE (7.1

EUR/MWh) are endogenously derived. The biggest part of these endogenous costs is spent for the dispatch of power plants. Furthermore, focusing on the endogenous variables of grid and storage expansion, it can be observed that in this scenario of the mid-term future significant investment into grid infrastructure represents the most important expansion measure. In contrast, storage expansion measures play a rather minor role in the overall model. The total overnight investment costs for the different regional scopes are displayed in Table 5.1. Grid investment costs of 8.9 bn. EUR represent roughly six times higher costs than the ones for storage expansion. Nevertheless, when observing the results only for Germany, the investment costs for storage expansion (1.5 bn. EUR) are even slightly higher than the ones for the inner-German grid expansion. All the investment into storage expansion is allocated at one single bus in the northeast of Berlin near to the northern interconnector to Poland as a long-term hydrogen storage of 1.6 GW nominal power. The exact regional allocation can be observed in Figure 5.1.

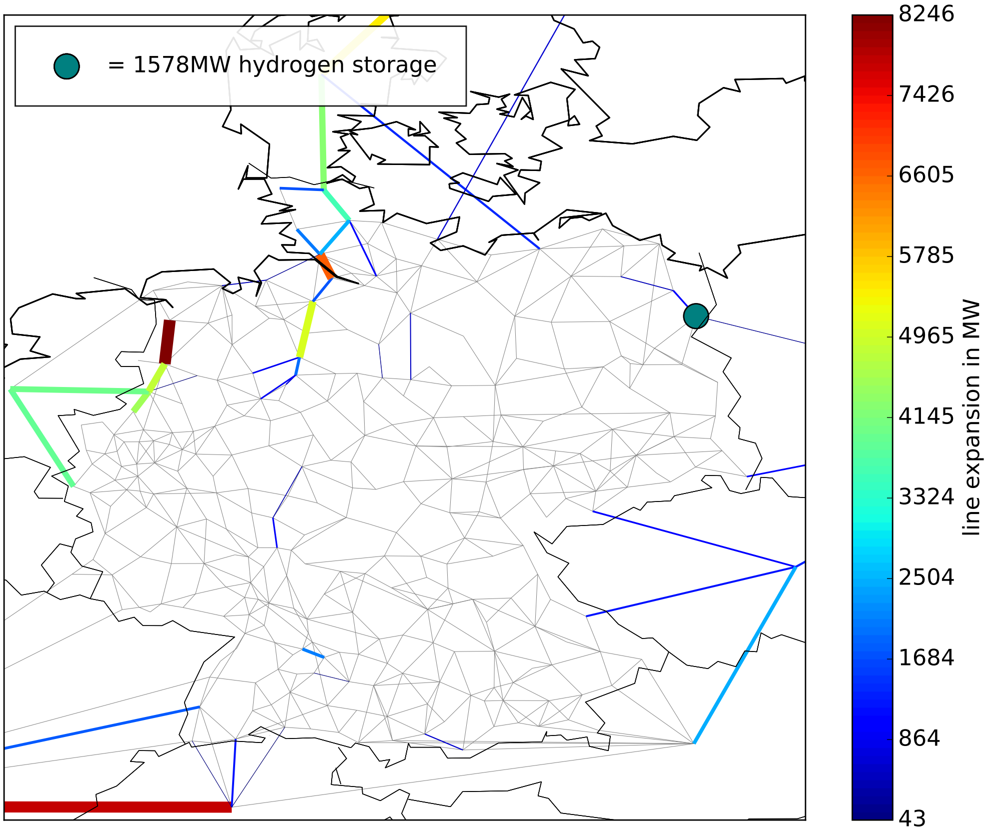

FIGURE 5.1: Spatial allocation of grid and storage expansion in the scenario *NEP 2035*.

This storage unit supplies flexibility primarily for the load centres in Berlin being charged by surplus wind on- and offshore generation being produced in Northern Germany and Denmark. The storage reduces on the one hand the flexible dispatch from conventional power plants and on the other hand the curtailment of the wind energy production. The storage bus is well connected to Berlin (380 kV), to Poland

(220 kV) and towards Rostock. In times of high wind production, high power flows coming from Denmark, Schleswig-Holstein and Mecklenburg-West Pomerania head towards Poland and then further south leading to loop flows towards Southern Germany. During these times the interconnetors from Denmark to Mecklenburg-West Pomerania (DC), from Mecklenburg-West Pomerania to Poland, and further from Poland to the Czech Republic, and finally to Switzerland and France via Austria are used to a very high extent. Therefore, these interconnetors are extended as much as possible, i.e. four times their original capacities (see Figure 5.1 and 5.2). At this time of RE overproduction the storage unit is charged. In contrast, in times of low northern wind energy production, the storage unit supplies power towards Berlin, which is accompanied by substantial imports from Poland where comparably low marginal priced conventional power plants (e.g. lignite) are dispatched.

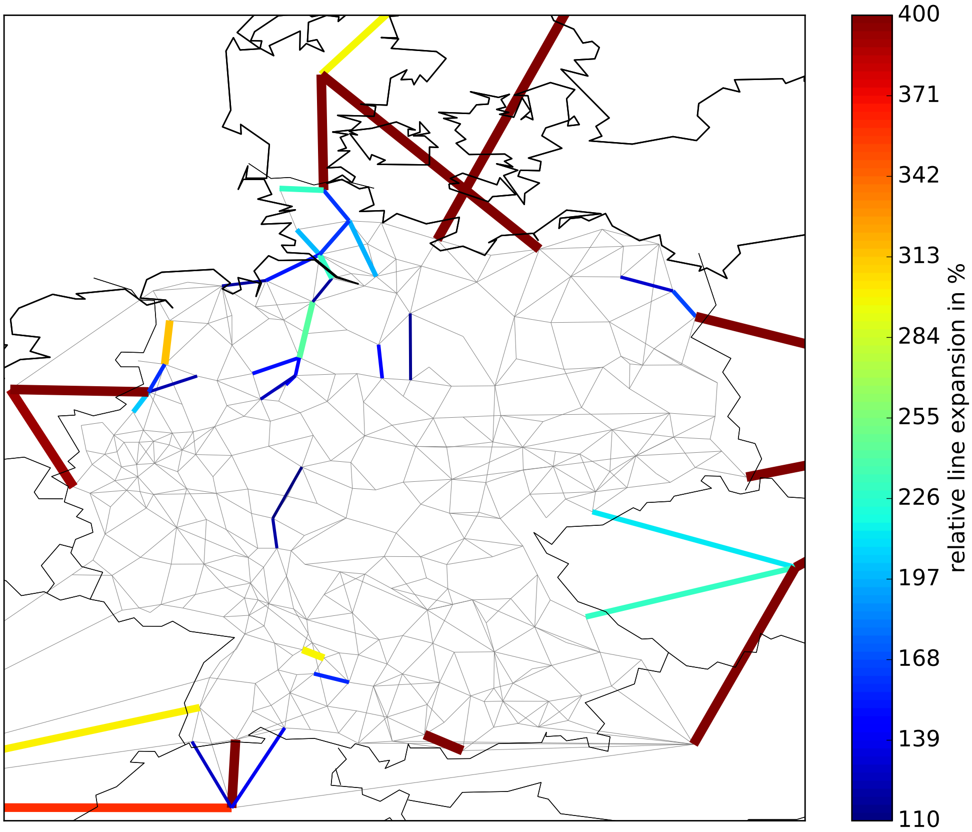

FIGURE 5.2: Expanded line capacities compared to the Status Quo capacities in the scenario *NEP 2035*.

Furthermore, the high feed-in of northern on- and particularly offshore wind power leads to substantial grid expansion mainly on two north-to-south routes in the northwest of Germany. The more eastern expansion route comes from Denmark and leads to Bielefeld in North Rhine-Westphalia. The cross-border capacity from Denmark is fully expanded leading to an expansion of 4.3 GVA (including generalized (n-1)-security margins). Due to more wind power feed-in coming from the west coast of Schleswig-Holstein, which is connected to the 380 kV main route by more than twice the status quo capacity, the further connection to Rendsburg, although less expanded, has a higher final capacity (see Figure 5.3). As the northern part of the offshore wind production from the North sea feeds into this route in Büttel at the river Elbe, the line crossing the river has to be expanded by 6.7 GVA, representing the highest expansion on this route. The following route segment is expanded a lot less due to a much higher original capacity. After that, energy can be used for the load centres in Bremen, which lower the need for further line expansion southwards. Yet, the expansion is higher because the original capacity is lower. Once getting to North Rhine-Westphalia, grid expansion is not needed since the existing capacities are sufficient for reaching substantial load centres in North Rhine-Westphalia and more southern regions. Another bottle-neck occurs then towards the city of Frankfurt. Here, the grid has to be expanded, although to a comparably low extent.

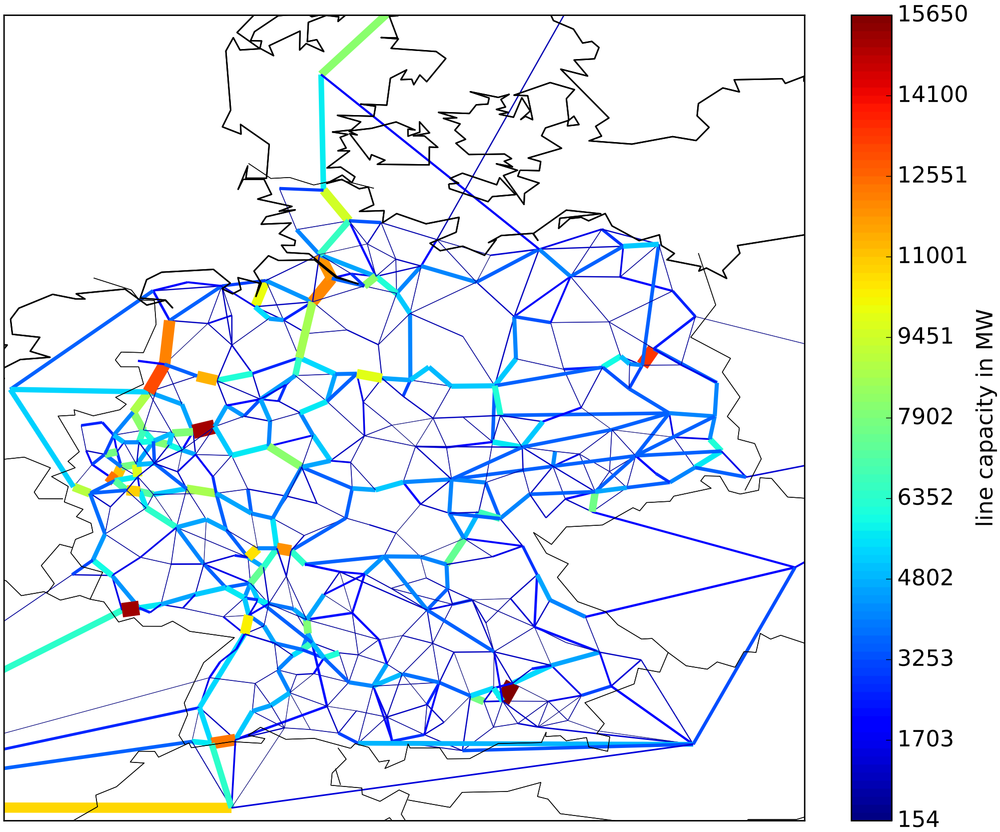

FIGURE 5.3: Final grid capacities in the scenario *NEP 2035*.

The other very important expansion route starts near the border to the Netherlands at the offshore feed-in bus Dörpen West. From this bus on southwards, an absolute expansion of 8.3 GVA is economically feasible. This value is the highest compared to all other expansion measures reaching the line's upper expansion limit. On this route southwards, less expansion is needed due to higher original capacities and additional connections to the south and especially to the Netherlands. This interconnector (the central one out of the three) to the Netherlands is heavily used for exports and loop flows to the south of Germany via the southern interconnector between the Netherlands and Germany. Similarly to the other main expansion route, this one transports primarily German offshore wind power to the load centres of North Rhine-Westphalia. Another similarity is that further southwards no grid expansion is needed to bring the remaining wind power to the more southern load centers.

Besides a few exceptions like the grid expansion at the west coast of Schleswig-Holstein driven by onshore wind feed-in, no distributed grid expansion is needed. Distributed power sources such as solar power plants in Southern Germany do not trigger local grid or storage expansion. Instead, the main driver for grid expansion is a massive offshore wind power production feeding in at few buses in the north. Additionally, the usage of the existing conventional power plants, which are located rather near to consumption and being well connected to the grid, lower the need for grid and storage expansion. Moreover, the grid and storage expansion needs are reduced by curtailment of available RE energy being to some extent economically feasible. Thus, the production of solar electricity is curtailed by less then 0.9 % whereas 4.6 % of the available onshore wind and 7.7 % of available offshore wind production is not dispatched throughout the year. Yet, the RE share on the German energy production, including 12.6 % imports, adds up to 64 %. Furthermore, loop flow behavior impede inner-German grid expansion especially between Northeastern and Southeastern Germany.

5.1.2 eGo 100

The realization of a 100 % RE scenario implies higher grid and storage investment costs compared to the *NEP 2035* scenario. Whereas grid investment costs have to be increased rather slightly, by 15 %, almost five times higher storage investment costs are economically feasible (see Table 5.1). Although the investment costs rise, due to a substantial decrease of the annual dispatch costs, the endogenous part of the systematic LCOE slightly decreases to a value of 6.9 Euro/MWh. The 924 million EUR/a fewer dispatch costs outnumber the 492 million EUR/a higher combined grid and storage investment annuity. The systematic LCOE, including the exogenous costs, decrease to a value of 55.6 Euro/MWh.

The majority of the additional grid expansion is invested into the German grid infrastructure. In Germany, 64 % more grid expansion leads to an overnight investment of 2.3 bn. EUR. In contrast, the cross-border and foreign interconnections do not increase substantially. Most of these interconnectors are already expanded four times their original capacity in the *NEP 2035* scenario leaving not much further expansion potential. The biggest difference here displays the interconnection between Austria and Switzerland which in the *eGo 100* scenario is fully expanded (see Figure 5.4). Due to the fact that the two scenarios are completely independent from each other, some of the expansion measures are even lower than in the *NEP 2035* scenario (e.g. the interconnetor from Denmark to Sweden). Nevertheless, the vast majority of

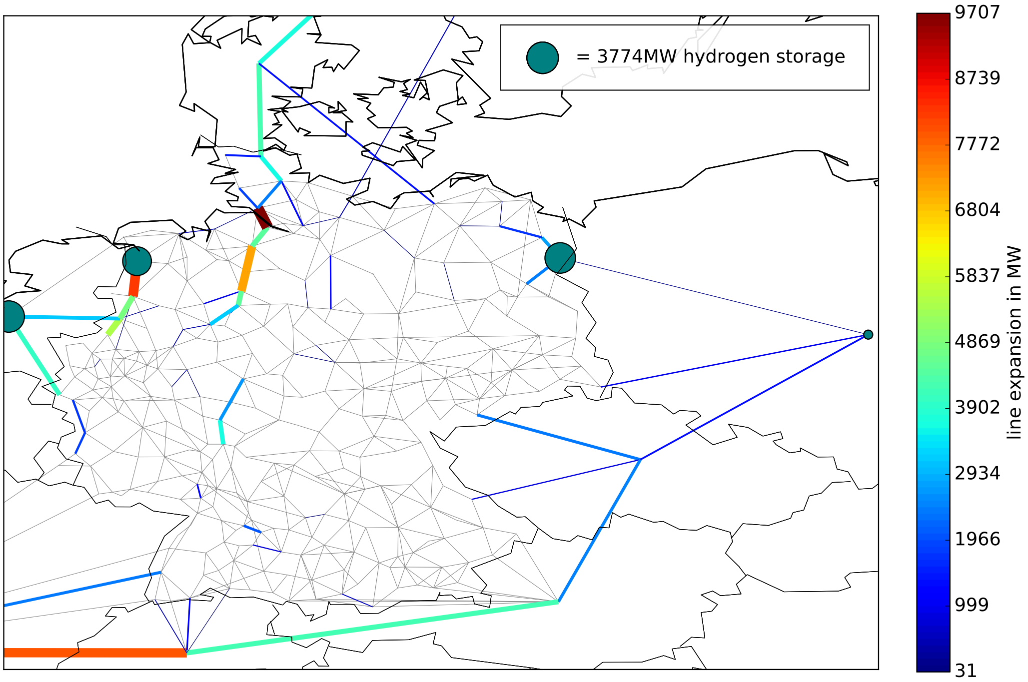

FIGURE 5.4: Spatial allocation of grid and storage expansion for the scenario *eGo 100*.

the expansion measures are consistent between the two scenarios. In simple terms, all lines which are expanded in the *NEP 2035* scenario are also expanded in the *eGo 100* scenario, however often to a higher extent.

The degree of expansion from Denmark towards Hamburg and Büttel remains the same leading to substantial curtailment of wind power in Denmark. The upper limit of grid expansion on the cross-border interconnector is already reached in the *NEP 2035* scenario impeding potential usage of the curtailed Danish wind power. Furthermore, a storage unit in this region is not feasible either. From the offshore feed-in bus Büttel southwards, the route is expanded significantly more. A crucial bottle-neck becomes a line near Bremen, which is now expanded 2.7 GVA more and is with 14.7 GVA at its maximum absolute capacity. This expansion most importantly enables a transportation of offshore wind power from Büttel southwards. Nevertheless, potential offshore wind (grid connection in Büttel) and onshore (at the west coast of Schleswig-Holstein) wind feed-in is curtailed significantly. This effect can be reduced if the upper limit of grid expansion would be loosened (see Section 5.2.2).

Due to higher wind power capacities in Sweden and the absence of coal fired power plants in Hamburg the power lines between the DC cable connection to Sweden (near Lübeck) and Hamburg are expanded. Although the DC line to Sweden is already expanded completely in the *NEP 2035* scenario its usage rate has risen leading to 12.8 % higher energy imports from Sweden.

The expansion route near the Dutch border cannot be expanded to a higher extent since the upper limit of the most northern segment is already reached in the

Parameter	Unit	Regional Scope	Scenario NEP 2035	eGo 100
Overnight Grid Investment	bn. EUR	Overall	9.6	11.0
		GER	1.4	2.3
		Crossb.	2.7	2.9
Overnight Battery Investment	million EUR	Overall	0	1.4
		GER	0	1.4
Overnight Hydrogen Storage Investment	bn. EUR	Overall	1.5	7.3
		GER	1.5	4.5
Annual Dispatch Costs	bn. EUR/a	Overall	10.5	9.6
		GER	3.3	2.4
Endogenous system LCOE	EUR/MWh	Overall	7.1	6.9
System LCOE	EUR/MWh	Overall	56.9	55.6

TABLE 5.1: Key cost parameters for the scenarios *NEP 2035* and *eGo100*

NEP 2035 scenario. Instead, in order to utilize more offshore wind power, a hydrogen storage unit with a nominal capacity of 3.2 GW is installed at Dörpen West. A slightly different situation occurs at the Dutch bus at which a hydrogen storage unit of 3.8 GW is built. This storage is also utilized to be charged in times of wind power overproduction and discharged in times of low wind power feed-in. In contrast to the situation at Dörpen West, the storage, when discharging, directly supplies the Dutch load decreasing the need for biomass power production.

The higher wind and less conventional energy production increases also the need for grid expansion in the Northeast. Especially the route from Rostock to the Polish border is expanded significantly more. Higher amounts of northern wind energy can be transported eastwards which is also reflected by higher usage rates of the DC interconnector from Denmark to Mecklenburg-West Pomerania. A storage unit of 3.6 GW is projected at the same bus where, in the *NEP 2035* scenario, a smaller one is feasible. The operational charateristics are very similar but scaled in the sense that more excess wind power can or has to be utilized and expensive conventional power is replaced. Thus, especially Berlin as a major load centre is even more fed by the storage unit in times of low fluctuating RE production. Consequently, the power line towards Berlin needs to be expanded due to higher necessary power flows.

The consistency of the grid and storage expansion measures between the two base scenarios is clearly detectable. This underlines that the expansion measures are mainly driven by wind power production, coming from on- and offshore. Similar to the *NEP 2035* scenario, distributed and northeast-to-southeast expansion can not be observed. Flexible power production from biogas power plants gain crucial significance. The overall installed biomass capacity rises by a factor of 2.6 (in Germany even 3.4) which partly compensates the missing conventional power generation and enables distributed power generation in times of low fluctuating RE generation. As a balancing power generation, the full load hours are with 3227 h rather low compared to the normal status quo operation strategy. Nevertheless, the availability of widespread biogas power plants reduces the need for flexibility supplied by additional storage units (see sensitivity analysis in Section 5.4.3).

5.2 The relevance of grid related assumptions

5.2.1 European interconnection

Restrictions on possible cross-border interconnections

As explained in Section 5.1 the cross-border interconnectors are highly extended, in many cases reaching the maximal possible value of four times the original capacity. Therefore, a sensitivity analysis on the restricting upper bound of cross-border grid expansion is performed. In Figure 5.9 the annual endogenous system costs for different sensitivity scenarios are displayed. The acronyms refer to the upper bound of possible cross-border (*cb*) capacities which are specified by numeric suffixes indicating by how many times the status quo capacities can be extended. Hence, the variants range from entirely disregarding cross-border capacities (*cb-0*) to completely unrestricting the upper bounds (*cb-inf*).

The increasing possibility for European interconnection is utilized in order to lower the dispatch costs. Consequently, the total endogenous system costs can be lowered. The higher cross-border capacities lead to higher imports, especially from Denmark, the Netherlands and Sweden to Germany. These cross-border investments imply also higher grid expansion in Germany but to a lower extent. In systems with low cross-border capacities, storage expansion becomes more important.

Compared to the base scenario (*cb-4*) in a system with unlimited possible European interconnection (*cb-inf*), grid expansion rises by 343 %. Complementary, dispatch costs are lowered by 32 % reducing the endogenous costs by 16 %. In absolute terms, this cost reduction translates into a 1.1 EUR/MWh lower LCOE. Including the exogenous system costs, the relative reduction compared to the 55.6 EUR/MWh in the base scenario is only 2 %. In contrast, in a system with today's interconnector capacities (*cb-1*) endogenous system costs increase by 12 % (0.8 EUR/MWh). Hence, almost twice as much storage expansion only partly compensate the missing cross-border capacities.

The spatial allocation of grid and storage expansion is generally consistent. In terms of storage, the storage at the Polish border as well as the one near the Dutch border is projected in all scenarios. The main grid expansion routes are also the same in all scenarios. As mentioned, the degree of expansion is different. In the most extreme case (see Figure 5.5), the northern cross-border line to Poland is expanded by 136 times its status quo capacity. In absolute terms, the highest expansion with 25 GVA is projected on the interconnector between Poland and the Czech Republic. Moreover, with low cross-border capacities, additional battery storage units are feasible at certain interconnectors to Poland, Austria and the Netherlands in order to increase the usage rates of the cross-border lines. In contrast, towards higher interconnection, starting with the *cb-6* sensitivity, storage units at the west coast of Schleswig-Holstein become economically feasible. In Figure 5.5 this effect can be observed in the case of the *cb-inf* scenario with no restrictions on the maximum cross-border grid expansion. Here, at the three west coast buses (Niebüll, Husum, Büttel) together 1.4 GW of hydrogen storage are installed. The increasing import from Denmark leads to the fact that the power lines southwards reach their maximal possible degree of expansion. Therefore these storage units in Schleswig-Holstein enable a higher usage of local wind production.

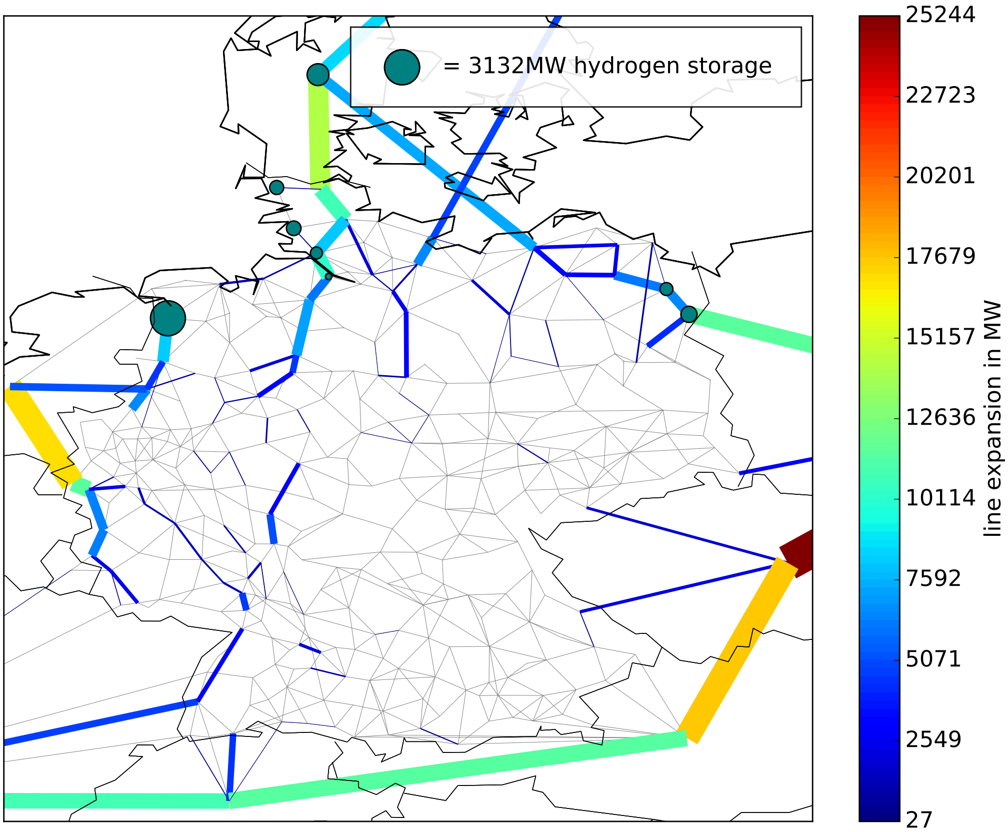

FIGURE 5.5: Spatial allocation of grid and storage expansion with perfect European interconnection (*cb-inf*).

A very unrealistic and extreme scenario is the *cb-0* variant. In this case, Germany does not use any cross-border capacities and has to supply the national demand at all times anywhere completely self-sufficiently. The endogenous system costs for Germany rise by 78 %, which is mainly induced by 5.8 times higher storage expansion costs. These costs are generated by an installation of 32.5 GW of hydrogen and 7.9 GW of battery storage. On the other hand, grid expansion decreases by 30 %. The spatial allocation of these expansion measures is displayed in Figure 5.6.

The biggest grid and storage expansion appear at the route from the offshore wind feed-in near the Dutch border southwards. Here, grid expansion reaches the

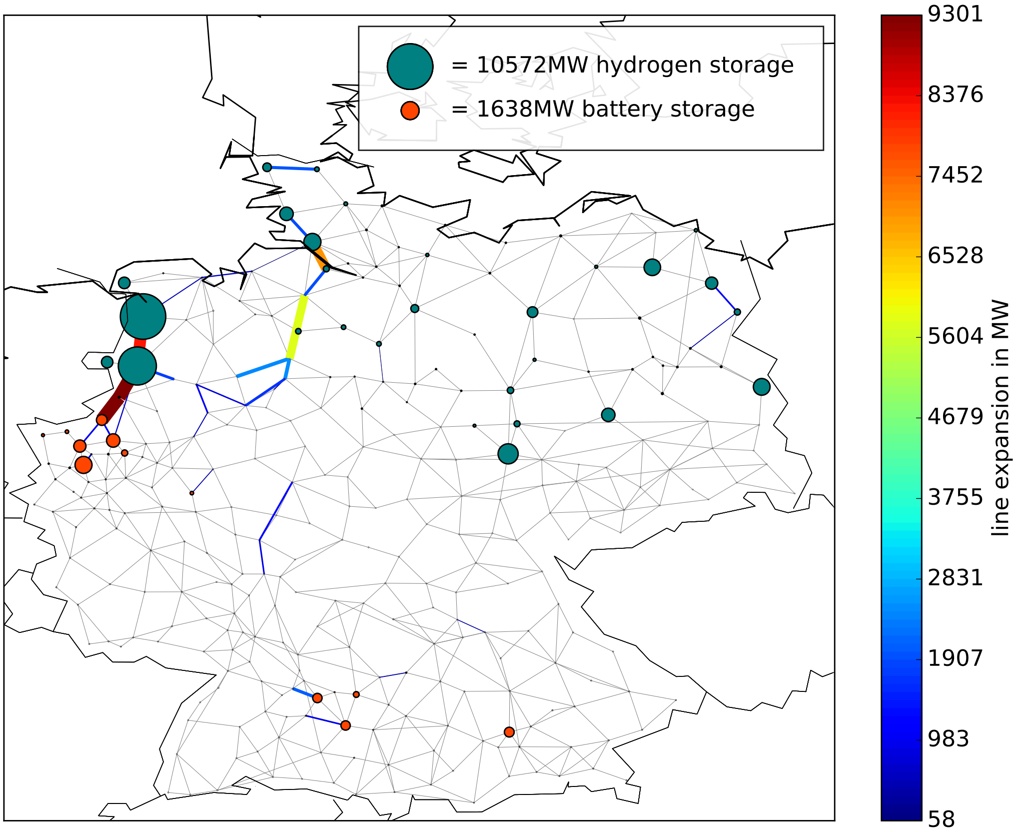

FIGURE 5.6: Spatial allocation of grid and storage expansion for autarkic Germany (*cb-0*).

upper bound of maximal expansion. Complementary, hydrogen storage capacities of 18 GW, subdivided into two big storage units on this route, exploit offshore wind generation to a high extent reaching 4086 full load hours. Nevertheless, offshore wind curtailment at this grid connection is the highest throughout the system, which has rather low curtailment rates. Despite the low curtailment of variable power sources, the biomass power plants reach full load hours of 4763 supplying 24 % of the total generation, providing a substantial amount of flexible power generation. Apart from the mentioned big storage units, the majority of the distributed storage units are not installed due to grid bottlenecks. Hence, more grid expansion cannot supply the same flexibility in this comparably small autarkic German system. Grid expansion remains to be induced mainly by the German offshore wind generation leading to the same major expansion routes as in the interconnected base case. Most prominently, less grid expansion occurs in Schleswig-Holstein from Flensburg to Hamburg and in the northeast of Germany. The absence of imports of mostly wind power generation from Denmark and Sweden leads to this effect. Instead, storage units supply energy in times of overall positive residual load. At the west coast of Schleswig-Holstein and in the northeast of Germany many distributed hydrogen storage units are economically feasible. Battery storage units are mainly feasible in the Ruhr area, near Stuttgart and near Munich. These storage units show a high amount of charging cycles supplying short-term flexibility.

The influence of cross-border and foreign reactances: A DC approach

The sensitivity analysis from the previous section shows that the modeling of the neighboring countries and their grid interconnection has an important impact on the optimization results on the German and European level. The physical behavior of the grid may lead to loop and transit flows, which do not necessarily correspond to the economic optimum i.e. the most cost-efficient use of power dispatch. Thus, the issue of loop and transit flows in Europe, in the light of energy transition, has been highly discussed (e.g. von Schemde et al., 2013). Consequently, countries like Poland, the Czech Republic and the Netherlands use phase shifting transformers at the cross-border interconnectors to Germany in order to control the power flows on these lines (Schlachtberger et al., 2017). In this section, it is presented how the results change when all cross-border interconnectors are modeled as DC lines, being controllable elements, which do not have to obey the passive power flow constraints as described in Equation 4.12.

The modeling change leads to a slight reduction of endogenous system costs of 4 % (see Figure 5.9, scenario *cb-dc* compared to base scenario *cb-4*). Storage expansion costs are halved whereas overall grid expansion increased by 19 % achieving a 3 % less expensive dispatch.

The regional characteristics of the grid and storage expansion can be observed in Figure 5.7. Compared to the base scenario results, a few striking differences shall be highlighted. First, the inner-German grid expansion, especially in the east of Germany, becomes an effective measure. The power lines connecting Thüringen and Sachsen with Bavaria are expanded. One can observe an additional expansion route from Mecklenburg-West Pomerania until the north of Bavaria. In total, 67 % higher investment into new grid infrastructure in Germany becomes economically feasible. In contrast, being another important difference, investments into foreign cross-border capacities are reduced by 70 %. Especially, the interconnection between France, Switzerland, Austria and the Czech Republic are not expanded at all. At last, the substantial storage unit at the Polish border is not needed any more. Apparently, the power flows, now controllable, between the mentioned countries are economically not optimal. Instead, a higher share of power flows via Germany from north to south while loop and transit flows are reduced. Consequently, a potential storage unit at the Polish border cannot benefit from high flows to Poland in times of high wind production.

Concerning the dispatch, RE curtailment in Germany is slightly reduced. In contrast, in Denmark more wind power production is curtailed due to less imports from Denmark to Germany. This also leads to less grid expansion in northern Schleswig-Holstein. In general, the net imports are significantly lower reaching only 1.7 % instead of 12.5 % in the base scenario. The largest trade balance difference is that

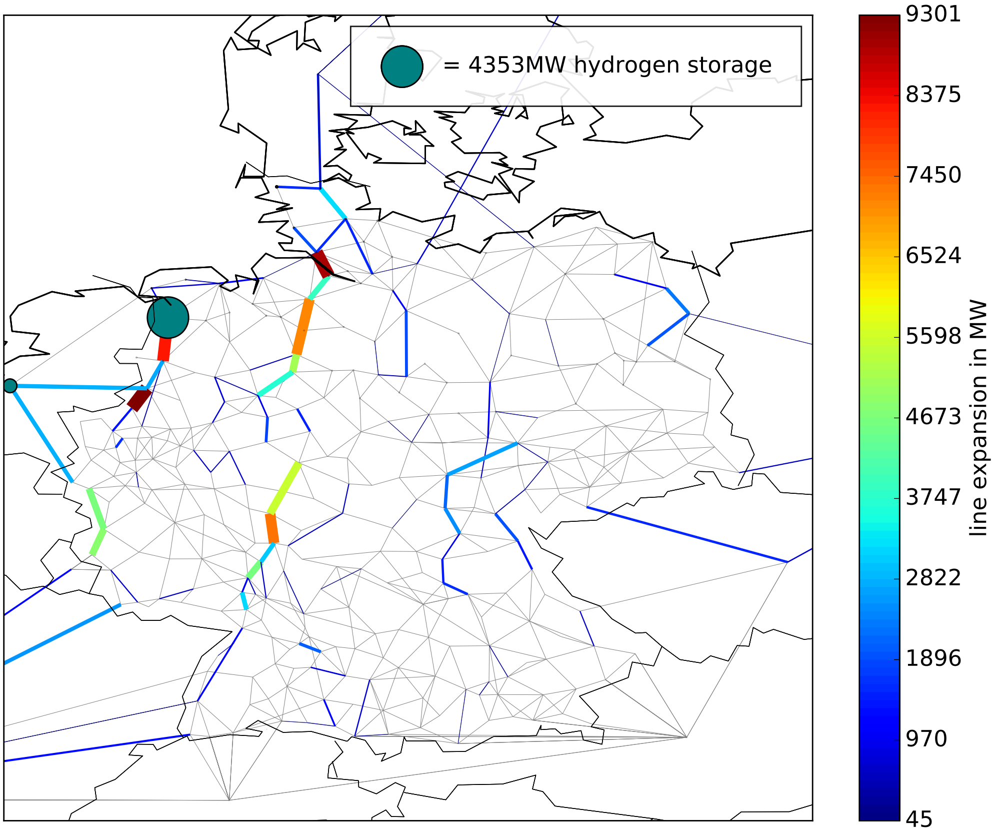

FIGURE 5.7: Spatial allocation of grid and storage expansion in a DC cross-border approach (*cb-dc*).

Germany exports a lot more energy to the Czech Republic, Switzerland and France and imports less from Denmark but more from the Netherlands.

In contrast to the storage at the Polish border, the one at the Dutch border is still needed. Here, the maximal possible grid expansion southwards is not sufficient to bring the offshore wind power to the load centres. An additional sensitivity scenario *cb-dc/D-inf* shows that if inner-german grid expansion is not restricted this storage will not be needed. Instead, grid expansion on the power lines heading southwards from the storage bus would be expanded by more than three times. Total grid expansion costs in Germany would rise by a factor of 2.9 while no significant amount of storage capacity would be needed (see Figure 5.9).

Consideration of grid connections to Belgium and Norway

Norway with its large potential of flexible hydro power (i.e. run-of-river, reservoir and pumped storage) might play a significant role in a future renewable European power system. In this context, a DC cable from Germany to Norway is under construction. As a sensitivity, the countries, which probably will be interconnected with Germany in the future are added to the model. Apart from the DC cable to Norway, a DC interconnector to Belgium is planned as well. Hence, Belgium and Norway are considered as additional electrical neighbors. The generation and load characteristics are consistently assumed as for the other countries. Therefore, the installed capacities are based on e-Highway 2050 project (2015b). In case of Norway, 28 GW run-of-river, 42.5 GW reservoir and 17 GW pumped storage are planned together with about 20 GW of wind and solar power plants. In addition to the direct connection to the two countries, the interconnectors to their other electric neighbors are considered. Consequently, Norway is also connected to Sweden, Denmark and, as Belgium, to the Netherlands. Belgium is moreover linked to France. The analysis in the following focuses on the influence of the interconnection with Norway being more relevant due to its available flexible power generation.

The results for this sensitivity variant *Be-No* are displayed in Figure 5.9 and geographically with the focus on storage and grid expansion in Figure 5.8. The endogenous system costs (Figure 5.9), although two additional countries are considered, are 6 % lower compared to the base scenario results. 9 % lower dispatch costs and 13 % fewer storage expansion costs overcompensate 39 % higher grid expansion costs. The flexible hydro power reduces the need for costly flexible biomass power. The biomass generation decreases by 14 %.

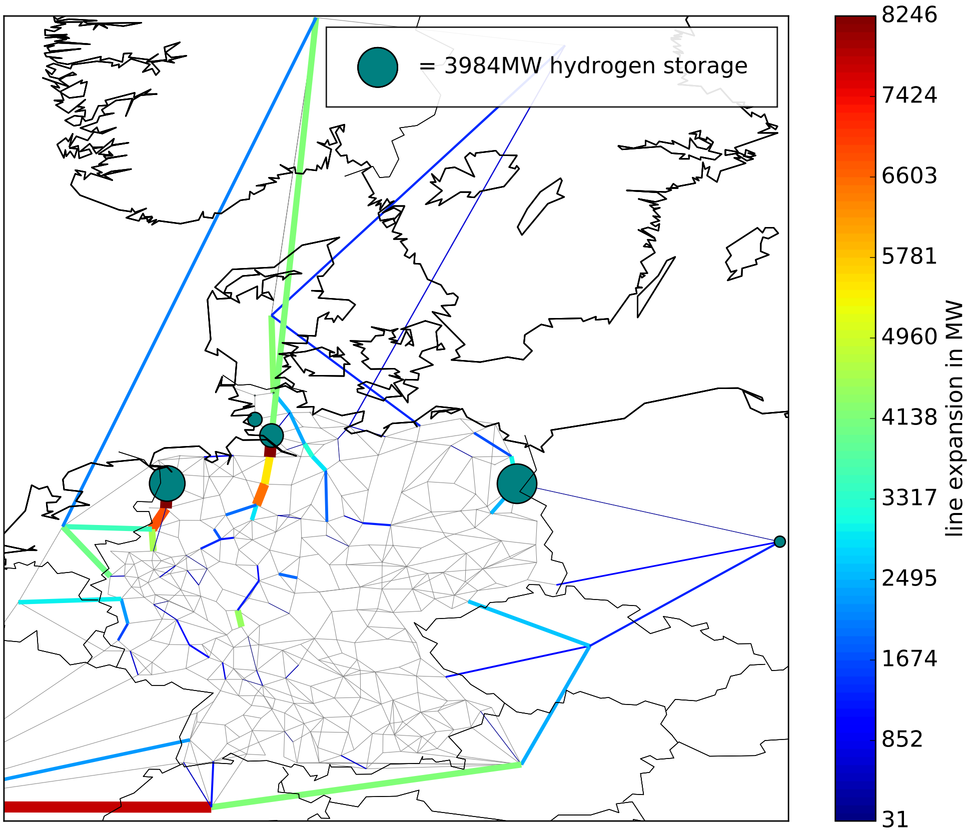

FIGURE 5.8: Spatial allocation of grid and storage expansion considering planned interconnection with Belgium and Norway (*Be-No*).

The power lines from Norway to the Netherlands and Germany are expanded completely up to the given upper bound of four times their planned capacity (see

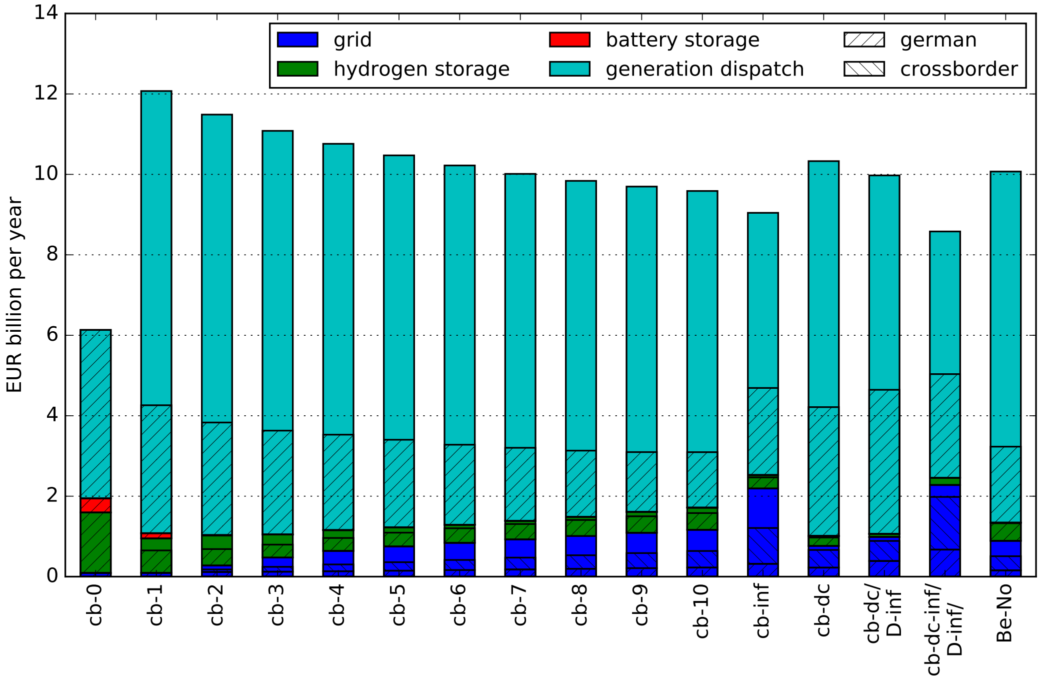

FIGURE 5.9: Annual endogenous system costs for sensitivity scenarios with different European interconnection settings. *cb-0* to *cb-inf* represent different restrictions on possible cross-border interconnections. *cb-0* represents Germany without any interconnections, *cb-1* with the status quo interconnector capacities, *cb-2* with twice the status quo capacity and so on. *cb-4* corresponds to the base scenario setting (as described in Section 5.1.2). *cb-dc* corresponds to a DC cross-border modeling approach (see Section 5.2.1). *Be-No* includes Belgium and Norway as electrical neighbors (see Section 5.2.1)

Figure 5.8). The motivation for these substantial grid expansion measures is originated in the flexible power generation of reservoir and run-of-river power plants, which is residually available apart from supplying the 123 TWh of Norwegian annual demand. A surplus of about 72 TWh is exported from Norway primarily to the Netherlands and Germany. As a consequence the hydrogen storage in the Netherlands is obsolete. In contrast, in Germany, storage expansion increases significantly. In Büttel, where the DC cable from Norway is connected to the German grid, a 1.4 GW hydrogen storage becomes economically feasible. As the upper bound of the interconnector to Norway as well as the Elbe crossing power line is reached, this storage units leads to a higher utilization of the flexible hydro power from Norway. The interconnector being the crucial bottle-neck, the flexibility in Norway cannot be used in order to avoid the economic feasibility of the storage unit in Büttel.

Although the major increase of grid expansion occurred to the cross-border interconnections, which are twice as high, a 16 % increase of grid expansion in Germany is noticable as well. As seen in Figure 5.8, the expansion route transporting power from Denmark southwards is now going mainly towards Hamburg, Braunschweig and further east. The route via Büttel towards North Rhine-Westfalia is already at its limit and receives substantial amounts of energy from Norway. Furthermore, in the west of Schleswig-Holstein, grid expansion is not needed. Instead a storage of 518MW is projected in Husum. The higher flows from north to south lead also to more expansion needs in North Rhine-Westfalia and southwards towards Frankfurt and Stuttgart.

The exogenously projected pumped storage capacity in Norway is not utilized, hence dispatched in the model. The extent of grid expansion from Norway to Germany and the Netherlands (being restricted by an upper bound) is only used for unidirectional power flows being supplied by reservoir and run-of-river power plants. These sources are sufficiently available to be utilized for export and local supply. This implies also higher net imports for Germany (16 %).

5.2.2 Restrictions on inner-German grid expansion

In this section, the influence of inner-German grid expansion is highlighted by comparing different sensitivities on the upper bound of German lines' capacities. Concerning the cross-border capacities, the base case assumptions are kept. In addition, in two extreme scenarios the two most adverse inner-German grid expansion sensitivities are combined with the two most adverse cross-border grid expansion sensitivities (as described in the previous section). The results of this sensitivity analysis are presented in Figure 5.10 and further analyzed in the following. The acronyms of the sensitivities are specified by a prefix and suffix. The prefix *D* indicates that only inner-German grid expansion upper bounds are altered by a relative factor (stated in the suffix) compared to the the base scenario setting *D-base* (as described in Section 5.1.2). Consequently, for instance the *D-0.25* sensitivity variant corresponds to a setting with 25% possible grid expansion compared to the base scenario setting.

As one can see in Figure 5.10, with increasing upper limit, starting from the *D-base* scenario, the overall cost reduction is only marginal. The *D-inf* scenario, which is characterized by no upper bound restrictions on the inner-German grid expansion, reaches only 2.7 % lower endogenous system costs compared to the ones in the base scenario. Nevertheless it can be highlighted that storage expansion is partly substituted by grid expansion. In Germany, storage expansion decreases by 37 % whereas grid expansion increases by 52 %. Instead of the substantial storage expansion at the Dutch border, the expansion route from the offshore feed-in Dörpen West southwards is expanded to a much higher extent. The first line segment of the route, which experiences the most expansion, is expanded more than twice as it is in the base scenario reaching a final capacity of 25.4 GVA. The shift from storage to grid expansion on this particular route characterizes the main difference leading to a partial substitution of biomass power production (full load hours drop from 3227 to 3120 h) by offshore wind generation (full load hours rise from 3161 to 3388 h). In the *D-2* scenario (twice as much possible grid expansion as in the base scenario) the line southwards form Dörpen West is (besides another power line near the Austrian border) the only power line which reaches its upper bound. Although this route

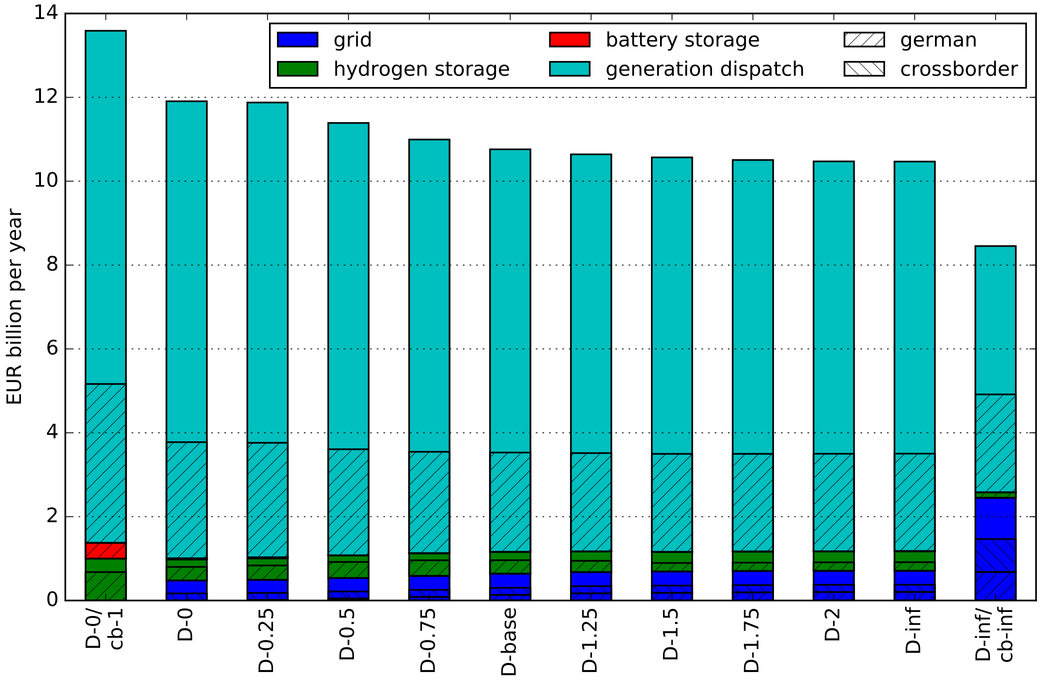

FIGURE 5.10: Annual endogenous system costs for sensitivity scenarios with different degrees of possible inner German grid expansion.*D-0* represents Germany without any possible grid expansion, *D-0.25* with 25% of the base scenario setting (*D-base*, as described in Section 5.1.2), and so on. On both extreme ends *D-0/cb-1* stands for no possible grid expansion in the entire system and *D-inf/cb-inf* corresponds to a perfect unrestricted overall grid expansion

still motivates more grid expansion due to the remaining offshore wind production, the hydrogen storage is already not feasible anymore in the *D-1.75* scenario. In the *D-1.5* sensitivity, a small storage unit is still feasible. Due to the higher exploitation of offshore wind energy, the net import characteristic is lowered by 30 % in the *D-inf* scenario. For example in case of the interconnection with the Netherlands, the net import behavior changes to a net exporting one. Moreover, the exports to France, Czech Republic and Poland are higher.

Combining the *D-inf* with the *cb-inf* (see previous section) approach, the cost reducing effect is substantially higher (see *D-inf/cb-inf* sensitivity in Figure 5.10). The endogenous costs can be reduced by 21 %. The shift from storage expansion (reduced by 75 %) towards grid expansion (283 % increase) becomes more evident. This by far highest grid expansion (out of all scenario variants) pays off with 39 % lower dispatch costs. Logically the share of biomass energy decreases to only 12 % combined with an increase of especially off- and onshore wind dispatch. Nevertheless, 14 % of the annual offshore wind and solar production and 17 % of the possible onshore wind generation remain to be curtailed.

The spatial allocation of the expansion measures is displayed in Figure 5.11 and shows predominantly a tremendous expansion from Denmark to Germany and moreover towards North Rhine-Westfalia and further south. Compared to

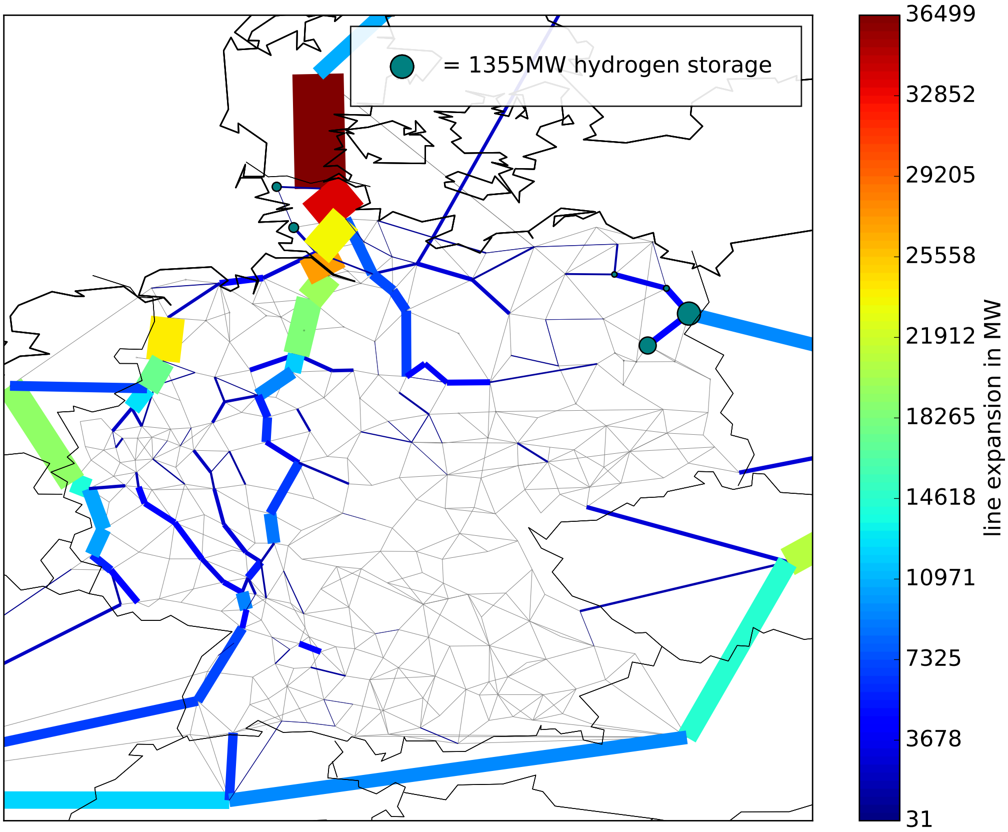

FIGURE 5.11: Spatial allocation of grid and storage expansion for the sensitivity *D-inf/cb-inf* with an completely unrestricted grid expansion on all lines.

the other scenarios, this north-to-south expansion route is continuously realized. Additionally, two expansion routes from the Ruhr area feed into the same direction being connected to the expansion route near Frankfurt and Mannheim. Moreover, an expansion route from Schleswig-Holstein via Hamburg towards Braunschweig, Wolfsburg, Magdeburg and finally Berlin is projected. Although a substantial increase in grid expansion can be observed, the northeast-to-southeast connections are not expanded as in the *cb-dc* approach (cf. Figure 5.7). Instead, the northeast-to-southeast cross-border interconnectors from Poland to Czech Republic and Austria are significantly expanded. In consequence to the expansion of the interconnection from Denmark, the imports towards Germany increase. In total, these higher imports are overcompensated by higher exports, especially to France, Switzerland and the Czech Republic. Therefore, the net imports are only at 4 %. i.e. reduced by 68 % compared to the base scenario results.

The remaining storage expansion is allocated near the Polish border, in Berlin and to a small extent at the west coast of Schleswig-Holstein. The storage units near the Polish border, which are not feasible in the *cb-dc* approach become feasible in this scenario due to a higher transit and loop flow behavior taking advantage of high RE flows towards Poland.

Reducing the maximal possible grid expansion towards no possible inner-German grid expansion (*D-0* scenario), the results react more sensitive. In the *D-0* scenario, 11 % higher endogenous system costs are caused by 11 % higher storage expansion and 14 % increased dispatch costs. The highest difference appears reducing the upper bound from 75 % to 50 % and 25 %. In contrast, the effect of only 25 % additional grid capacity is rather marginal.

In Figure 5.12, the spatial allocation of storage and cross-border line expansion in the case of the *D-0* scenario can be observed. Although more storage expansion is necessary, the extent is remarkably low for a 100 % RE scenario. The 7.5 GW of storage in Germany are allocated in a more distributed way compared to the two big storage units in the base scenario. Storage units are built at the same buses where in the base scenario storage units are feasible. At these buses the level of extension is lower due to grid bottle-necks. In addition to the 2 GW storage at the dutch border, another offshore wind driven storage unit (1.4 GW) is projected at the other German north-sea offshore feed-in bus at Büttel. Apart from these largest storage units and the one at the Polish border (1.2 GW), eight smaller hydrogen storage units are allocated near the Dutch border, in Schleswig-Holstein and near the Polish border. Furthermore two smaller battery storage units (263 and 391 MW) are feasible in the north of the Ruhr area and near Stuttgart. High curtailment rates are tolerated, especially the offshore wind curtailment increases from 32 % in the base scenario to 45 %. Consequently, biomass production increases by 13% reaching 3634 full load hours. In addition, Germany heavily relies on net imports of 20 % (instead of 12.5 % in the base scenario).

As one can discover in Figure 5.10, the extreme scenario *D-0/cb-1*, without any possible grid expansion, leads to 26 % higher endogenous system costs compared to the base scenario. Storage expansion in Germany increases by a factor of 3.4 leading to 22.6 GW of storage capacity. Especially offshore wind energy production is curtailed even more reaching a relative value of 51 %. Due to no cross-border expansion, the net imports are reduced to 11 %. The substantially higher dispatch costs can be explained by a high share of biomass energy generation reaching 4009 full load hours and additional storage losses.

5.2.3 The German high voltage grid

The consideration of the upper distribution level, i.e. the high voltage grid, ensures the reflection of local grid infrastructure in the context of a high spatial model resolution. Therefore, local grid restrictions on the one hand and transit flow behavior on the other hand may affect the results. In order to depict the relevance of the high voltage grid, comparative analyses are undertaken and their results are presented in this section.

Particularly, results of the *eGo 100* base scenario presented in Section 5.1.2 are

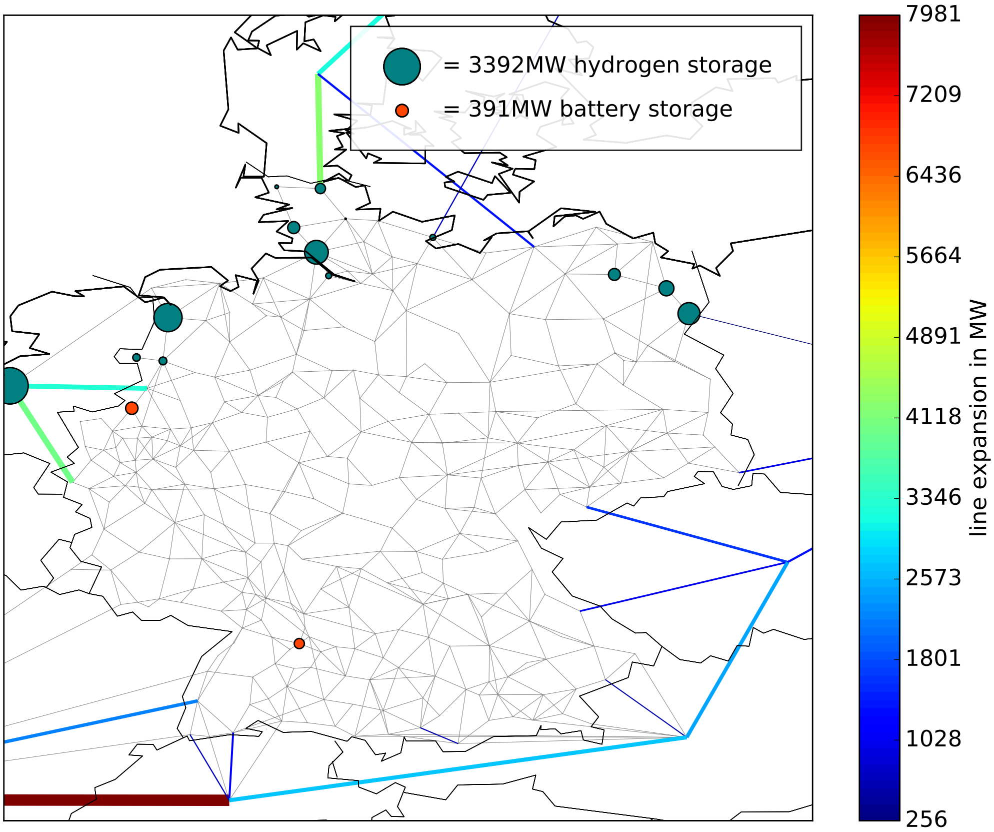

FIGURE 5.12: Spatial allocation of grid and storage expansion for the sensitivity *D-0* with no possible grid expansion in Germany

compared to alternative results being generated by a modeling approach which disregards the high voltage grid (as described in Section 4.4.1). The alternative approach, except neglecting the HV level, is subject to the same assumptions as applied in the *eGo 100* base scenario. The reduced EHV model is further reduced to 300 buses by applying the same k-means algorithm which is used in the base approach.

These two opposing modeling approaches are labeled as *EHV+HV* (base setting including the HV level) and *EHV* (excluding the HV level). In Table 5.2 the annual endogenous system costs for the results of the two approaches and their relative differences are presented for the *eGo 100* base scenario. Moreover, in order to deepen the evaluation, additional scenario variants are considered (also presented in Table 5.2). At first, the *eGo 100* base scenario is focused on. Afterwards the additional scenario variants are complementarily analyzed.

Concentrating initially on the *eGo 100* base scenario comparison, one can depict from Table 5.2 that the *EHV* model approach leads to 6.5 % higher system costs. In Figure 5.13, the corresponding spatial allocation of grid and storage expansion can be observed. Compared to the results of the base scenario (see Figure 5.4) the overall characteristics can be described very similar. Total grid expansion costs stay the same, although in Germany in terms of MVA*km 6 % more grid expansion occurs. Furthermore, the maximal grid expansion is 940 MVA lower. This difference can be

Scenario variants	Annual endogenous system costs		
	approach *EHV+HV*	approach *EHV*	rel. difference
	bn. EUR	bn. EUR	%
eGo 100	10.8	11.5	+6.5
eGo 100 D-inf/cb-inf	8.5	8.7	+2.6
NEP 2035 (dispatch)	12.8	13.5	+5.4
Status Quo (dispatch)	9.9	10.2	+2.8

TABLE 5.2: Annual endogenous systems costs of approach *EHV+HV* and *EHV* and the relative difference for different scenario variants.

mainly explained by lower upper bounds on aggregated routes due to the nonconsideration of HV systems, which may be installed in parallel with EHV ones in the base approach. For instance, the important bottle-neck route crossing the Elbe from Büttel southwards has a 26 % lower upper bound resulting into a maximal expansion of only 7.2 GVA, which is entirely used. Similarly, the crucial AC cross-border capacity to Denmark can only be expanded to a lower extent leading to less grid expansion needs on the route from Flensburg to Rendsburg. In contrast, a feasible hydrogen storage unit of 0.5 GW in Flensburg near the Danish border is installed to partly compensate the lower cross-border capacity. In total, storage expansion is 10 % i.e. 1 GW higher. Besides the additional storage unit in Flensburg, the storage unit at Dörpen West ends up with a 0.8 GW higher capacity whereas the storage unit at the Polish border is 0.3 GW smaller. Similarly, to the storage in Flensburg, the one in Dörpen West compensates fewer possible grid expansion southwards reducing the effect of increasing wind power curtailment. Nevertheless, as displayed in Figure 5.14, wind power curtailment increases significantly. Instead of building yet additional storage capacities, wind power production is curtailed to a higher extent and mainly compensated by flexible biomass power dispatch. This different generation characteristic is the main reason for the rise in system costs. 93 % of the increase in system costs leads back to the different dispatch, only the remaining 7 % are explained by the additional investment into storage expansion.

In order to isolate the effect of transit flows and local grid restrictions from the mentioned difference in the maximal possible upper bounds for grid expansion, additional scenario variants neglecting the HV level are performed. Once the restriction on the upper bound is neglected the cost difference of both approaches becomes smaller leading to 2.6 % higher system costs (see scenario *eGo 100 D-inf/cb-inf* in Table 5.2) . In order to generate more converging results, in terms of MVA*km, 23 % more grid expansion would be needed in the German grid. Yet, the remaining difference is still mainly due to an expensive shift from wind power production to biomass power generation. Especially in the southwest and southeast of Germany more biomass is dispatched. This is cheaper than investing into more grid expansion in order to lower the dispatch costs. Consequently, less wind energy can be exported to neighboring countries in the south leading to more biomass dispatch

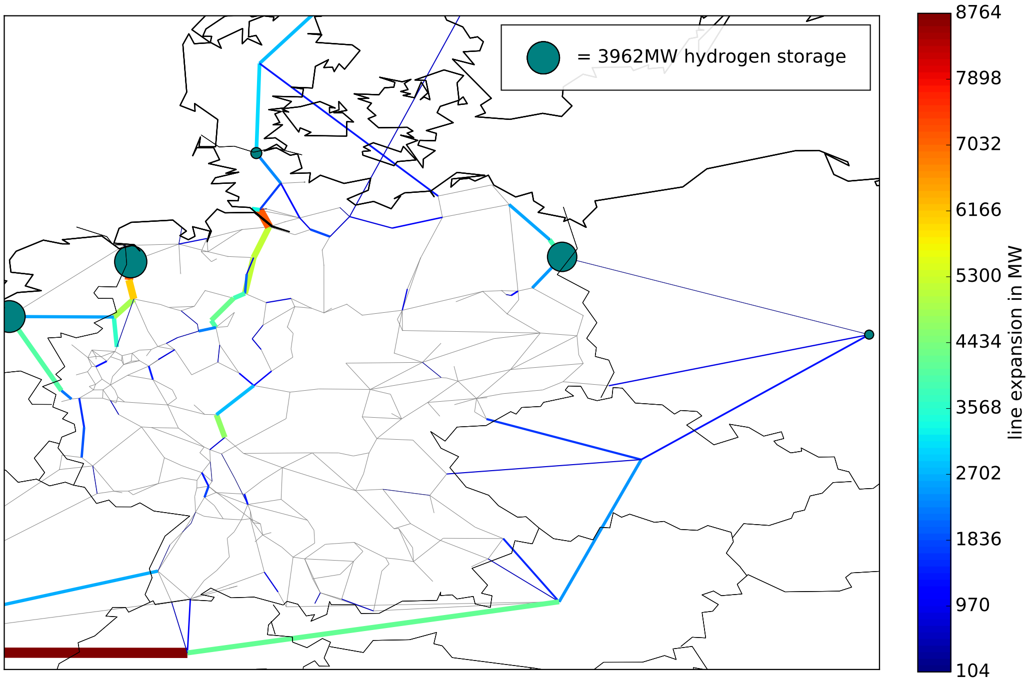

FIGURE 5.13: Spatial allocation of grid and storage expansion for the scenario *eGo 100* neglecting the HV grid.

in these countries as well. The largest export difference is the one to the Czech Republic. Here, the net export is lowered by 43 % and 3 TWh. The lack of energy is compensated mainly by higher dispatch of biomass in the Czech Republic and Poland. Thus, the net imports from Poland increase transporting biomass energy to the Czech Republic.

The effect of higher dispatch costs can also be analyzed when optimizing only the dispatch disregarding any grid and storage expansion possibilities. This approach is only physically possible for the *NEP 2035* and *Status Quo* scenario. The results show that with increasing generation of distributed RE the cost increasing effect becomes more significant (see Table 5.2).

Altogether the results show that positive transit flow effects outnumber the costly necessity to overcome local bottle-necks in the HV level. The already installed status quo capacity in the HV level supplies additional power flow possibilities mainly from the north to south. Especially at the west coast of Schleswig-Holstein this transit flow effect can be noticed. In the *eGo 100 D-inf/cb-inf* approach this effect could have been diminished completely by grid expansion. Instead, some dispatch differences are tolerated due to higher economical feasibility.

Besides considering transit flows like in the west of Schleswig-Holstein, in other cases the k-means algorithm may create false transit possibilities. This effect has to be born in mind and will be further analyzed and discussed in Section 5.2.5 and 6 respectively.

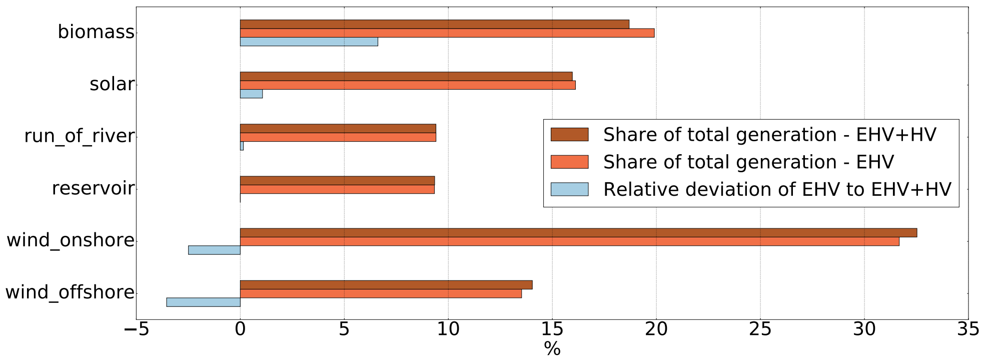

FIGURE 5.14: Deviation of annual power dispatch between the approach considering the HV level (*EHV+HV*) and the one neglecting the HV level (*EHV*) for each generation type in relation to the dispatch of the base approach (*EHV+HV*). The results are based on the *eGo 100* scenario. Only technologies with major generation shares are presented.

5.2.4 Capital cost assumptions of grid expansion

In Figure 5.15 a sensitivity analysis on the specific investment costs of grid expansion is illustrated. The assumed specific investment costs are increased in 25 % steps until a doubling of the assumption from the base scenario (i.e. from variant *grid_cost-1.25* to *grid_cost-2*). Considering the other extreme, 25 % (sensitivity *grid_cost-0.75*) up to 87.5% (*grid_cost-0.125*) lower costs are simulated.

A doubling of specific grid investment costs only leads to 3 % more endogenous system costs, 14 % higher storage costs and 11 % lower grid investment costs. The higher specific capital costs are overcompensated by 40 % less grid expansion in terms of installed MVA*km. These changes lead to 2 % higher annual dispatch costs. As grid expansion gets higher, storage expansion becomes slightly more attractive. With 50 % higher specific grid investment costs, a hydrogen storage of 1.5 GW nominal capacity is feasible in Denmark. In the subsequent sensitivity two more but smaller hydrogen storage units of each about 100 MW nominal capacity are projected. One is located at the Niebüll bus and the other one accompanies the big storage unit at the northern interconnector to Poland at the neighboring bus in the north-west reducing the need for grid expansion between these two buses.

A 87.5 % reduction of specific grid costs provokes 5 % lower endogenous system costs, 3 % higher storage costs and 75 % lower grid expansion costs. The lowering of the grid expansion costs corresponds to 34 % more physical grid expansion in terms of MVA*km. Consequently, the dispatch becomes slightly cheaper (1 % reduction).

Overall, the effect of lowering the specific capital costs is higher than increasing them. For example, a decrease of 25 % of specific costs (sensitivity *grid_cost-0.75*) reduces grid expansion costs by 15 %, although 10 % more physical capacity can be installed. The endogenous system costs are reduced by 1.3 %. In contrast, the increase of 25 % (sensitivity *grid_cost-1.25*) scale up the system costs by 1 %. Nevertheless, the influence on the physical grid capacity is even higher being reduced by 14 %, yet

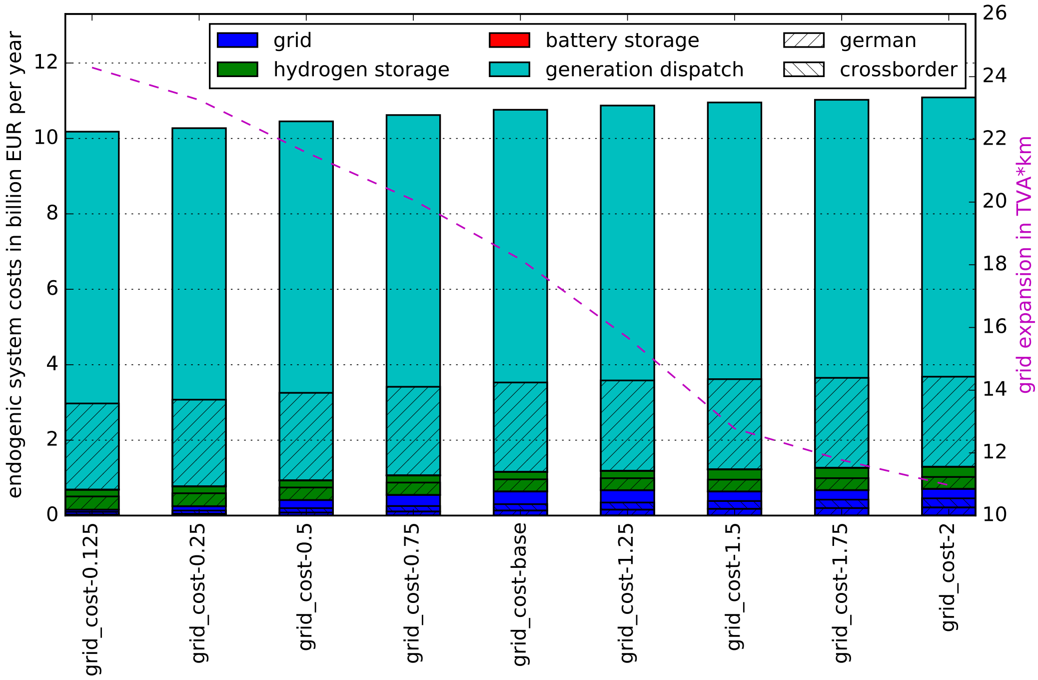

FIGURE 5.15: Annual endogenous system costs and grid expansion for sensitivity scenarios with different specific grid investment costs. The base case is plotted as reference (*grid_cost-base*). The *grid_cost-1.25* scenario stands for 25% higher specific grid investment costs, *grid_cost-0.75* for 25% lower ones, and so forth.

leading to 5 % higher grid expansion costs.

In terms of the spatial allocation of grid and storage expansion, the changes are small. The two big storage units in the base scenarios are in all scenarios feasible, varying a bit in their sizes. The major grid expansion routes are expanded in all scenarios varying in the extent. With very low grid costs the north-to-northeast and north-to-northwest lines are expanded, which are not expanded in the base scenario. This leads two a higher usage of offshore wind generation. Hence, here the curtailment is reduced by 8 %. Concerning the other fluctuating RE the curtailment rates do not change significantly in the analyzed sensitivities.

5.2.5 K-means clustering

Different k resolutions

The spatial resolution is an important aspect in this work. Thus, a sensitivity analysis of how the results are influenced by changes in spatial detail will be presented in the following. In 50-k steps, between the sensitivities *k-50* (50 cluster buses) and *k-500* (500 cluster buses), the resolution is changed applying the k-means clustering as described in Section 4.4.1. In Figure 5.19 the corresponding cost results for all calculated sensitivities are presented. Furthermore the mentioned extreme cases are presented in Figures 5.16 and 5.17 concerning the spatial distribution of grid and storage expansion.

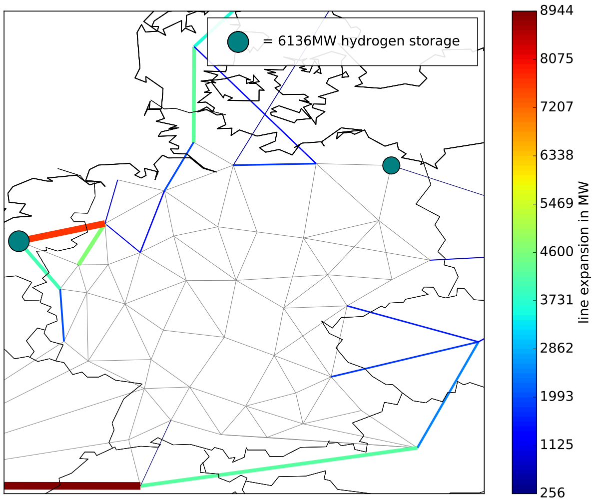

FIGURE 5.16: Spatial allocation of grid and storage expansion for the *k-50* sensitivity

The results can be categorized in two different groups, one showing solutions, as in the base scenario with a storage unit at the offshore feed-in bus near the Dutch border, and another one where this storage is not feasible, instead grid expansion southwards is substantially higher. The *k-250*, *k-350* and *k-400* scenario results belong to the latter mentioned group. Here, from the feed-in bus southwards, instead of the 8.3 GW line expansion in the base scenario, the expansion is at most (in the *k-400* scenario) almost doubled. Different positions of the relevant buses provoke an advantageous line aggregation in the clustering process (i.e. more lines get aggregated between the offshore feed-in bus leading southwards) causing a higher possible upper bound on this crucial bottle-neck section. Consequently, the higher grid expansion makes storage expansion at this bus obsolete. Furthermore, more offshore wind power is dispatched at this bus leading to less imports from the Netherlands (and therefore more storage expansion in the Netherlands), fewer biomass dispatch and therefore less dispatch costs. Thus, the endogenous system costs are in this group consistently 1.5 % lower than in the base scenario.

The other mentioned group is principally already well described by the base scenario results. One outlier in this group displays the *k-150* scenario, in which the described sensitive hydrogen storage expansion at the Dutch border is comparably extremely high being even accompanied by additional battery storage expansion. This scenario reaches the highest (i.e. 7% higher) endogenous system costs. Altogether, except the mentioned outlier, the influence on the overall costs results is rather low.

In particular, especially when considering the spatial allocation of the grid and expansion measures, two main trends can be pointed out. First, with higher spatial detail, more distributed storage units become feasible. Starting with the *k-350*

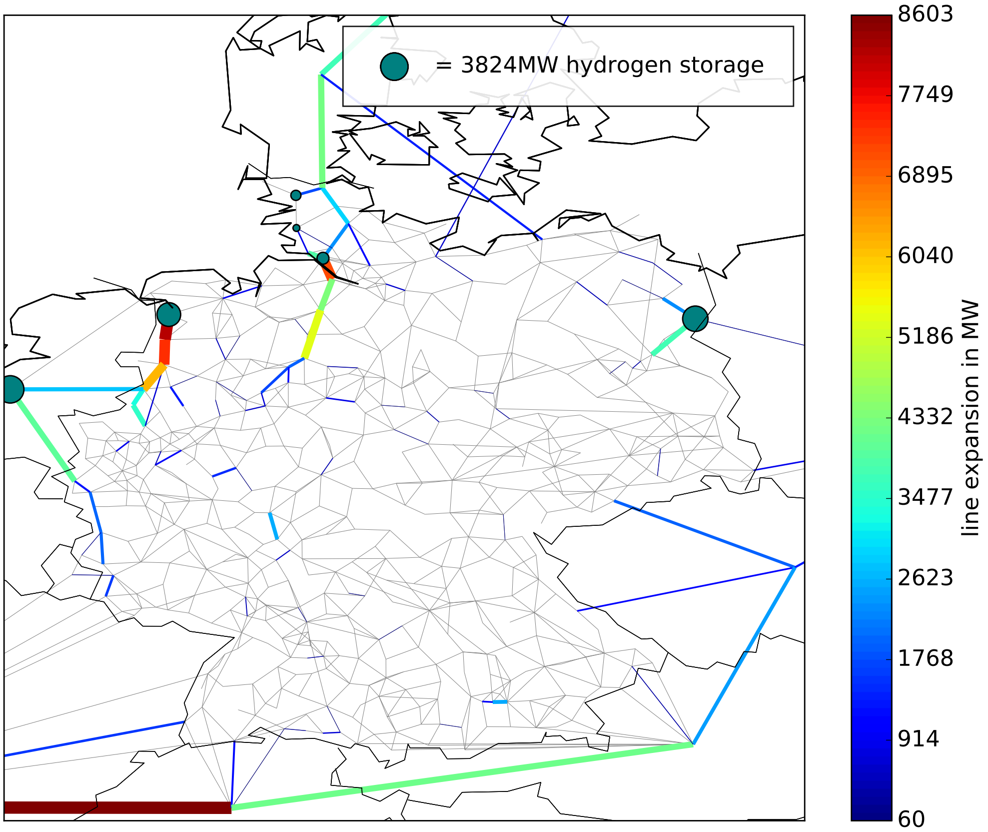

FIGURE 5.17: Spatial allocation of grid and storage expansion for the *k-500* sensitivity

sensitivity, hydrogen storage units in Schleswig-Holstein are projected. In the *k-500* scenario this effect occurs to the highest extent (see Figure 5.17). In this case, the largest storage of the ones in Schleswig-Holstein is the one at the offshore feed-in bus in Büttel with 723 MW nominal capacity. Second, fewer spatial detail leads to underestimation of grid expansion. Especially in the *k-100* and *k-50* scenario (see Figure 5.16) the main expansion routes are heavily underestimated due to the lack of significant bottle-necks. Hence, in Germany 37% fewer grid expansion investment are necessary in the *k-50* scenario.

Different initial random busmaps

As described in Section 4.4.1 the k-means algorithm produces reproducible results starting from the same initial (random) busmap. By analyzing six sensitivity results (called *busmap-1* to *busmap-6*), which correspond to different initial, randomly generated busmaps, the impact of the random initialization is evaluated. The endogenous cost parameters of the calculated solutions are part of Figure 5.19. One can observe that the overall cost results are very much alike. The mean deviation is at most +1 % concerning grid expansion costs and otherwise concerning storage expansion, dispatch and overall endogenous costs below 0.1 %.

The structural clustering effect which shows the high sensitivity concerning local grid and storage expansion at the German northwestern offshore feed-in bus, described in the previous section, can also be analyzed in this set of sensitivities. In case of the *busmap-1* sensitivity, the mentioned storage is not feasible (see Figure 5.18). Instead, grid expansion from that bus southwards is almost doubled. Therefore, the clustering effect (in combination with the upper bound restriction) can also be observed when assuming the same number of buses as in the base scenario but a different initial busmap. This effect leads to 3 % more grid and 2 % less storage expansion, dispatch and total endogenous costs. The overall storage expansion is not lowered more substantially because the missing storage unit at the described offshore feed-in bus is partly compensated by more storage capacities in the Netherlands and small ones in Schleswig-Holstein. This effect has been already described in the previous section and can be studied in Figure 5.18 and 5.19.

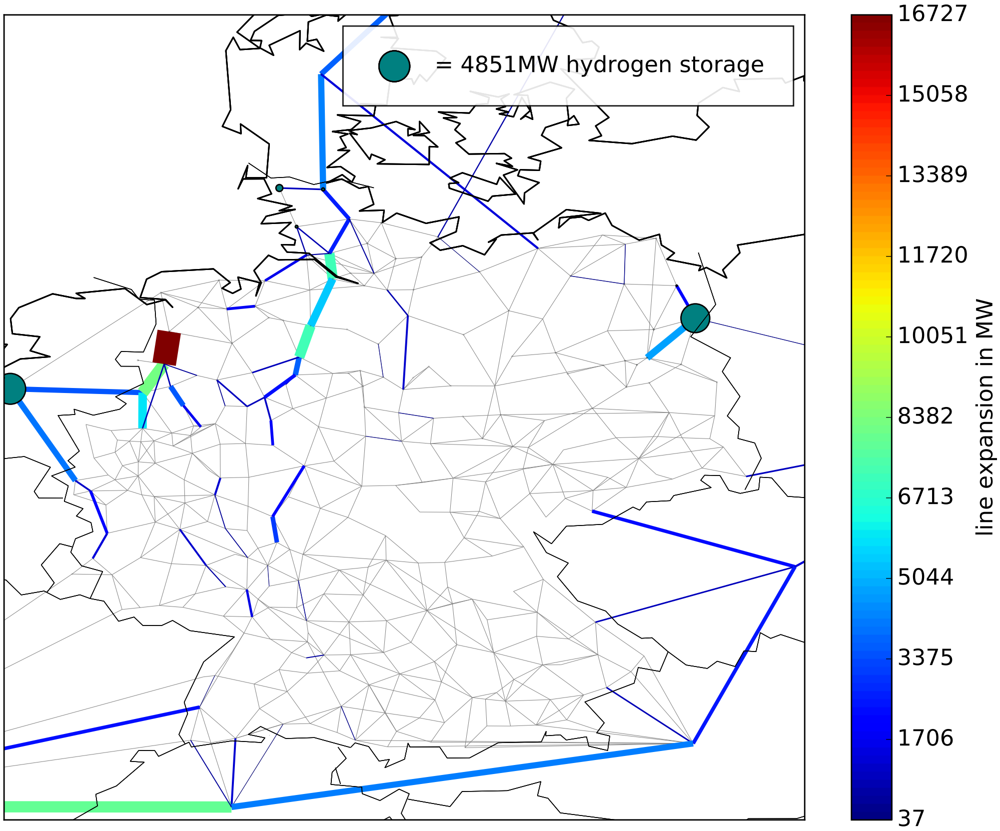

FIGURE 5.18: Spatial allocation of grid and storage expansion for the sensitivity *busmap-1*

The opposed extreme, which shows the highest endogenous system costs (1.3 % higher compared to the base scenario) is the sensitivity *busmap-4*. In this case, in Schleswig-Holstein a few small storage units are feasible due to the fact that less grid expansion southwards across the river Elbe is possible due to a different line aggregation caused by a different initial busmap.

Apart from these - compared to the mean deviation - two extreme cases (which

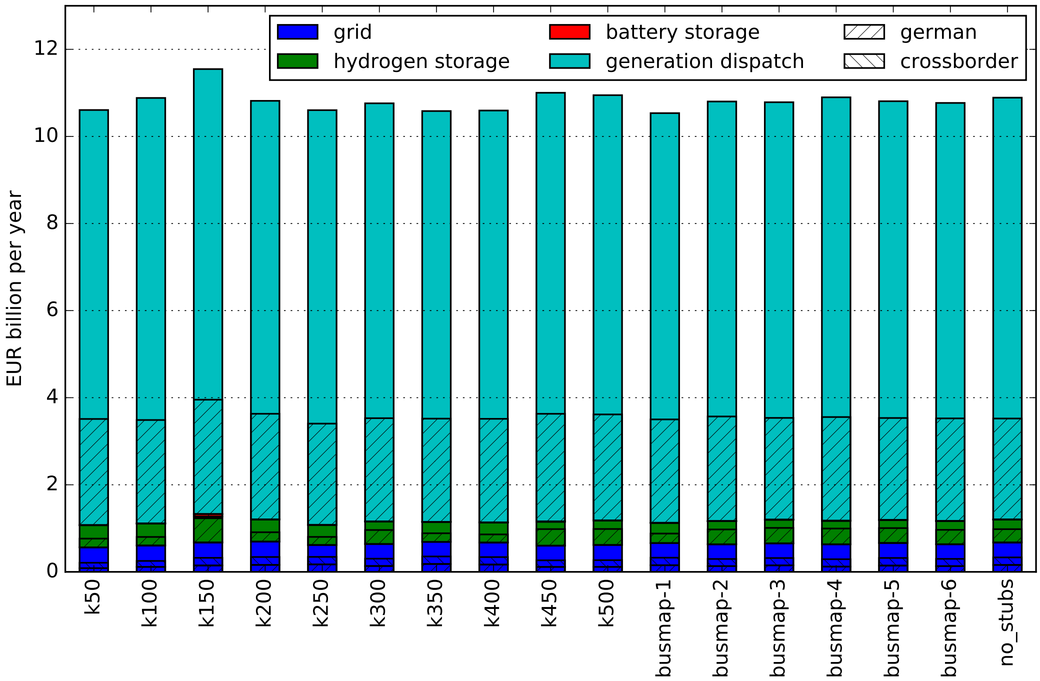

FIGURE 5.19: Annual endogenous system costs for sensitivity scenarios concerning the k-means clustering.The *k-50*, *k-50* and so on stand for different spatial resolution with different k buses. The *busmap-1*, *busmap-2* (...) represent different initial random starting position of the k-300 buses base scenario setting. For the *no_stubs* sensitivity, stubs are removed before the k-means clustering.

in overall terms show still very small influence on the results), the other sensitivities are extremely homogeneous with deviations below 0.5 % concerning the mentioned cost parameters.

Initial stub removal

As mentioned in Section 5.2.3, the k-means algorithm produces false interconnections of spatially nearby but electrically disconnected grid topology. This effect can be minimized by initially removing all stubs. Consequently, in case of spatially nearby stubs, no false interconnections can evolve. A drawback of this approach is that spatial detail is lost, which can be represented with increasing consideration of k buses. For instance, in Figure 5.17 one can see stubs being modeled (e.g. from Niebüll towards the island of Sylt) which would be eliminated beforehand. This approach has been tested in the sensitivity *no_stubs*. Its results are displayed in Figure 5.19 and 5.20. When analysing the results, one should keep in mind that the effect of a different initial busmap (which is produced in this context) is inherent as well. This additional effect might bias the sensitivity result to an extent as described in the previous section.

In Figure 5.20, the different grid topology can be observed. The degree of interconnection is lower. One clear example is the missing interconnection in Southwestern Germany in the area of the Black Forest. Here, two 110 kV stubs reach into the Black Forest from the east and west side and become spatially very close leading to a false connection in the base scenario. Moreover, especially the east-west interconnections at the former inner-German border are substantially reduced towards a more realistic representation. Apart from the topological changes the spatial allocation of grid and storage expansion is displayed. The main aspects of the distribution is very similar as in the base scenario. In particular, a few differing characteristics can be highlighted. Concerning grid expansion, more lines, although to a low extent, are expanded. Regarding storage expansion, two additional small storage units with a nominal capacity of 353 and 150 MW in Schleswig-Holstein are feasible and the storage unit at the Dutch border is with 2.2 GW significantly smaller.

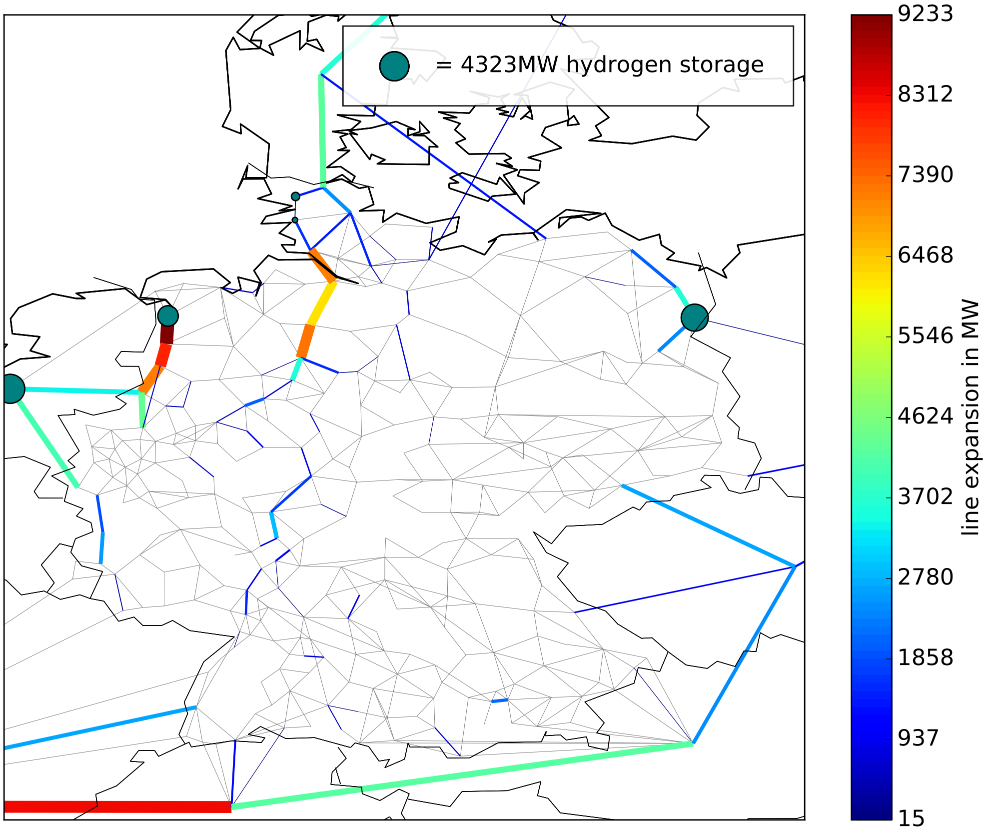

FIGURE 5.20: Spatial allocation of grid and storage expansion for the sensitivity *no_stubs*

In terms of overall costs, Figure 5.19 reveals that the influence is only marginal. As expected, the highest influence is observed concerning grid expansion. In the overall system these costs are 5.5 %, in Germany even 18.6 % higher. Due to a bigger storage unit in the Netherlands, storage expansion is in total 2.2 % higher, although in Germany storage expansion is 5 % lower due to above described reason of a smaller storage unit at the Dutch border. The influence on the dispatch costs is minor being not even 1 % higher leading to only 1.2% higher total endogenous system costs.

5.3 Sensitivity analysis on storage related parameters

5.3.1 Exogenous storage expansion in foreign countries

As the focus of the work is the optimal grid and storage expansion in Germany, one could argue that the exogenously defined hydrogen and battery storage capacities in the foreign countries (as described in Section 4.3.5) shall not be endogenized. Therefore, a sensitivity is performed to analyze the influence on the results when assuming these storage units in the foreign countries as exogenous. The corresponding overall cost results of the sensitivity scenario *store_foreign_ex* are shown in Figure 5.22. One has to keep in mind that the endogenous costs in this particular scenario do not include the costs for the exogenously defined foreign hydrogen and battery storage units. Hence, the comparison to other scenarios has to be carried out carefully. The breakdown of the costs shows that the additional exogenous foreign capacities of 39.7 GW hydrogen and 16.7 GW battery storage lead to 18 % less storage expansion in Germany, 27 % less grid expansion and 9 % lower dispatch costs in the overall system. Thus, more fluctuating RE can be harvested in the neighboring countries. In particular, solar curtailment is reduced by 41 % to a relative value of 8 %. Wind on- and offshore are also curtailed less (i.e. 18.6 % and 31 % respectively). These additional capacities, which, due to the storage units, offer flexible power, lead to higher net imports to Germany (14 %).

The spatial allocation of the foreign exogenous and German endogenous storage expansion can be observed in Figure 5.21. The two big hydrogen storage units at the Dutch and Polish border are still feasible. Whereas the nominal capacity of the storage unit at the Polish border slightly increases, the 1.7 GW of storage capacity near the Dutch border stands for only about half as much capacity as modeled in the base scenario. Consequently, 9 % less offshore wind power can be dispatched from this feed-in bus. This missing energy production is compensated by more imports from the Netherlands. Due to the substantial storage capacity there, more RE, especially wind power can be dispatched and utilized for more exports towards Germany.

Analyzing the spatial allocation of grid expansion (see also Figure 5.21) it can be emphasized that the majority of the reduction is attributed to the foreign grid expansion. This category of investment costs is halved. Particularly, the interconnector capacities from Denmark to Sweden (no expansion), from Austria to Switzerland and from Switzerland to France are significantly lower. The higher local storage capacities decrease the need for energy interexchange between countries. Especially the existing flexibility in terms of pumped storage and reservoir power plants in Sweden, Switzerland and Austria becomes less valuable.

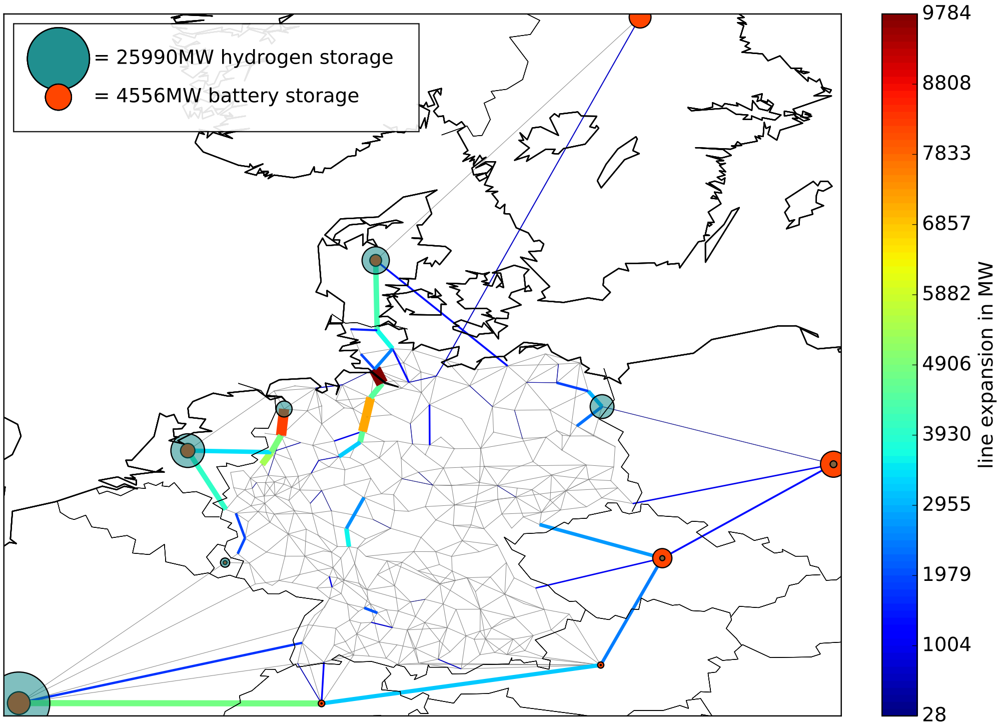

FIGURE 5.21: Spatial allocation of grid and storage expansion for the sensitivity *store_foreign_ex* with exogenous foreign hydrogen and battery storage expansion.

5.3.2 Capital cost assumptions of storage expansion

As in Section 5.2.4 specific grid investment costs are varied, in this section the influence of lower or higher specific storage investment costs are analyzed. In contrast to the grid components, the hydrogen and battery storage technologies are comparably innovative. Therefore, unforeseeable cost reductions, like it has happened in case of PV technology, are more likely to develop in the upcoming decades. Hence, especially sensitivities assuming lower storage costs are interesting. In Figure 5.22, the results of the performed sensitivity analyses are presented. In 25%-steps, the specific capital costs are lowered and increased from the perspective of the base scenario assumption. Additionally, two scenarios with extremely low specific investment costs of 12.5 % (*store_cost_0.125* sensitivity) and 5 % (*store_cost_0.05* sensitivity) compared to the base scenario assumption are simulated.

As the specific investment costs increase, investment into additional storage capacities becomes less attractive. An increase of 25 % in specific costs lead to 25 % lower i.e. 5.1 GW storage capacity in Germany. With yet higher specific costs, the German storage expansion stays rather constant. Whereas the two big hydrogen storage units consistently end up with lower capacities with rising specific costs, a small battery storage of 157 MW at the southern interconnector to Poland becomes feasible when specific costs are assumed to be 50 % higher. This effect becomes stronger with increasing investment costs leading to a 805 MW battery when specific costs are doubled. This trend compensates partly the lowering of hydrogen storage

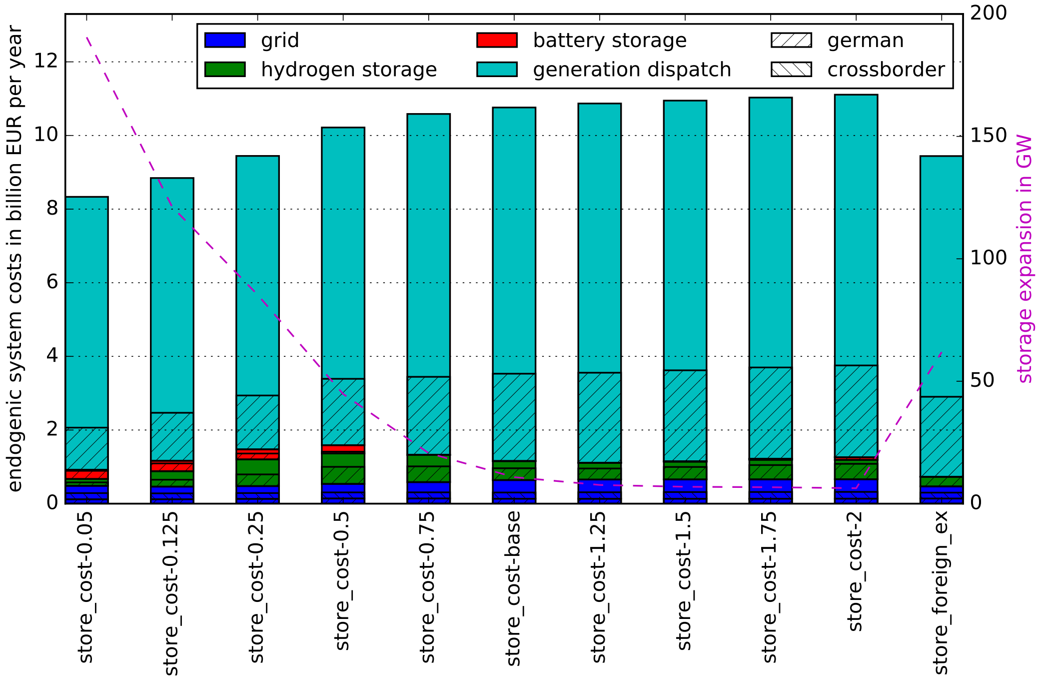

FIGURE 5.22: Annual endogenous system costs and storage expansion for sensitivity scenarios with different specific storage investment costs and assumptions on the foreign storage expansion (*store_foreign_ex*). The base case is plotted as reference (*store_cost-base*). The *store_cost-1.25* scenario stands for 25% higher specific storage investment costs, *store_cost-0.75* for 25% lower ones, and so forth. In the *store_foreign_ex* scenario all foreign hydrogen and battery storage units are exogenous.

capacity leading to a total capacity of 5.2 GW in Germany (*store_cost_2* scenario). In terms of storage expansion costs the described development implies at first a reduction of 12 % and then 5 %. Thus, lower storage expansion overcompensates the higher specific storage investment costs. Then, with a significantly higher share of battery expansion and once higher specific investment costs the storage investment are 8 % (*store_cost_1.75* scenario) and 16 % (*store_cost_2* scenario) higher.

The lower storage expansion in terms of installed capacity comes along with a slightly increasing investment into grid expansion (at most by 3.7 %). These additional investments do not compensate the slight negative effect on the annual dispatch costs which increase by 2.5 % in the *store_cost_2* scenario. Furthermore, the endogenous system costs are then 3.2 % higher. Overall, the effects of higher specific storage costs influence the results rather marginally.

In contrast, the effect of lower specific storage investment costs is substantial. Figure 5.22 clearly shows that storage expansion increases over-proportionally. A reduction of 25 % leads to almost twice as much storage capacity in Germany. In the most extreme scenario (*store_cost_0.05*) the German storage expansion is even 21 times higher. The 138 GW installed capacity are accompanied by almost the entire possible storage expansion in the neighboring countries leading to a total capacity of 190 GW of which 59 % are battery storage units.

Assuming a little less extreme cost reduction, the storage expansion in the variant *store_cost_0.125* is significantly lower. Especially the battery expansion reacts very sensitive to these low specific investment costs. Hence, the share of battery storage is, with 42 % of a total expansion of 121 GW, lower than in the most extreme scenario and substantially higher than in the scenarios with higher specific investment costs. In Figure 5.24 the nodal allocation of the storage expansion can be observed. Concerning the battery expansion two main effects can be emphasized. First, batteries are projected at buses next to cross-border interconnectors, where geographically no hydrogen storage may be built. Second, at many buses in the north, battery storage units are jointly feasible with hydrogen storage units being situated at the same bus. The first mentioned effect is mainly linked to the restriction on the maximal cross-border capacities. The batteries increase the possible exchange with the neighboring countries. Furthermore, the increasing battery installations in the north correlate with the effect of higher utilization of fluctuating RE, in particular solar generation. This implies more need for intra-day short-term flexibility (as demonstrated in Figure 5.23), which together with better efficiency rates motivate the higher extent of battery expansion. For instance, the battery storage units in Schleswig-Holstein are about as large as the hydrogen storage units at the same buses.

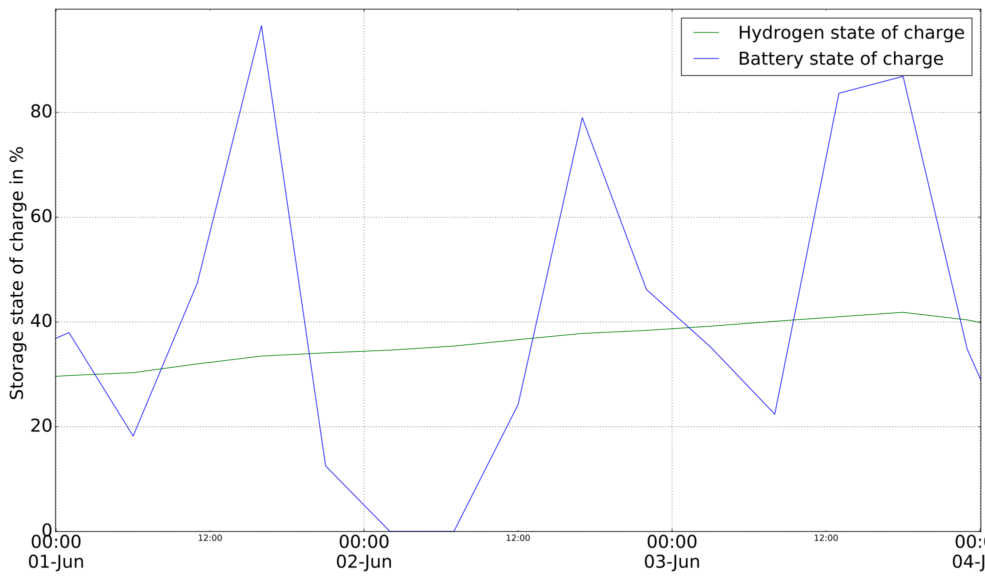

FIGURE 5.23: Overall storage state of charge of hydrogen and battery storage units during the first four days in June in case of the sensitivity scenario *store_cost_0.125*

As mentioned, in the *store_cost_0.05* sensitivity, the general effect of increasing battery storage capacities becomes even higher. Hence, in the example of Schleswig-Holstein, the battery capacities surpass the hydrogen ones. The first significant appearance of battery storage occurs in the *store_cost_0.5* scenario. Yet, the share in Germany with 10 % is still rather low. Here, mainly the two large hydrogen storage units from the base scenario increase substantially (9.5 GW in the northwest and 5.1 GW in the northeast) and additional but smaller ones in northern Schleswig-Holstein (580 MW in Niebüll, 613 MW in Husum, 688 MW in Flensburg and 267 MW in Rendsburg) reach feasibility. In the *store_cost_0.25* scenario, predominantly the hydrogen storage unit in France (in *store_cost_0.5* scenario 2.5 GW of capacity) becomes with 21 GW the biggest one in the system. In addition, the increase of battery storage units becomes highly visible, structurally similar to the spatial allocation in Figure 5.24. Compared to the displayed results, primarily, the battery capacities at the bus at Dörpen West and more southward buses on that route, although existent, are comparably lower.

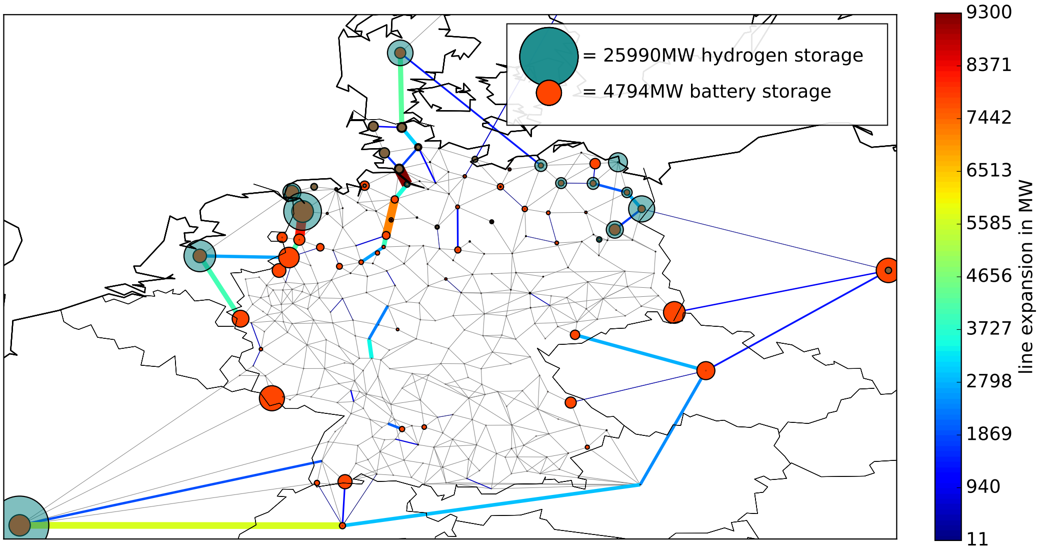

FIGURE 5.24: Spatial allocation of grid and storage expansion for the sensitivity *store_cost_0.125* with 12.5% specific storage investment costs compared to the base scenario.

As a consequence of the significant storage investment, German net imports increase (by 31 % in the *store_cost_0.05* sensitivity) and generally curtailment of fluctuating RE decreases substantially. In the most extreme case, solar curtailment is more than halved to 6 %, off- and onshore wind curtailment is reduced less but significantly to 19 % and 15 % respectively. Due to the higher usage of fluctuating RE, the dispatch costs can be reduced by 23 %. Moreover, the low specific storage investment costs overcompensate the high expansion reaching 15 % lower storage expansion costs. Although the storage capacity is expanded up to 21 times, grid expansion is not reduced anti-proportionally being at lowest 25 % below the base case expansion. The spatial allocation of the grid expansion measures (as seen in Figure 5.24 remain principally the same. In some cases, lines are expanded less, in particular concerning the foreign power lines e.g. between Austria, Switzerland and France. Overall, the endogenous system costs, similar to the lower dispatch costs decrease by 22 % in the most extreme case.

5.4 Sensitivity analysis on dispatch related parameters

5.4.1 Temporal resolution

Figure 5.25 shows how the modeling of the temporal resolution changes the overall endogenous system costs. Besides the sensitivity with the most coarse resolution of using every sixth hour of the year (*skip-6* sensitivity) the endogenous system costs are very much alike regardless of the considered resolution. Whereas the sensitivities *skip-4* and *skip-2* show slightly lower costs (below 0.3%) compared to the base assumption of choosing every fifth hour of the year, *skip-3* and *skip-6* have higher costs of 1.3 % and 9 % respectively. The considerably high difference of the latter primarily corresponds to 7 % higher dispatch costs. In contrast, the ones with a higher resolution have slightly lower dispatch costs (between 0.8 % and 2.6 %). Grid expansion costs are in all sensitivities in a range of 2.5 to 3.5 % higher. Also commonly higher values occur concerning storage expansion. In contrast, in this case, the difference is significant. The in principle superior temporal resolutions display all about 41 % higher storage expansion.

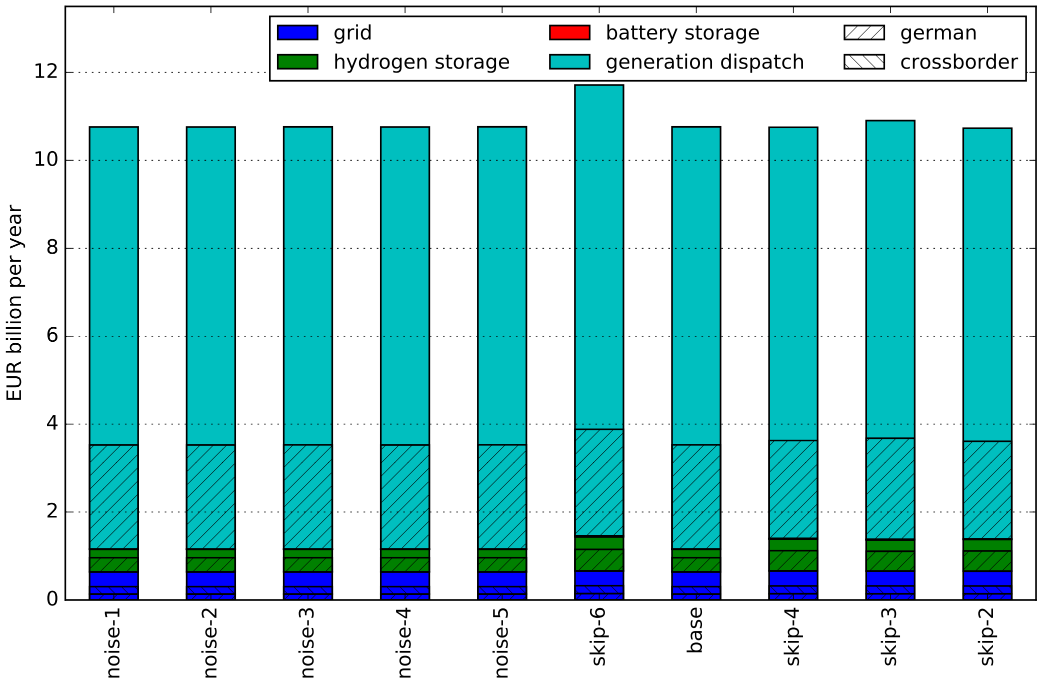

FIGURE 5.25: Annual endogenous system costs for different temporal resolutions and generators' marginal costs random noises. As the *skip-2* sensitivity represents a temporal resolution of every second hour of the year, the other *skip* scenarios use every third, forth, fifth (*base*) and sixth hour of the year. The *noise* sensitivities stand for different randomly generated marginal cost noises.

These higher storage capacities allocate mainly at the same buses where storage expansion occurs in the base scenario. Hence, the two main storage units in the base scenario become larger. Especially the storage unit at the Dutch border increases substantially by 63 % in the *skip-2* scenario. The one at the Polish border increases by 19 %. Apart from these main changes a small hydrogen storage unit (155 MW) is projected in Niebüll in northern Schleswig-Holstein and a small battery storage (291 MW) is situated at the southern interconnector to Poland.

5.4.2 The random noise on generators' marginal costs

The minor random noise (with a standard deviation of 0.01 EUR) on the marginal costs of the generators (as explained in Section 4.1.1) does not seem to have any influence on the results. In Figure 5.25, five results (indicated as *noise-1* to *noise-5*) being based on different noises are displayed. In all cost categories, out of all sensitivities, the maximal difference stays below 0.05 %.

5.4.3 Biomass power generation

Biomass power plants apart from gas fired plants are the only flexible generators in the *eGo 100* system being modeled with notable marginal costs. Due to the higher marginal costs, gas fired power plants are hardly dispatched at all in the presented results. In contrast, biomass power plants substantially supply flexible electricity. At the same time, the use of biomass electricity production has been critically addressed due to various reasons. Thus, e.g. Brown et al. (2018c) did not consider any biomass for energy use due to concerns about the sustainability of fuel crops and assuming that sustainable second-generation biofuels will be needed for the hard-to-defossilize sectors such as industrial process heat, aviation and shipping. Therefore, in this section it is analyzed if and how the system setting changes and performs if power production by biomass is available to a lower extent. In this sense, the installed capacities and the available biomass are downscaled in different sensitivity scenarios.

Installed capacities

In the *bio-NEP* sensitivity, the installed capacity of biomass power plants in Germany is downscaled to the *NEP 2035* capacity which is in the range of the status quo capacity. Thus, instead of 27.8 GW, 8.3 GW are installed in the German power system. The 19.5 GW fewer biomass power plant capacity is partly compensated by higher full load hours. Nevertheless, the annual energy production by biomass plants is reduced by 5 %. The missing energy is compensated by fluctuating wind and solar generation. Hence, onshore wind and solar potential generation is curtailed about 10 % less. Wind offshore potentials are exploited even 20 % more. This is only possible by investing substantially more into the grid and storage infrastructure (see Figure 5.27). Whereas the grid expansion annuity only rises by 6 %, storage expansion costs increase by a factor of 2.4. Although the investments lead to 2.5 % lower overall dispatch costs, the endogenous costs are 5 % higher compared to the base scenario results.

Spatially, the grid expansion in Germany stays very much alike. The main differences occur on the cross-border expansion towards Austria and the Czech Republic. These changes facilitate higher imports. Consequently, some of the lacking flexible energy in the south is compensated by higher imports from the southern neighbors, France, Switzerland, Austria and the Czech Republic. Overall, the net imports increase by 54 % leading to 19 %. Moreover, the imports are enabled by storage expansion at various interconnectors. Battery storage units are projected at the border to Switzerland (920 MW), Poland(1035 MW) and the Netherlands (500 MW). Hydrogen storage units are located at the DC cable to Sweden (180 MW) and in Flensburg (560 MW). Furthermore, to harvest more on- and in particular offshore wind power, the hydrogen storage units at Dörpen West (8 GW) and in the Netherlands (6.7 GW) are expanded to a much higher degree. Apart from these large central storage units (the one at the Polish border is also still feasible (3.7 GW)), smaller ones in Schleswig-Holstein in Husum (560 MW), Niebüll (410 MW), Rendsburg (300 MW) and Büttel (140 MW) are needed. The storage unit at the Polish border is accompanied by two medium sized hydrogen storage: a 1.7 GW near Berlin and another one with a capacity of 860 MW in Mecklenburg-West Pomerania near Neubrandenburg.

Combining the *bio-NEP* approach with the assumption that grid expansion in Germany can be expanded without upper bound (as evaluated in Section 5.2.2) the main difference is that the storage in Dörpen West can be sized substantially smaller (2.9 GW). Instead the grid expansion from Dörpen West southwards is more than doubled reaching 20 GW. Overall, grid expansion rises, whereas storage expansion slightly decreases leading to slightly smaller overall endogenous costs, although still above the base scenario results (2.7 %) (see Figure 5.27 sensitivity *bio-NEP_D-inf*).

Additionally, the just explained setting is combined with the approach to model the cross-border interconnectors from Germany to its neighbors as DC cables (as evaluated in Section 5.2.1). This leads to the additional effect that more inner-German grid expansion, in particular from middle-western and eastern Germany towards the south, substitutes grid expansion in neighboring countries and storage expansion near the Polish border. Moreover, storage expansion is mainly happening in Northern Germany as hydrogen storage in a rather distributed way with installed capacities of up to 700 MW (for the spatial allocation see Figure 5.26). A distributed allocation of small battery storage units, although for the overall results hardly important, are feasible at many buses in the Ruhr area. Overall, this setting is 4 % cheaper than the solution in the base scenario (see Figure 5.27, sensitivity *bio-NEP_D-inf_cbdc*) reaching 74 % more grid and 26 % more storage expansion and being 17 % less dependent on imports from the neighboring countries.

Assuming no available biomass capacity in Germany but instead 20 % more wind and solar capacity in the entire system, the spatial allocation of grid and storage expansion is principally similar to the one in the *bio-NEP* sensitivities. Whereas grid expansion also lies within the same overall range, the storage capacities in the *bio-NEP* sensitivities are upscaled, in total by a factor of 1.3 in the *bio-0_vRE-1.2*

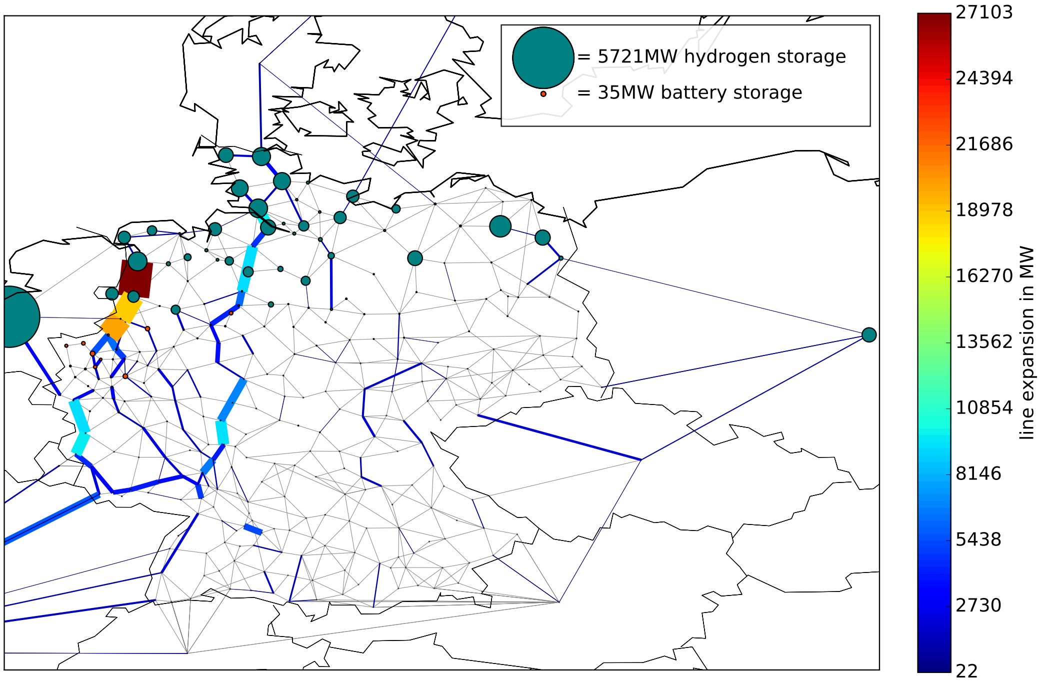

FIGURE 5.26: Spatial allocation of grid and storage expansion for the sensitivity *bio-NEP_D-inf_cbdc* with a *NEP 2035* biomass capacity in Germany, unrestricted grid German grid expansion and a cross-border DC flow approach.

scenario (see Figure 5.27) leading to 3.2 higher storage expansion costs compared to the base scenario results. In the *bio-0_vRE-1.2_cbdc* variant, the usual shift from storage expansion to grid expansion occurs. This setting leads to dispatch costs, which in Germany are non-existent, and in total are about 30 % lower than in the base scenario. These lower costs overcompensate the high investment costs ending up with a 20 % less costly system in endogenous terms. Due to the 20 % higher exogenous capacity of solar and wind and the non-existent biomass capacity in Germany, the generator investment annuity becomes 8 % higher accounting for 6.2 bn. EUR per year. Thus, the higher exogenous costs overcompensate the 2.3 bn. EUR lower annual endogenous costs.

Restrictions on maximal full load hours

Another central aspect of biomass energy production is the resource availability. In a sensitivity scenario *bio-flh* the full load hours of the *eGo 100* biomass plants of each country are set as an upper bound for the annual production with respect to the e-Highway results (e-Highway 2050 project, 2015b). This approach has been applied by Wingenbach (2018) arguing that these full load hours (2514 h in Germany) in combination with the installed capacities (27.8 GW in Germany) lead to a reasonable resource consumption of 70 TWh/a.

As shown in Figure 5.27, this restriction has a significant impact on the results. Overall, the endogenous system costs rise by 14 % being originated by 174 % more

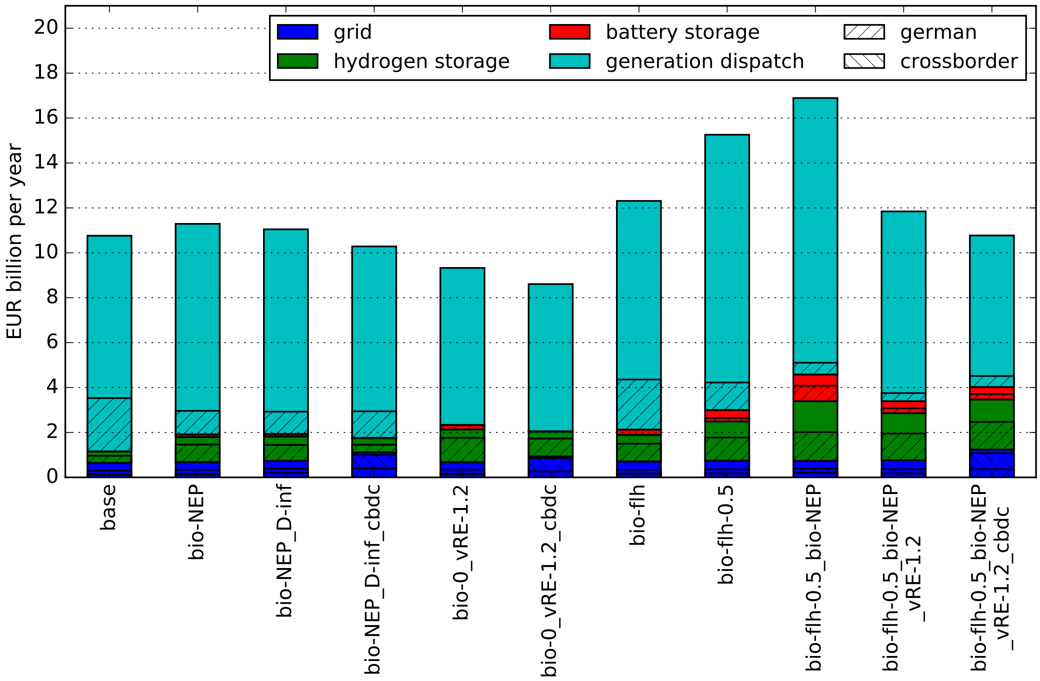

FIGURE 5.27: Annual endogenous system costs of sensitivity scenarios with different biomass power settings in terms of available capacities and resources.

storage expansion, 11 % more grid expansion and at the same time 6 % higher dispatch costs. In contrast, logically in Germany the dispatch costs are reduced (by 6 %) due to the lower possible dispatch of biomass power plants. In the foreign countries the biomass generation has to be reduced as well but is not only compensated by more dispatch of fluctuating RE but also by dispatch from gas fired power plants. Especially Poland, Czech Republic, Austria and France use this fossil energy significantly, leading to overall full load hours of 1894 h of the 28.5 GW installed capacities. This fossil power generation compensates 70 % of the 76 TWh fewer biomass power generation. The remaining 30 % are supplied by a higher usage of available RE sources. Hence, solar curtailment, mainly due to the mentioned higher investment into storage expansion, is reduced to 11.5 %, wind on- to 20.3 % and offshore to 25.6 %.

Spatially, the storage expansion in the foreign countries is characterized by a big hydrogen storage unit in the Netherlands as well as battery storage units in France and Poland. In Germany, the big storage units at Dörpen West and at the Polish border are upscaled to 9 GW and 5.9 GW. Additionally, a hydrogen storage capacity of 1.7 GW, subdivided as four units, is installed in northern Schleswig-Holstein.

The sensitivity *bio-flh-0.5* restricts the available biomass resource once more. The e-highway upper limits per country from the *bio-flh* sensitivity are averaged over all countries. This value is then halved in order to reach the order of magnitude of today's biomass production (comparing the resulting German upper limit with its electricity production from 2017 of 32 TWh (BMWi, 2017)). As a consequence, storage expansion rises once more to be 4.4 times higher than in the base scenario, whereas grid expansion only slightly increases. The storage capacities allocate similar to the distribution in the *bio-flh* scenario, only that the units are upscaled. A new hydrogen storage unit of 1.4 GW is situated at the Danish bus. Although the investments enable a slightly higher utilization of fluctuating RE, overall dispatch costs rise by 28 % due to a significant dispatch of gas fired power plants in the neighboring countries. These power plants reach in total full load hours of 5409 h. Together, the high investment into storage units and the substantial use of fossil gas lead to 42 % more endogenous system costs.

The most restricted sensitivity is designed as a combination of the *bio-NEP* and the *bio-flh-0.5* sensitivity. Hence, the maximal full load hours of biomass production for the entire system of 1209 h are coupled with a reduced German capacity of 8.3 GW. As Figure 5.27 shows, this setting leads to the highest storage expansion and overall endogenous costs of all sensitivities (sensitivity *bio-flh-0.5_bio-NEP*). Compared to the *bio-flh-0.5*, the dispatch costs only rise marginally. The higher gas fired power plants dispatch (9 % increase) is compensated by 21 % less biomass production. The high storage expansion (640 % higher than in the base scenario, 42.3 GW alone in Germany) enables comparably very low curtailment rates (solar: 7.5 %, onshore wind: 16 %, offshore wind: 21 %) but cannot overcompensate the missing biomass production leading to 57 % higher overall endogenous costs compared to the base scenario. This expensive setting comes along with the highest net importing behavior of Germany compared to all other sensitivities. 21 % of the German load has to be produced in other countries.

The incorporation of 20 % additional wind and solar capacities, as realized in the *bio-flh-0.5_bio-NEP_vRE-1.2* sensitivity, affects the results substantially. The fewer biomass production can now be substituted by solar and wind power production to a higher extent with the help of less storage expansion (410 % more than in the base scenario). Nevertheless, in the neighboring countries the gas fired power plants are still dispatched, reaching 3490 full load hours.

Additionally, reducing passive flow effects by modeling all cross-border lines as DC lines (*bio-flh-0.5_bio-NEP_vRE-1.2_cbdc*, see Figure 5.27) stimulates higher grid expansion in Germany (170 % net increase) and on the cross-border lines from Germany to the neighboring states (320 % net increase). At the same time investment into the lines interconnecting the neighboring states are halved. Spatially, this effect can be observed in Figure 5.28. Storage expansion remains to be rather high (31.3 GW in Germany), but due to the DC approach is generally shifted from the east to the west. Although the gas fired power plants in the neighboring countries still reach 2427 full load hours, the dispatch costs are effectively lowered by 30 % compared to the base scenario. Consequently, solar and wind generation reach a significantly higher share of the total production (72 % compared to 63 % in the base scenario). The lower dispatch costs compensate the higher investment costs, such that the total endogenous costs are the same as in the base scenario. One has to bear in mind, that (as stated in the previous section) the additional wind and solar capacity together with the lower biomass capacity sum up to 7.3 bn. EUR/a higher annualized exogenous costs.

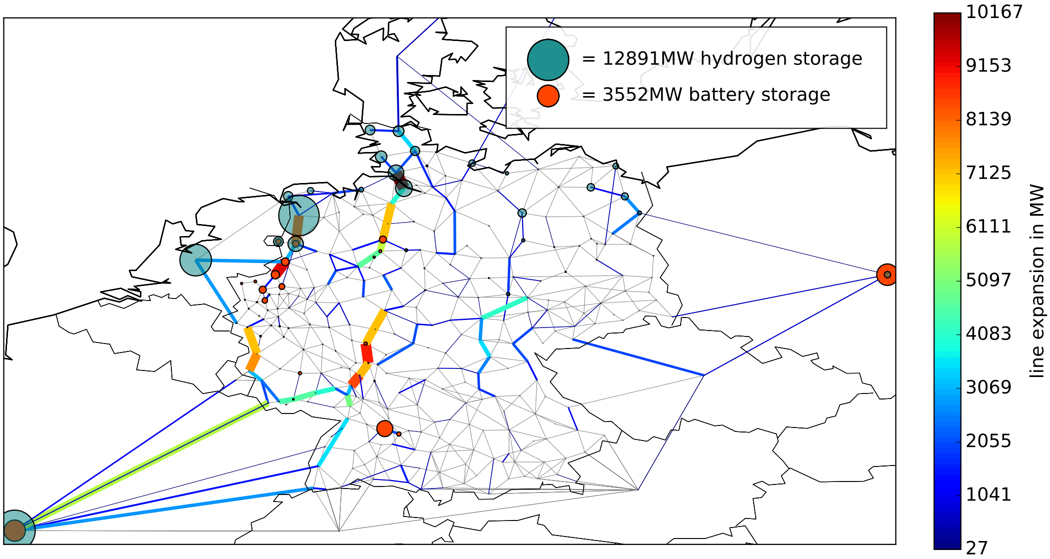

FIGURE 5.28: Spatial allocation of grid and storage expansion for the sensitivity *bio-flh-0.5_bio-NEP_vRE-1.2_cbdc* with a status quo biomass capacity and resource setting and 20% higher installed capacities of solar and wind generators.

5.4.4 Solar and wind power generation

The most important fluctuating RE sources are wind and solar. Their presence characterizes the German electricity system transformation predominantly and motivates grid and storage expansion. As their development is not part of the optimization, in this section it is analyzed how the results change when one modifies the installed capacities or restricts the maximal possible curtailment.

Installed capacities

As one can see in Figure 5.29, grid expansion stays rather constant throughout the sensitvities from *vRE-0.8* up to *vRE-1.2* representing a range of ±20 % installed solar and wind capacities (equally scaled). In Germany, grid expansion increases slightly with rising existence of solar and wind capacity (by 5 % in the *vRE-1.2* sensitivity with 20 % more installed wind and solar capacity). This effect is overcompensated by a decrease of expansion costs concerning the interconnectors between the neighboring countries. Especially between Denmark and Sweden less capacity is needed. Overall, the grid expanion costs are lowered up to 5 %. Besides very slight changes, spatially, no significant changes between the different scenarios can be observed.

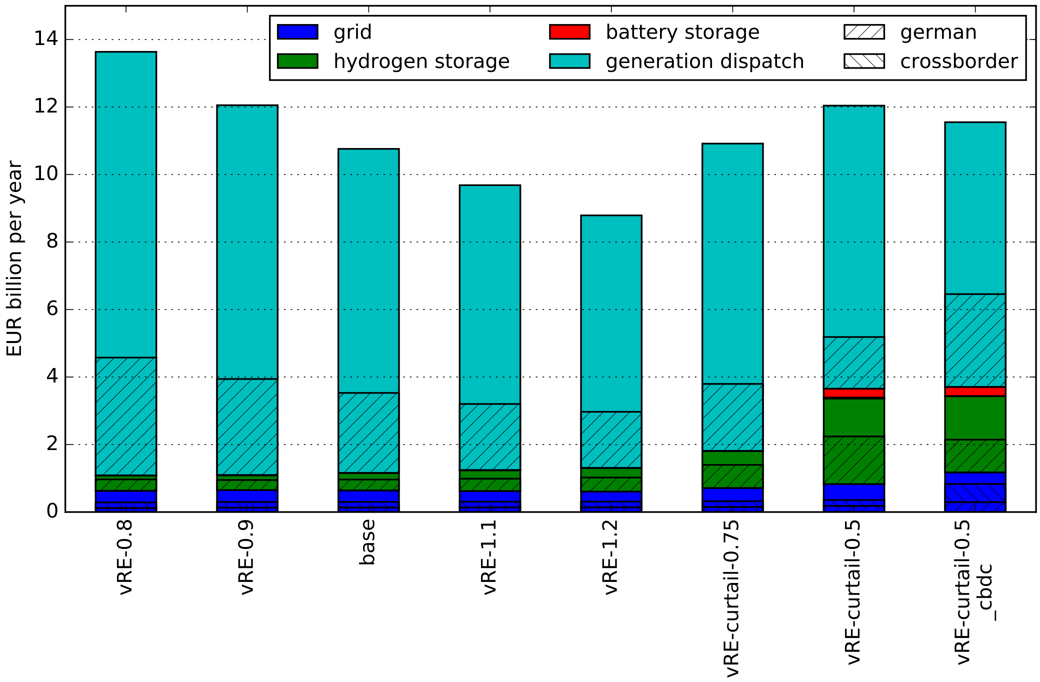

FIGURE 5.29: Annual endogenous system costs for sensitivity scenarios of different solar and wind power expansion settings and their maximal possible curtailment.

In contrast, storage expansion reacts more sensitively. Especially with rising solar and wind capacities, storage expansion increases up to 35 % in the *vRE-1.2* sensitivity. On the other end, in the sensitivities *vRE-0.8* and *vRE-0.9* storage expansion is 12 % and 14 % lower. Spatially, mainly the two big storage units are scaled. In addition, in the *vRE-1.1* sensitivity a small hydrogen storage unit (76 MW) in Niebüll in northern Schleswig-Holstein is feasible. This trend becomes stronger when the capacities are scaled by a factor 1.2. Hence, the storage near Niebüll becomes larger (297 MW) and is accompanied by one in Flensburg (122 MW) and another one in Husum (63 MW).

The biggest change is certainly connected to the dispatch. The dispatch costs decrease almost linearly (with a slightly decreasing slope) anti-proportional to the increase of solar and wind capacity. Consequently, the dispatch costs in the *vRE-0.8* sensitivity are 29 % higher and the ones in the *vRE-1.2* sensitivity 22 % lower. This trend correlates directly with the change in the dispatch of biomass power plants (gas fired power plant dispatch does not occur). In the *vRE-1.2* setting, the biomass power plants altogether have 2515 full load hours. In contrast, in the other extreme case, they rise up to 4208 h. The differences in dispatch costs almost completely translate into the overall endogenous cost development. Solely, in case of higher costs, the fewer investment costs and in case of lower costs, the more investment costs slightly attenuate the effect. However, the endogenous cost development of +3 and -2 bn. EUR/a comes to a price of an endogenous costs development of ±9.8 bn. EUR/a.

Maximal curtailment

Since the overall curtailment rates of solar (13.5 % i.e. 40 TWh), wind on- (22.8 % i.e. 154 TWh) and offshore (32.4 % i.e. 109 TWh) are considerable, the question is how the results change if the unrestricted curtailment is forced to a lower upper bound. Thus, the mentioned economically optimal curtailment rates from the base scenario are reduced by 25 % (i.e. sensitivity *vRE-curtail-0.75*) and 50 % (i.e. sensitivity *vRE-curtail-0.5*). Naturally, the overall costs will be more expensive, as illustrated in Figure 5.29.

In order to stay below the target value, more investment into grid and storage is necessary. In the *vRE-curtail-0.5* sensitivity, grid expansion costs are 29 % higher and investment into storage rise by a factor of 5.5. Although the dispatch costs are being reduced by these means to 87 % of the original value, the endogenous system costs rise by 12 %. When modeling the German cross-border lines as DC lines the overall cost increase is reduced to 7 % (sensitivity *vRE-curtail-0.5_cbdc*). Here, more grid expansion and fewer storage expansion lead to higher dispatch savings. Germany is then only net importing 5 % of its electricity, which is 60 % less than in the base scenario. Spatially, grid and storage expansion allocate similar as displayed in Figure 5.28, except that the order of magnitude of storage expansion is 10 % and of grid expansion is 5 % lower. In particular, the battery expansion in Germany is not being modeled in this scenario. In contrast, the big hydrogen storage at the western north-sea offshore feed-in bus is about 1 GW larger (see Figure 5.30).

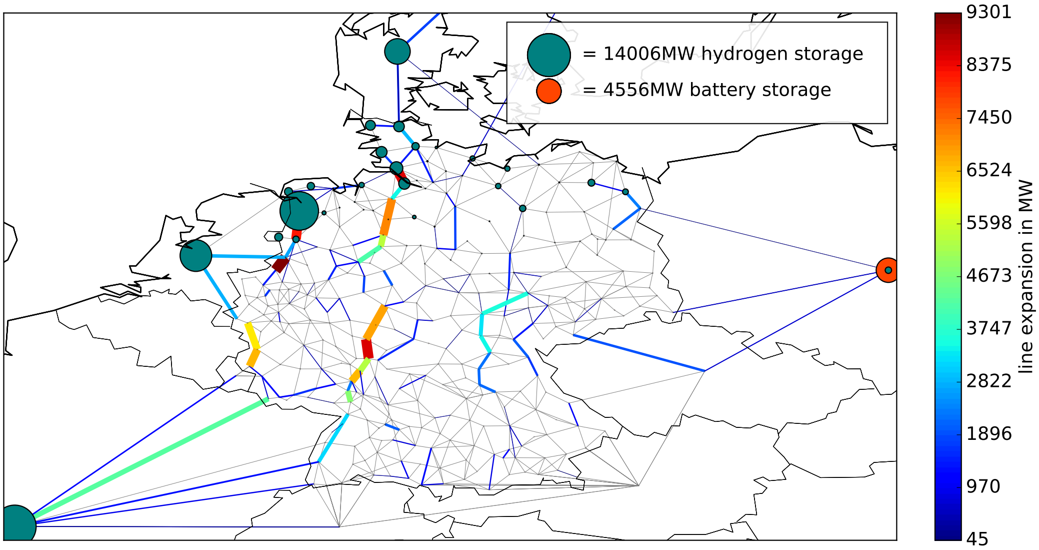

FIGURE 5.30: Spatial allocation of grid and storage expansion for the sensitivity *vRE-curtail-0.5_cbdc* with a maximal curtailment of solar and wind potentials of 50% of the economically optimal values of the base scenario.

As the above mentioned curtailment rates are halved, the biomass full load hours are reduced to 2641 h. In contrast, in Germany the curtailment rates in the base scenario are lower (3.8 % solar, 10.6 % wind on- and 21 % wind offshore potential are curtailed) and are reduced in the *vRE-curtail-0.5_cbdc* to very low values. Thus, solar power is curtailed by 1.2 %, onshore wind by 0.9 % and offshore wind by hardly any means. At the same time, biomass full load hours in Germany are with 3128 h higher than in the overall system.

Chapter 6

Discussion

In this section, the results presented in the previous section are at first compared to results from state-of-the-art research (presented in Section 2). The comparison aims to interpret the results considering the status quo of relevant research. Furthermore, the results are addressed critically by pointing out weakness and limitations of the applied methods. Finally, the research hypotheses from Section 3 are assessed.

6.1 Comparison of the results to state-of-the-art scenarios

The comparison exclusively focuses on studies, which generate results for Germany or Europe. The most relevant works from transmission, sub-transmission and systematic grid expansion planning, storage expansion planning and co-optimized approaches are taken into consideration. Since the combination of co-optimization and spatial detail of this work is innovative, studies which somewhat meet these criteria are concentrated on. Furthermore, official reports like the German *NEP* or the European *TYNDP*, due to their high degree of concrete relevance are of particular interest.

Besides the results of the *NEP 2035* scenario and a few special evaluations (in particular in context of Section 5.2.3), all results for the *eGo 100* scenario (base case and 87 sensitivities) are summarized in Figure 6.1. Several boxplots depict how the annualized costs spread concerning the optimization variables i.e. dispatch, grid and storage expansion. Moreover, the sum of these annualized costs i.e. the total endogenous system costs are displayed. The median, quartiles and whiskers give a graphical impression of the variability of the 88 different results. In addition, besides the *eGo 100* base results nine other sensitivity results, which will be directly referred to in the following discussion, are explicitly plotted emphasizing their position within the data set range. Thus, the visualization of the results' range shall serve the comparison to results generated by other studies.

The line-sharp official TEP for Germany, the *NEP* (50Hertz et al., 2015b) reveals significantly higher grid expansion costs compared to all results generated in this work. In particular, 50Hertz et al. (2015b) calculated costs between 20 to 36 bn. EUR (until 2025), which being annualized (by assuming the same assumptions on interest rate and component lifetime as stated in Section 4.1), translate to a range between

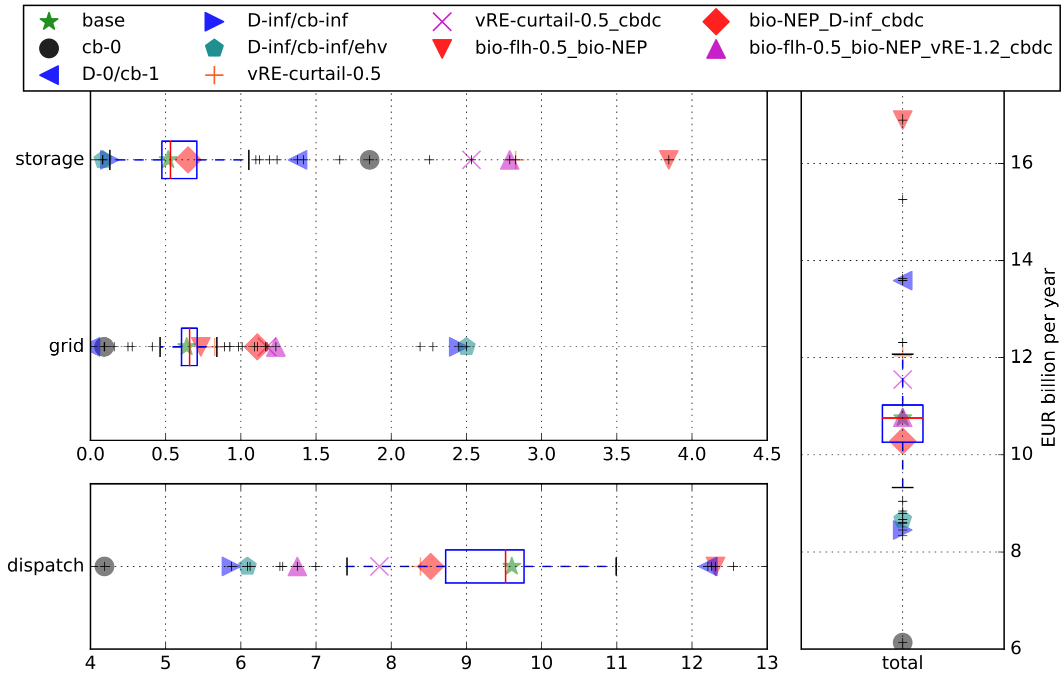

FIGURE 6.1: Boxplots with median, quartiles, whiskers (1.5 of the interquartile range) and outliers of the annual costs (in EUR billion per year) of the optimization variables grid, storage expansion and dispatch as well as the resulting total endogenous system costs for the *eGo 100 - base* scenario and its 87 sensitivities. A selection of important solutions are explicitly plotted. Note that, the *cb-0* only accounts for the German system costs. Moreover, mind that for some sensitivities, the exogenous costs change.

1.2 and 2.1 bn. EUR/a. In contrast, the adapted *NEP 2035* base scenario depicts for the inner-German grid expansion costs of 82 million EUR/a (1.4 bn. EUR overnight costs, cf. Table 5.1). Out of many reasons, the most important methodical difference is that the official *NEP* does not co-optimize grid with storage investment and generation dispatch decisions. Storage investment adds 103 million EUR/a to the investment costs and allowed curtailment rates for wind power generation are with 7.6 % (offshore) and 4.5 % (onshore) higher than the allowed 3 % maximal curtailment rate in the official *NEP* approach. Spatially, the calculated expansion corridors (as in Figure 5.1) are principally in line with the official planning. Beyond these measures, the official *NEP* plans with far more projects e.g. a DC overlay grid, which is not considered as an option in this work. It can be stated, that (considering a different modeling approach) significantly less grid expansion is necessary leading to an economical optimal solution for the year 2035 while accepting a lower share of RE.

In the long term 100 % RE future, the *eGo 100* scenario results get closer to the ones proposed by the official *NEP*. Nevertheless, the German grid expansion costs in the base scenario still end up comparably low but are accompanied by a more than three times higher storage investment (see Figure 6.1). Yet, the sum of these two investment costs remains to stay below the proposed *NEP* costs (at least by 66 %). If grid expansion is not restricted by an upper bound, the gap becomes smaller once more. The sensitivities *D-inf/cb-inf* and *D-inf/cb-inf/ehv* reach the highest grid expansion costs (see Figure 6.1). Hence, together with storage expansion, these two sensitivities end up with only 23 % and 37 % lower investment costs for Germany. In these scenarios the investment pays off due to lower dispatch costs becoming the most cost effective solutions in total (see Figure 6.1). Theses lower dispatch costs are explicitly reached by significantly reducing offshore wind curtailment. In contrast, in the *vRE-curtail-0.5* sensitivity the curtailment rates of all fluctuating RE are forced to be halved. This restriction, which methodically goes into the direction of the *NEP* assumptions, leads to high investment costs. Considering the upper bound of grid expansion, especially storage expansion is comparably high. Consequently, with 1.6 bn EUR/a, the joint annuity of German grid and storage expansion (of which almost 90 % are storage costs) is in the range of the *NEP* results. Furthermore, the sensitivities have shown that modeling the crossborder interconnectors as active DC elements, which may be represented by phase shifting transformers to countries like Poland and the Netherlands, leads to higher possible grid investments, which are in line with the *NEP* projections and partly avoid more costly storage expansion. Hence, in case of the *vRE-curtail-0.5_cbdc* variant, the overall German investment costs are reduced to 1.3 bn EUR/a (of which 70 % are storage costs).

On the German distribution grid level, two prominent studies (i.e. Agricola et al., 2012; Büchner et al., 2014) have generated grid investment costs for two scenarios from 50Hertz et al. (2012) for the year 2030 which are intended to be complementary to the costs in the transmission grid. Depending on the scenario, Agricola et al. (2012) calculated 932 million or 1.5 bn. EUR/a (annualized by the author) for the sub-transmission grid. The more up-to-date study, Büchner et al. (2014) identified according to the same scenarios 19 % to 14 % lower costs and stated that if no underground cables are necessary the cost reduce to one third. Consequently, the lowest annuity of 252 million EUR/a is probably the value closest to the results presented in this work, which does not consider cabling costs. However, due to the holistic optimization approach, once assuming significantly higher specific investment costs (see Section 5.2.4), physical grid expansion is reduced to a necessary minimum avoiding an increase of grid expansion costs.

Although the sub-transmission grid is included providing additional level of spatial detail, due to the clustering approach, it is not possible to clearly distinguish voltage level specific costs. Nevertheless, it is obvious that the investment costs are mostly allocated to the transmission corridors. This becomes clear when comparing the integrated results with the EHV-only results (see Section 5.2.3). In contrast, the most prominent example for clear HV grid investment can be observed in Schleswig-Holstein. In particular, the lines from the west coast south- and eastwards are expanded significantly for the transport of onshore wind. The general finding of minor grid investment in the HV level applies for all sensitivities. However, two effects i.e. increasing spatial detail (see e.g. the *k-500* sensitivity) and the obligation to harvest more distributed fluctuating RE (cf. e.g. sensitivities *bio-flh-0.5_bio-NEP_vRE-1.2_cbdc*, Figure 5.28 and *vRE-curtail-0.5_cbdc*, Figure 5.30) lead to more investment into the HV level.

Furthermore, in contrast to the consecutive, separated approach in the mentioned state-of-the-art studies (without an holistic optimization), which produces additional grid expansion costs, the evaluation of the integrated EHV/HV grid modeling in Section 5.2.3 shows that considering the HV level leads to less overall grid expansion in Germany. Additionally, the power plants can be dispatched more cost effectively. Hence, the systematically positive effect of transit flows overcompensates the negative effect of considering HV grid restrictions. This result principally stays in line with the results from van Leeuwen et al. (2014) and Hoffrichter et al. (2018), which first revealed significant transit flows on the HV level. However, in Müller et al. (2018a) it was falsely concluded that the effect of considering HV bottle necks outnumbered the effect of adding additional transport capacities leading to overall higher system costs. This distorted finding was biased by a false representation of the HV line reactances in the clustered grid and has been corrected in the context of the evaluations in Section 5.2.3.

This code bug affected the results of other previous paper (i.e. Wienholt et al., 2018; Müller et al., 2019b) as well. Moreover, compared to the latter mentioned (which also co-optimized grid and storage expansion), three additional changes, which have a comparably low influence on the results, are realized. First, the LOPF is iterated four additional times (instead of one) after the first run. Second, minor inaccuracies concerning the exogenously defined generation capacities were corrected. Third, the inner-German upper limit for expansion was changed to a voltage level specific absolute value instead of a uniform relative value (four times the status quo capacity). Consequently, the results of this work to the ones in Müller et al. (2019b) are different to some extent. Whereas the spatial distribution of hydrogen storage expansion is similar, battery storage units were feasible in the base scenario setting. Overall, storage expansion was calculated twice as high compared to the *eGo 100* base scenario results. Grid expansion was a lot more distributed and did not have this clear focus on transmission corridors. This difference in grid expansion, in particular when comparing the results with other studies, makes the more recent results of this work appear more plausible. Overall grid expansion costs were 20 % lower, whereas in Germany 80 % higher.

Various TEP studies (i.e. Brown et al., 2016; e-Highway 2050 project, 2015a; Papaemmanouil et al., 2010; Schaber et al., 2012b,a) have derived results for entire Europe. Unfortunately, they did not specify the grid expansion costs for Germany. Then again, since the scope of this work does not cover entire Europe, it is not possible to quantitatively compare the results to these studies. In qualitative terms, a basic similarity can be observed to e-Highway 2050 project (2015a) stating that an invariant set of reinforcements including major North-South corridors connecting Scandinavia and Northern Germany has been determined throughout all scenarios. Apart from the interconnectors to Denmark and Sweden which are extended at least four times their original capacities in basically all sensitivities, also the interconnector to Norway in the corresponding sensitivity *Be-No* is expanded to the model-specific highest possible extent. Focusing on the 100 % RE scenario (which was the base for the *eGo 100* scenario), the finding that additional interconnector capacities from Southern Germany to Switzerland and Austria are rarely or not needed is also in line with the e-Highway 2050 project (2015a) results. Higher interconnections from Germany to the Netherlands, Poland and France are congruent as well, whereas the additional crossborder capacities to the Czech Republic are not determined by e-Highway 2050 project (2015a).

As described in Section 2.2, storage expansion has been derived for Germany and Europe without considering grid constraints or its optimization. Schill (2014), modeling Germany as an copper plate island, stated that storage investment is hardly necessary until 2032 (assuming a power system as proposed by 50Hertz et al. (2012)) if flexible power plants are existent and curtailment of 1 % of the annual potential production of fluctuating RE is allowed. This finding is basically in line with the results of the *NEP 2035* scenario. Furthermore, Schill (2014) calculated for a scenario of the year 2050, which assumed 27 % lower demand and significantly lower generation capacities as in the *eGo 100*, a storage expansion in the range of 10 to 54 GW depending on the allowed curtailment. The lower end is characterized by an unrestricted curtailment. Despite all the modeling differences, the storage expansion of 14.6 GW or 8.8 GW in the sensitivities with only status quo (*cb-1*) or possibly twofold crossborder capacities (*cb-2*) are close to the lower end calculated by Schill (2014). In case of the other extreme, the sensitivities with forced lower curtailment, show significantly increased storage expansion in a comparable order of magnitude. Compared to the base scenario, storage expansion in Germany increases then maximally by a factor of 4.5 (*vRE-curtail-0.5* sensitivity). Actually modeling Germany as an autarkic island, although assuming optimal curtailment, lead to 40.4 GW storage expansion, far above the 10 GW proposed by Schill (2014).

In Wienholt et al. (2018), without considering grid expansion, for a 67 % RE share in the *NEP 2035* scenario 13.6 GW storage expansion were calculated. The co-optimized results for the same scenario show that most of the storage expansion can be substituted by grid expansion. In particular, the storage expansion driven by offshore wind feed-in can be substituted entirely by grid expansion. Applying the basic assumption of disregarding grid expansion as in Wienholt et al. (2018) to the *eGo 100* scenario, 22.6 GW storage expansion in Germany are feasible (sensitivity *D-0/cb-1*). In contrast, the co-optimized solution in the base setting needs 3.4 times less storage.

Cebulla et al. (2017), using the model *REMix*, determined storage expansion of 30 GW for Germany assuming an exogenous grid based on ENTSO-E (2012). The majority of expansion is realized by hydrogen (10 GW) and battery storage (16 GW). Although these values are higher compared to the results in this work, a major finding of Cebulla et al. (2017) can be confirmed. The long-term hydrogen storage units are utilized primarily for offshore wind feed-in. Therefore, similar to the results of this work, the largest storage expansion capacity (as hydrogen storage) occurs, in their region model, in the northwest of Germany. Apart from this similarity, the rather homogeneously wide-spread battery expansion throughout the country cannot be shown by this work. Only if the flexible biomass power feed-in is restricted and fluctuating RE capacities are increased, battery storage units become an option (apart from a massive drop in specific investment costs). Then, storage expansion in Germany reaches up to 42.3 GW (15.5 GW battery and 26.8 GW hydrogen storage). On the one hand, since Cebulla et al. (2017) still counted on flexible conventional generation, at least in the order of magnitude of the assumed biomass plants in the *eGo 100* scenario, it seems unlikely that these sensitivities are comparable. On the other hand, the higher marginal costs of conventional power plants promote investment into storage. However, another central finding of Cebulla et al. (2017) was that battery expansion correlates with solar power feed-in due to the diurnal characteristics. As the share of solar power in the exogenously defined generation capacities is substantially higher than in the *eGo 100* scenario, this might explain less solar driven storage expansion.

Furthermore, Cebulla et al. (2017) performed one sensitivity with endogenous interzonal grid expansion. Consequently, storage expansion was reduced significantly by 39 %. In particular, the hydrogen storage expansion could be substituted. The same substituting effect, although to a higher extent, can be observed in this work.

As in this specific sensitivity, other studies have generally focused more on a co-optimized approach and generated results for Europe as well. Due to the European focus, absolute cost values cannot be compared. Consequently, mostly general effects and relative parameters such as LCOE are used for comparison. The model *GENESYS* has been used for many publications. Rather recently, Bussar et al. (2016) have derived concrete results for the EU/MENA power system in 2050. The above mentioned correlation of wind power feed-in and long-term hydrogen storage is emphasized by the authors as well. In contrast to Cebulla et al. (2017), more in line with this work's results, the majority of the storage expansion is projected as hydrogen storage although the overall power plant portfolio is solar-dominated due to the consideration of southern countries. These costs are more than four times higher compared to the ones generated by investment into batteries. Although, surprisingly, besides hydrogen storage appearances in the northern countries, Bussar et al. (2016) do not model any in Northern Germany. The overall costs for grid and storage in terms of LCOE are very high compared to results in this work. Whereas the total storage expansion in this work accounts for at most 2.5 EUR/MWh (0.3 EUR/MWh in the base scenario), Bussar et al. (2016) calculated LCOE of about 15 EUR/MWh for hydrogen and 3 EUR/MWh for battery storage. A reasoning for this difference could be given by the spatial distribution of the storage units revealing that the vast majority is installed in southern countries, which are not considered in this work.

As the grid investment costs of almost 10 EUR/MWh are far higher than at most 4 EUR/MWh (2 EUR/MWh in the base scenario; including the value of the status quo grid), it can be assumed that the longer lines surrounding central Europe account for a non-linear cost increasing effect. In principal, the average optimal grid expansion of 5-10 GW per interregional connection is in line with this works's results, especially when comparing them with the unrestricted grid expansion sensitivities.

Pleßmann and Blechinger (2017) also modeled a power system for the year 2050 with almost 100 % RE production. However, the necessary investment costs are a lot closer to the results derived in this work. Apart from grid expansion (LCOE of about 2 EUR/MWh), power-to-gas-to-power storage provided the main flexibility leading to approximately 2.5 EUR/MWh (accompanied by battery storage accounting for about 0.5 EUR/MWh). These costs are still located at the upper end of the cost range calculated in this work, yet that the two flexibility options show a certain degree of inverse correlation. In the case of highest combined grid and storage investment costs (*bio-flh-0.5_bio-NEP* sensitivity) the LCOE for grid (2 EUR/MWh, including the value of the status quo grid) and storage (2.5 EUR/MWh) are very similar to the above mentioned values. Yet, this sensitivity accounts for about twice as much flexible generation (hydro, gas, biomass) as in Pleßmann and Blechinger (2017). One can assume that with less availability of these non-storage and non-grid flexibilities, costs would rise significantly. Spatially, grid expansion in Pleßmann and Blechinger (2017) show some similarities. The interconnectors from Denmark and Sweden to Germany are expanded substantially. The first mentioned interconnector shows the highest absolute expansion in the system enabling high exports of wind power generation from Denmark to Germany. The same effect can be especially well observed in the *D-inf/cb-inf* sensitivity. Here, the final capacity with 37 GVA, additionally substracting the (n-1)-security margins, is in a comparable range with the 20 GW from Pleßmann and Blechinger (2017).

Whereas most of the studies show somewhat higher LCOE, Child et al. (2019) derived significantly lower overall LCOE of 51 EUR/MWh. They argued that "significantly lower costs of storage and markedly lower costs of interconnections contributed to lower LCOE" Child et al. (2019, p. 97). In this sense they saw great potential for an altruistic prosuming behavior, which favors battery storage investment being an important flexibility option in their modeling. Nevertheless, in northern countries gas storage was seen to provide more flexible energy. The overall relevance of storage investment was comparably high, accounting for a share of up to 28 % of the LCOE. Besides storage expansion, they modeled fourfold grid expansion compared to the status quo. In this study's base scenario, the crossborder lines are overall only doubled. However, in the unrestricted variant (sensitivity *D-inf/cb-inf* the crossborder lines from Germany to other countries reach, three, and the other foreign lines, four times the size of today's capacity. Moreover, Child et al. (2019) showed that the majority of the grid expansion is needed before the year 2035. This result can be backed up by this work's findings, which show that the vast majority of the grid expansion in the base scenarios is already feasible in the *NEP 2035* scenario.

Modeling Europe at a spatial scale of 118 nodes, Held et al. (2018) claimed to combine the co-optimization approach with a high spatial resolution. Certainly, out of the European transshipment models considered in this work, they modeled the highest number of grid buses. With a LCOE share of 1.5 Euro/MWh, grid investment is expected to be rather low only accounting for at most 2.6 % of the overall system costs. In comparison, in the *eGo 100* base scenario, 4 % of the system costs are assigned for grid investment. Although Held et al. (2018) only reaches a RE share of 70 % the results seem somewhat comparable because in the *eGo 100* base setting the flexible hydro and biomass power plants reach about 40 % of the total power generation. Adding hydro and biomass production to the 30 % fossil production, Held et al. (2018) modeled almost 50 % of the generation as flexible generation. Therefore, it does not seem astonishing that they conclude that besides the existing pumped storage units no additional storage units are necessary. The manifold sensitivities in this work verify that grid expansion is more cost-effective than storage expansion. Moreover, the need for both increases if the availability of flexible generation (e.g. from biomass) decreases.

Similar to Held et al. (2018), Zappa et al. (2019) did not model any storage expansion needs. In contrast, they modeled a system with a 100 % RE share. However, similar to the results in this work, flexible biomass production played an important role providing about 20 % of the total generation. Overall, the share of fluctuating RE stayed below 70 %. The grid expansion, modeling country-to-country interconnections, is with 240 % more grid than today and a 4.7 % share in system costs comparable to the results derived in this work.

Apart from the explicit grid expansion plans, none of the so far considered optimization approaches from literature have used a power flow model. In the following, two papers i.e. Hagspiel et al. (2014) and Hörsch and Brown (2017), which modeled the passive power flow behavior and derived results for the European power grid, while considering up to 256 buses, are used for discussing this work's findings. In both studies, fewer flexible generation is available than in the *eGo 100* scenario setting. Hagspiel et al. (2014) assumed about 1 % of the annual generation from biomass sources whereas Hörsch and Brown (2017) did not consider any. Furthermore, Hagspiel et al. (2014) assumed considerable amounts of somewhat flexible hydro power, which Hörsch and Brown (2017) only modeled marginally. In total, Hörsch and Brown (2017) (similar to Brown et al., 2018c) utilized approximately 5 % flexible generation. These circumstances give an explanation for higher grid and storage expansion as well as higher systematic LCOE.

Hagspiel et al. (2014) explicitly addressed the possibility to utilize distributed biomass power production to avoid grid expansion (if restricted) and to replace storage expansion needs. Furthermore, the biggest principal similarity in terms of grid expansion is the important expansion corridor near the Dutch border transporting wind power to the Ruhr area. In terms of storage expansion neither in total numbers nor concerning the spatial distribution information for comparison can be used. Moreover, Hagspiel et al. (2014) emphasized the importance and difficulty to consider the effect of loop flows by modeling the passive behavior of the AC grid. The sensitive behavior of the model when representing the crossborder interconnectors as DC lines, as realized in the sensitivity analysis, fortifies these conclusions.

Analyzing the spatial distribution of grid and storage expansion in Hörsch and Brown (2017) (concerning the scenario with 256 buses and a doubling of today's grid capacity) several similarities to the results of this work can be found. Most of the grid expansion in Germany is situated in the north. In the northwest, the corridor towards the Ruhr area is highly expanded. Moreover, a central corridor from the southwest of Schleswig-Holstein towards North Rhine-Westfalia and Hesse is extended significantly. The north-to-east corridor towards Poland was modeled but to a far higher extent, similar to the one in the *cb-inf* sensitivity. Moreover, the north-to-south expansion reached further to the south. However, here the expansion stayed comparably low. Principally, the crossborder expansion was similarly modeled as in this work. Northern interconnectors such as between the Netherlands and Germany gain capacities, as well as the northern interconnector to the Czech Republic. In contrast, the interconnectors to Austria and Switzerland are hardly expanded. Besides the spatial similarities and differences, in total the grid expansion seems to be significantly higher than the one in the base scenario and would rather correspond to sensitivities with high grid expansion. Concerning storage expansion, it is striking that no storage units were placed in Germany (except for possible pumped storage sites). Battery expansion was realized in solar dominated southern countries like Spain (which are not considered in this work) and hydrogen storage were significantly situated in the wind-dominated Denmark. Principally, storage wise, these findings are in line with the results of this study, although hydrogen storage are mostly situated in Northern Germany and the Netherlands.

Consequently, Hörsch and Brown (2017), among others, stated that high grid expansion is economically favorable. The more grid expansion is possible, the more wind off- and then also onshore wind power is feasible, the less solar generation and storage units are projected. Nevertheless, Brown et al. (2018c); Hörsch and Brown (2017); Schlachtberger et al. (2017) emphasized that the cost benefits of grid expansion decrease non-linearly with rising grid expansion. In other words, the most benefits are reached already with comparably low grid expansion. Consequently, Hörsch and Brown (2017) stated that more than half of the benefit is already reached when expanding the grid by 25 %. Initially, Schlachtberger et al. (2017), in a spatially less detailed model, determined a grid with the fourfold of today's capacity as a compromise of locking in 85 % of the cost reduction with an optimal grid expansion of 9 times of today's capacity. The sensitivity analysis in this work shows a similar non-linear effect. Although due to the ceteris paribus approach of separately addressing the interdependent crossborder and inner-German expansion restrictions it is not as clearly evaluable. Analyzing the inner-German grid expansion, the optimal relative grid expansion (according to sensitivity *D-inf*) accounts for 6 % (accompanied with roughly a doubling of the crossborder capacities) of today's capacities. Due to the high spatial resolution and the consideration of the HV level in Germany, the not-expanded capacities are a lot bigger leading to a comparably small relative value. Utilizing about 60 % of this maximal grid expansion in Germany in the base scenario, 80 % of the benefits are locked in. Furthermore, the base setting reaches 43 % of the overall cost savings which are produced in the optimal crossborder expansion setting (*cb-inf*). Hence, only 15 % of the optimal expansion of 430 % for the German crossborder lines and only 30 % of the optimal expansion of 230 % for the other foreign interconnectors are necessary to reach the compromise setting.

6.2 Critical appraisal

In the following, the most important limitations of the applied methods are discussed in order to appraise the results more precisely. Thus, assumptions and approaches concerning the developed data model and optimization are addressed. Most of the following issues have already been outlined in previous related work (i.e. Medjroubi et al., 2017; Müller et al., 2018b; Wienholt et al., 2018; Müller et al., 2018a, 2019b,a).

6.2.1 Data model

Developing and utilizing the first open grid model integrating the German transmission and sub-transmission level comes with the inconvenience of difficult validation. The results of the mentioned previous works and especially the results of this work affirm the plausibility of the model. Moreover, there have been several attempts (e.g. Kähler, 2018; Medjroubi et al., 2017; Scharf, 2015; Vespermann, 2017) to evaluate the quality of openstreetmap data and the applied simplified assumptions concerning electrical parameters. Whereas the mentioned studies concentrated on the transmission level, in particular the availability of official data on the sub-transmission level on a national scale is scarce and incomplete. Consequently, so far the data model lacks a thorough validation.

A related issue, which especially accounts for the sub-transmission level, is the lacking knowledge of open switches in the grid. In particular, the sub-transmission grid is not operated as one interconnected grid in Germany. The sub-transmission grid operators try to avoid interconnections with other operators' grids in order to ease operation and foster security e.g. in case of a ground fault. However, in this model no open switches are assumed. Adequately modeling open switches would probably make the results less cost-effective. In particular, the positive effect of transit flows via the sub-transmission grid, which is shown in this work would decrease.

Due to the high computational burden, the spatial distribution is reduced by a k-means algorithm. The reduction of spatial complexity implies a few drawbacks.

Whereas the transmission grid topology is represented properly, certainly, the spatial resolution of about 3,600 additional sub-transmission substations is only partly represented by considering up to 500 buses. Apart from examples such as Schleswig-Holstein, where the HV topology is clearly modeled in a few separate meshes, in many cases the HV level is merged with the EHV topology only being reflected by additional parallel line capacity. Hence, a tendency of losing local grid restrictions has to be stated, especially in the context of assessing the third hypothesis. Apart from losing intra-zonal grid constraints, the problem of over-meshing the inter-zonal interconnections of the reduced grid has been observed. By initially removing the stubs, as realized in Section 5.2.5, this effect can be reduced risking to lose relevant grid constraints. However, if separated meshes come geographically close to each other the false inter-zonal connection can still occur. Nevertheless, due to the spatial resolution of at least 300 buses, that effect occurs mainly in less important high voltage topologies. Consequently, the sensitivity in Section 5.2.5 shows only a minor influence on the results.

The high spatial resolution also enables to model demand and generation of high resolution. The future generation capacities are allocated proportional to the status quo distribution. This rather simple approach might not represent the most probable future development. A more potential oriented or socially accepted distribution as developed in Wingenbach (2018) might be more realistic.

Furthermore, concerning the temporal behavior of solar and wind power generation, a few reasons for underestimating extreme potential feed-in peaks can be emphasized. First, only one weather year is considered. Second, linear correction factors are used to downscale the curves of potential feed-in. Third, snapshots are skipped (and weighted) in order to reduce temporal complexity. The latter mentioned affects the demand patterns as well. However, the effect of higher solar and wind peaks as well as the potential influence of the snapshot skipping is addressed in different sensitivities. Consequently, most importantly it is shown, that whereas grid expansion and the spatial distribution of storage expansion reacts rather insensitive to the chosen snapshot skipping setting, the sizing of the projected storage units is influenced significantly. Thus, the base results tend to underestimate the extent of storage expansion. Regarding the demand, no decreasing or increasing future development is considered. The latter could be a probable future development due to the expected synergies of sector coupling (see also Brown et al., 2018c). Moreover, one should bear in mind that the temporal behavior of the distributed demand was derived from a bottom-up method based on a variety of standard load profiles. Therefore, the need for a high spatial resolution was addressed. A downside is that the resulting overall time series for Germany does not fit the commonly used ENTSO-E load curve (ENTSO-E, 2015). As the ENTSO-E demand time series is modeled and biased by assumptions as well (Schumacher and Hirth, 2015), it is uncertain whether the applied bottom-up approach is less accurate. The general shape-wise similarities as well as the more extreme characteristics of peaks and troughs seem to estimate the temporal load behavior in an adequate and rather conservative way. However, in comparison with other studies, this modeling approach might cause significant differences.

6.2.2 Optimization

The LOPF method assumes an ideal dispatch and redispatch market with perfect foresight and accepts nodal pricing such that operational decisions compete with investive ones. Consequently, RE can be curtailed substantially. Furthermore, since the cost optimization is not accompanied with a CO_2 emission constraint, biomass or in the foreign countries gas fired power plants (with respect to the *eGo 100* scenario) can be dispatched significantly. Therefore these aspects (e.g. full load hours of biomass power plants) were addressed in the results section, especially in the context of the thorough sensitivity analysis. This cost-based deterministic approach is not in line with the current market design. Hence, the *NEP* studies apply a different approach being one central reason for differing results.

Furthermore, the linearity of the optimization problem comes with a few drawbacks. First, no grid losses and reactive behavior are considered. Especially in the case of the high voltage grid where the x/r ratio becomes smaller, this simplification has a higher influence than in the transmission grid in which it is widely accepted to choose the linear approximation of the power flow problem. However, the ex-post performed non-linear power flow converged for all snapshots in all results. Consequently, at least the linearly derived solutions are able to meet the non-linear power flow constraints including a simplified assumption for a reactive power demand. Nevertheless, the robustness of this ex-post evaluation is limited. Besides a general check of convergence, the ex-post non-linear results were not focused on and therefore not evaluated in-depth. For instance, to a limited extent additional line loadings may occur already in normal operating mode which can violate the (n-1)-security margins. Second, the inflexible behavior of fossil power plants (e.g. intertemporal constraints) is not considered. This only affects the *NEP 2035* scenario results and may lead to an underestimation of system costs. Third, in traditional grid planning grid expansion is determined discretely. In contrast, the continuous optimization applied in this work determines line capacities not being available on the market. Hence, grid expansion costs tend to be underestimated.

In energy system modeling, it is common to use generalized assumptions on maximal line usages in order to address (n-1)-security. This simplified assumption is applied in this work as well. From a perspective of traditional grid planning, this is another weakness. In contrast, (n-1)-contingency analysis would be performed, especially when dealing with a complex grid topology. However, the assumed component-sharp security margins with 30 % (in the EHV level) and 50 % (in the HV level) can be assessed to be rather conservative.

6.3 Assessment of the hypotheses

The hypotheses formulated in Chapter 3 are assessed by relating them to the developed methods, results and discussion (as described in Chapter 4, 5 and 6). Hence, in the following, each hypothesis is recapped and evaluated.

> *It is possible to model the German power grid down to the 110 kV grid level on the basis of open source and open data to derive cost optimal future grid and storage expansion settings.*

Chapter 4 describes how it is possible to model the German power grid down to the HV level using open data and open source software. Topological grid data is used from openstreetmap and combined with assumptions from literature in order to derive a highly meshed grid model (of more than 11,000 buses and almost 20,000 branches), which suits linear and non-linear power flow approaches considering active and passive behavior of DC and AC components. Furthermore, it is possible to add necessary open data of generation and consumption behavior being spatially sufficiently detailed to be allocated to more than 4,000 substations. The generation and consumption, especially due to the storage modeling, is modeled for each hour of one year including realistic solar and wind weather characteristics. The resulting high computational burden for a joint optimization of grid and storage under consideration of many relevant technical constraints including a linear approximation of the power flow equations is addressed by minimizing the spatial and temporal complexity to a, with respect to the requirements of the hypothesis, acceptable extent. Thus, a German grid model with up to 500 buses and over 1000 lines remains to be of a unique high spatial resolution showing significant distribution-like topological structures (e.g. in the west of Schleswig-Holstein). Finally, the results reassure, that it is possible to allocate cost optimal future grid and storage expansion settings to this grid of high spatial detail.

> *A joint modeling of the transmission and sub-transmission grid (including its passive flow behavior) enables a spatially detailed and possibly diverse allocation of economically co-optimal grid and storage expansion in a future German power system.*

The second hypothesis can be assessed by concluding the main findings of this work. A diverse set of different spatially detailed allocations of co-optimal grid and storage expansion are derived through a variety of sensitivity analyses. The most important different spatial distributions and their main drivers are highlighted in the following.

The base scenario results of the *NEP 2035* and *eGo 100* show very consistent results, primarily meaning that, the grid expansion of the *NEP 2035* scenario is highly congruent to the one in the *eGo 100* scenario. Accordingly, the two main north-to-south expansion corridors plus some comparably minor distributed grid expansion are feasible in both scenarios. In terms of storage expansion, in the *eGo 100* scenario two larger hydrogen storage units of together about 7 GW are installed near the Polish and Dutch border, whereas in the *NEP 2035* scenario only the one at the Polish border is feasible with a size of 1.6 GW.

The base result of the *eGo 100* scenario with highly centralized characteristics is only one out of a diverse set of interesting solutions, which become optimal under different circumstances. The results' wide range of additional 87 sensitivities is compiled in Figure 6.1 highlighting the most important and extreme variants.

The degree of European interconnection has a high influence on the results. In an autarkic Germany, on the one hand, storage expansion needs would increase substantially by a factor of 6. These storage units would be spread throughout the country as hydrogen storage units in the north and as battery storage in the Ruhr area, near Stuttgart and near Munich. On the other hand, grid expansion would decrease, although showing a similar spatial allocation. In contrast, a solution with unrestricted crossborder expansion particularly leads to higher usage of wind energy from Denmark and the Netherlands causing significantly higher grid expansion of the interconnectors but also within Germany. Moreover, various hydrogen storage units, with a combined capacity of 1.4 GW, at the west coast of Schleswig-Holstein become feasible.

The effect of north-to-south loop flows, especially via the eastern countries, also influences immensely the distribution of grid and storage expansion in Germany. Once the interconnectors are modeled as active components, the hydrogen storage near the Polish border is not feasible anymore. Instead, northeast-to-southeast grid expansion becomes relevant.

Including Norway into the model substantially reduces the system costs, especially the dispatch costs due to the high amount of additional hydro flexibility in the system. As grid expansion is a limiting factor, significant hydrogen storage expansion on the German side in Büttel becomes feasible in order to utilize more Norwegian hydro power. The pumped storage units in Norway are not needed (in the context of the spatial scale of this work excluding many European countries).

Assuming an unrestricted grid expansion throughout the entire system (*D-inf/cb-inf* sensitivity), about 3 bn. EUR/a can be saved compared to a setting with today's grid capacities (*D-0/cb-1* sensitivity). This would result into, compared to the base scenario, substantial grid expansion, especially on the transmission level from the north and northwest to the southwest. Minor storage capacities in Schleswig-Holstein and at the Polish border would even be shifted to more northeast-to-southeast grid expansion in case of modeling interconnectors as active DC elements.

Although the change of specific grid investment costs is correlated with the total physical grid expansion, the principal spatial distribution of grid and storage expansion does not differ significantly. In contrast, whereas higher specific storage investment costs only slightly influence the results, lower ones lead to an increase of storage expansion up to 138 GW in Germany, if specific technology costs decrease

95 % more than expected. Under these conditions, battery storage is with a 60 % share more important than hydrogen storage. The storage units are distributed primarily in the north and at interconnectors.

Focusing on the level of spatial detail in the modeling approach, a few effects can be emphasized. First, grid expansion is substantially underestimated when considering 100 or less buses due to the absence of significant bottle-necks. Second, when considering higher spatial resolutions, distributed grid restrictions become more relevant inducing the need for more grid expansion on this level. Nevertheless, the overall cost effect is not significant. Third, storage expansion at the west coast of Schleswig-Holstein becomes increasingly relevant when reaching resolutions from 350 to 500 buses (assuming base assumptions on upper limits of grid expansion).

The importance of biomass as a local flexible power source becomes clear when reducing its potential. Assuming a low biomass capacity as in the *NEP 2035* scenario (slightly higher than in the status quo power system) and additionally no upper grid restriction in Germany and a crossborder DC approach (*bio-NEP_D-inf_cbdc* sensitivity), storage expansion turns out to be very different compared to the base setting. Hydrogen storage units are allocated at almost all buses in the north with capacities of up to 700 MW. Furthermore, in the Ruhr area many small storage units with each about 35 MW capacity are projected. Despite the substantially increased number of storage units, the total storage capacity is only slightly increased. In contrast, reducing also the available biomass resource to about half of today's consumption and instead increase solar and wind capacities by 20 %, storage expansion increases to more than 31 GW in Germany being situated mainly in Schleswig-Holstein, at the offshore wind bus near the Dutch border, in the Ruhr area and near Stuttgart (the latter two as batteries). Moreover, grid expansion is wide-spread and increased by 170 %. A similar change occurs, only without the mentioned battery expansion, if curtailment of solar and wind is restricted such that in Germany only about 1 % gets curtailed.

Comparing the findings to results from other state-of-the-art studies, it can be stated that the results are principally plausible. In particular the base results show rather low investment costs and a dominating effect of wind power driven grid expansion. Considering a wide range of literature results on the one hand while spanning a diverse set of sensitivities on the other hand, shows that the results lie within the range of literature results.

> *Distributed power flow problems and flexibility investments effect the overall optimum.*

In a comparative study it was shown that additional grid capacities from the HV level lead to possible transit flows lowering the need for grid expansion by 23 %, leading to a minor endogenous cost reduction of less than 3 %. Therefore, transit flow effects outnumber the costly necessity to overcome local bottle-necks in the HV level. Consequently, this last hypothesis can also be affirmed. However, the limited detail of spatial resolution and corresponding false inter-zonal meshing effects weaken the affirmation of this hypothesis.

Chapter 7

Conclusion

The transformation of the power system towards a distributed renewable power supply calls for models being able to allocate distributed grid and storage expansion while producing minimal costs for the entire system. In an innovative approach, which uses only open data, the German transmission and sub-transmission grid is integrated into a power system model for Germany and its European neighbors. Although computational burden implies the need for spatial complexity reduction, for the first time, co-optimal grid and storage expansion is allocated to a spatially detailed grid with up to 500 buses and more than a 1000 lines. Within the optimization, the passive flow behavior of the AC components is considered by a state-of-the-art linear approximation.

A thorough analysis and discussion of a mid-term and long-term 100 % renewable future power system is performed. Grid and storage expansion in Germany is mainly driven by offshore and onshore wind feed-in. Two main north-south transmission corridors are feasible connecting the northsea offshore feed-in buses with load centres in the Ruhr area. In contrast, distributed grid expansion plays only a minor role. In the long-term future, if inner-German grid expansion is restricted by an upper limit, two large hydrogen storage units, with capacities above 3 GW, are situated in the northwest (near the Dutch border) and northeast (near the Polish border). The latter can be avoided by impeding loop flow effects through the eastern European neighbors leading to significant inner-German northeast-to-southeast transmission expansion. Moreover, the storage at the Dutch border can be substituted by grid expansion southwards if extensive grid expansion is possible. In this setting, which is dominated by transmission grid expansion, besides flexible hydro power, distributed flexible biomass power feed-in plays an important balancing role. Once this flexible power is less available, RE curtailment is restricted or specific storage investment costs decrease significantly, distributed storage expansion, mostly as long-term hydrogen storage in the north, becomes a feasible option. Up to 100 storage aggregates with a combined capacity of 138 GW can then contribute flexibility.

The consideration of the HV level leads to a high spatial distribution and the recognition of relevant grid constraints. The effect of additional grid restrictions are over-compensated by the cost-reducing effect of transit flows. Consequently, the need for grid expansion is lowered by 23 % leading to a minor endogenous cost reduction of less than 3 %.

The developed model and its results can help investors and authorities to make local investment decisions, which are in line with a macro-economic optimum. Policy should foster primarily inner-German and cross-border transmission grid expansion and secondarily focus rather on investments into large-scale long-term storage in Northern Germany instead of into small-scale distributed short-term technologies.

Chapter 8

Outlook

The modeling in this work can be further developed in order to enhance the quality and robustness of the results as well as to answer new research questions. In the following, possible future research focuses based on this work are outlined.

Concerning the developed data model, several improvements can be realized in the future. First and foremost the openstreetmap-based grid model should be further validated. In this context, the main challenge, especially on the sub-transmission level, has been the lack of official open grid data. Policy should address this important obstacle in order to strengthen open, spatially detailed, grid-based modeling increasing the probability of a successful publicly accepted energy transition at low societal costs. Without policy changes the highly restricted confidential transmission grid and scenario data (in context of the German grid development plans) being available with respect to §12f EnWG (EnWG, 2019) can be utilized for validation of the transmission grid model. Dissolving the discrepancy of ensuring confidentiality on the one hand and the openess of the model on the other hand will be a worthwhile task. Another possibility for further validation, which does not necessarily require policy changes, is to model the grid expansion as similar as possible to the official *NEP* planning approach and compare the results.

Furthermore, the spatial complexity reduction of the grid can be enhanced by various means. First, addressing the false inter-zonal meshing effect, as explained in Section 6.2, the k-means complexity reduction method might be improved by considering the shortest paths in the grid from a representative bus to its cluster medoid. Although initially removing stubs did not influence the results significantly (see Section 5.2.5), this improvement should make the reduced model more accurate. Second, methods to augment the degree of spatial detail once more while keeping computational burden feasible could be developed. For example a method of defining different levels of spatial detail within Germany could enable higher spatial detail in some regions of interest whereas others are modeled less accurately. In a master thesis (i.e. Hansen, 2018) this idea was realized, such that Schleswig-Holstein was modeled at highest spatial complexity while the rest of the grid was reduced to a few buses. This approach could be developed further in the future. Moreover, as computational burden is mainly affected by spatial and temporal complexity, more sophisticated snapshot clustering approaches as in e.g. Kotzur et al. (2018) can be utilized to lower temporal complexity without weakening the modeling quality and in contrast enabling higher spatial detail. Without having to develop or implement such a new method, at first, it would be interesting to re-calculate the sensitivity results with a higher temporal resolution, i.e. skipping only every fourth hour. Consequently, while having to deal with higher computational burden, the effect of underestimating the size of feasible storage units, as shown in Section 5.4.1 for the base case, can be evaluated for the other sensitivity settings. Third, as the results are very sensitive to the interexchange of power within Europe, it should be considered to amplify the spatial coverage towards the rest of Europe including important countries like Great Britain or Italy.

Having mentioned temporal complexity, demand and generation behavior are fundamental in this context. The temporal behavior of weather-dependend resources (affecting wind, solar and hydro power generation) as well as of the demand should be considered in a more diverse manner. In future research, the robustness of the results should be investigated once weather or demand pattern become more extreme. The linear down scaling of the coastdat2-weather data and the usage of standard load profiles are two approaches to be altered in the future in order to simulate more extreme situations. Furthermore, the variation of different weather years and multi-annual modeling should be considered. Concerning the rather flexible RE technologies such as hydro and biomass, flexibility constraints should be further addressed. The results have shown that the flexibility of theses generation technologies offer a substantial value to the system. Therefore, a more complex modeling of intertemporal constraints (e.g. biogas storage behavior) and hydro weather dependency (e.g. reservoir inflow and spillage) shall be considered in future research.

Apart from the modeling of generators' temporal behavior, the siting and sizing issue can be exogenously varied assuming different developments. As already critically addressed in Section 6.2 the linear allocation of future generation capacities to the existing sites is not very sophisticated. Hence, more potential oriented or socially accepted distribution as developed in Wingenbach (2018) might be more realistic. Moreover, it would be very interesting to refrain from defining the generation development exogenously but instead to integrate the generation siting and sizing into the optimization. This co-optimal approach would find the cost optimal allocation of grid, storage and generation expansion. The problem of rising computational burden would have to be addressed and might lead to lower spatial or temporal accuracy.

More optimization variables would also be introduced when coupling the power sector with other energy sectors like mobility and heating. As Brown et al. (2018c) show synergies between sector coupling and a European-wide transmission grid expansion, it is highly interesting to introduce such a approach into this model of yet higher spatial resolution. This task will imply a significant modeling effort and is focused on in a new research project called eGo^n.

In contrast to focus on a broader scope of integrating additional energy sectors, the constraints for the optimization of power grid expansion can be modeled more in detail. In particular, it would be interesting to focus on determining discrete grid expansion, considering the non-linear power flow equations, and (n-1) contingencies in order to further discuss the results of this work and to address new research questions.

References

50Hertz, Amprion, TenneT, and TransnetBW (2012). Netzentwicklungsplan Strom 2012 – Zweiter überarbeiteter Entwurf der Übertragungsnetzbetreiber. Online available at: https://www.netzentwicklungsplan.de/de/netzentwicklungsplaene/netzentwicklungsplan-2022.

50Hertz, Amprion, TenneT, and TransnetBW (2012-2019a). Netzentwicklungsplan Strom. Online available at: https://www.netzentwicklungsplan.de/de/netzentwicklungsplaene.

50Hertz, Amprion, TenneT, and TransnetBW (2014). Kraftwerksliste zum Entwurf Szenariorahmen NEP/O-NEP 2025. Online available at: https://www.netzentwicklungsplan.de/sites/default/files/paragraphs-files/nep_2015_kraftwerksliste_entwurf_140430.pdf.

50Hertz, Amprion, TenneT, and TransnetBW (2015a). NEP 2025 - Methodik der Modellierung wetterabhängiger erneuerbarer Energien (zu Kapitel 2.2.2). Online available at: https://www.netzentwicklungsplan.de/de/methodik-der-modellierung-wetterabhaengiger-erneuerbarer-energien-zu-kapitel-222.

50Hertz, Amprion, TenneT, and TransnetBW (2015b). Netzentwicklungsplan Strom 2025, Version 2015 – Erster Entwurf der Übertragungsnetzbetreiber. Online available at: https://www.netzentwicklungsplan.de/sites/default/files/paragraphs-files/NEP_2025_1_Entwurf_Teil1_0.pdf.

50Hertz, Amprion, TenneT, and TransnetBW (2015c). Offshore-Netzentwicklungsplan 2025 (O-NEP 2025), Version 2015 – Erster Entwurf der Übertragungsnetzbetreiber . Online available at: https://www.netzentwicklungsplan.de/sites/default/files/paragraphs-files/ONEP_2025_1_Entwurf_Teil1.pdf.

50Hertz, Amprion, TenneT, and TransnetBW (2019b). Netzentwicklungsplan Strom 2030, Version 2019 – Zweiter Entwurf der Übertragungsnetzbetreiber. Online available at: https://www.netzentwicklungsplan.de/de/netzentwicklungsplaene/netzentwicklungsplan-2030-2019.

50Hertz, Amprion, TenneT, and TransnetBW (2020). Grundsätze für die Ausbauplanung des deutschen Übertragungsnetzes. Online available at: https://www.tennet.eu/fileadmin/user_upload/Our_Grid/Stakeholders_DE/%C3%9CNB-PlGrS_Juli_2020.pdf.

ABB (2018a). Baltic Cable - An HVDC cable links Sweden with Germany. Online available at: https://new.abb.com/systems/hvdc/references/baltic-cable.

ABB (2018b). Kontek - Zealand's second international interconnection. Online available at: https://new.abb.com/systems/hvdc/references/kontek.

Abedi, M. H., Hosseini, H., and Jalilvand, A. (2019). Sub-transmission substation expansion planning considering load center uncertainties of size and location. *International Journal of Electrical Power & Energy Systems*, 109:413 – 422.

Aboumahboub, T. (2012). *Modeling and Optimization of the Global Electricity Generation System with High Shares of Fluctuating Renewable Energy Sources*. Dissertation, Technische Universität München.

ACER/CEER (2016). *Annual Report on the Results of Monitoring the Internal Electricity Markets in 2015*. Agency for the Cooperation of Energy Regulators and the Council of European Energy Regulators. Online available at: http://www.acer.europa.eu/Official_documents/Acts_of_the_Agency/Publication/ACER%20Market%20Monitoring%20Report%202015%20-%20ELECTRICITY.pdf.

Ackermann, T., Martensen, N., Brown, T., Untsch, S., Tröster, E., Geidel, S., Koch, M., Bauknecht, D., Heinemann, C., Ritter, D., and Hennenberg, K. (2014). *Verteilnetzstudie Rheinland-Pfalz*. Energynautics GmbH, Öko-Institut e.V., Bird & Bird LLP. Online available at: https://mueef.rlp.de/fileadmin/mulewf/Themen/Energie_und_Strahlenschutz/Energie/Verteilnetzstudie_RLP.pdf.

Agricola, A.-C., Höflich, B., Richard, P., Völker, J., Rehtanz, C., Greve, M., Gwisdorf, B., Kays, J., Noll, T., Schwippe, J., Seack, A., Teuwsen, J., Brunekreeft, G., Meyer, R., and Liebert, V. (2012). Ausbau- und Innovationsbedarf der Stromverteilnetze in Deutschland bis 2030 (kurz: dena-Verteilnetzstudie): Endbericht. Online available at: http://www.dena.de/fileadmin/user_upload/Projekte/Energiesysteme/Dokumente/denaVNS_Abschlussbericht.pdf.

Alvarez, R., Thien, T., Moos, M., Chen, H., Cai, Z., Leuthold, M., Sauer, D., and Moser, A. (2013). Optimal allocation and capacity of renewable energies, storage systems and transmission grid in the future European power system. In *Internationaler ETG-Kongress 2013 - 05.-06.11.2013 in Berlin*. VDE VERLAG GMBH, Berlin, Offenbach.

Amme, J., Pleßmann, G., Bühler, J., Hülk, L., Kötter, E., and Schwaegerl, P. (2018). The eGo grid model: An open-source and open-data based synthetic medium-voltage grid model for distribution power supply systems. *Journal of Physics: Conference Series*, 977:012007. SciGRID International Conference on Power Grid Modelling, 30–31 March 2017, Oldenburg, Germany.

Amprion (2011). Erläuterungsbericht - 380-kV-Höchstspannungsfreileitung Wehrendorf – St. Hülfe (Bl. 4196) - Neubau im Bundesland Nordrhein-Westfalen - Anlage 1. Online available at: https://www.bezreg-detmold.nrw.de/200_Aufgaben/010_Planung_und_Verkehr/Planfeststellung___Plangenehmigung/Info_zu_Planfeststellungsverfahren/Verfahrensuebersicht/380_kV-Leitung_Wehrendorf-St_Huelfe/Planungsunterlagen/Planungsunterlagen/Erl__uterungsbericht.pdf.

Andrey, C. and Fournié, L. and Gabay, M. and de Sevin, H. (2016). *The role and need of flexibility in 2030: focus on energy storage*. European Commission, Directorate General for Energy. Online available at: https://op.europa.eu/en/publication-detail/-/publication/2f3ff8c1-714e-11e9-9f05-01aa75ed71a1/language-en/format-PDF/source-96288412.

Bayatloo, F. and Bozorgi-Amiri, A. (2019). A novel optimization model for dynamic power grid design and expansion planning considering renewable resources. *Journal of Cleaner Production*, 229:1319 – 1334.

Becker, S., Rodriguez, R., Andresen, G., Schramm, S., and Greiner, M. (2014). Transmission grid extensions during the build-up of a fully renewable pan-European electricity supply. *Energy*, 64:404 – 418.

BMWi (2017). Erneuerbare Energien in Zahlen. Online available at: https://www.bmwi.de/Redaktion/DE/Publikationen/Energie/erneuerbare-energien-in-zahlen-2017.pdf?__blob=publicationFile&v=27.

Borchard, T. and Haubrich, H. (2008). Evaluating the benefit of voltage comprehensive planning of high and medium voltage networks. In *2008 Third International Conference on Electric Utility Deregulation and Restructuring and Power Technologies*, pp. 823–828.

Brakelmann, H. (2004). Netzverstärkungs-Trassen zur Übertragung von Windenergie: Freileitung oder Kabel? Online available at: http://www.ieea.uni-duisburg.de/brakelmann/Freileitung_Kabel.pdf.

Braun, M., Krybus, I., Becker, H., Bolgaryn, R., Dasenbrock, J., Gauglitz, P., Horst, D., Pape, C., Scheidler, A., and Ulffers, J. (2018). *Verteilnetzstudie Hessen 2024–2034*. Fraunhofer IEE and BearingPoint GmbH. Online available at: https://www.house-of-energy.org/mm/2018_Verteilnetzstudie_Hessen_2024_bis_2034.pdf.

Brijs, T., van Stiphout, A., Siddiqui, S., and Belmans, R. (2017). Evaluating the role of electricity storage by considering short-term operation in long-term planning. *Sustainable Energy, Grids and Networks*, 10:104 – 117.

Brown, R. E., Jiuping Pan, Xiaorning Feng, and Koutlev, K. (2001). Siting distributed generation to defer T D expansion. In *2001 IEEE/PES Transmission and Distribution*

Conference and Exposition. Developing New Perspectives (Cat. No.01CH37294), volume 2, pp. 622–627.

Brown, T., Bischof-Niemz, T., Blok, K., Breyer, C., Lund, H., and Mathiesen, B. (2018a). Response to 'burden of proof: A comprehensive review of the feasibility of 100% renewable-electricity systems'. *Renewable and Sustainable Energy Reviews*, 92:834 – 847.

Brown, T., Hörsch, J., and Schlachtberger, D. (2018b). PyPSA: Python for Power System Analysis. *Journal of Open Research Software*, 6(4).

Brown, T., Schierhorn, P. P., Tröster, E., and Ackermann, T. (2016). Optimising the European transmission system for 77% renewable electricity by 2030. *IET Renewable Power Generation*, 10(1):3–9.

Brown, T., Schlachtberger, D., Kies, A., Schramm, S., and Greiner, M. (2018c). Synergies of sector coupling and transmission reinforcement in a cost-optimised, highly renewable European energy system. *Energy*, 160:720 – 739.

Brummitt, C. D., Hines, P. D. H., Dobson, I., Moore, C., and D'Souza, R. M. (2013). Transdisciplinary electric power grid science. *Proceedings of the National Academy of Sciences*, 110(30):12159–12159.

Büchner, J., Katzfey, J., Floercken, O. D., Moser, A., Schuster, H., Dierkes, S., van Leeuwen, T., Verheggen, L., Uslar, M., and van Amelsvoort, M. (2014). Moderne Verteilernetze für Deutschland (Verteilernetzstudie). Online available at: `http://www.bmwi.de/BMWi/Redaktion/PDF/Publikationen/Studien/verteilernetzstudie,property=pdf,bereich=bmwi2012,sprache=de,rwb=true.pdf`.

Bundesamt für Kartographie und Geodäsie (2016). Verwaltungsgebiete VG250. Online available at: `http://www.geodatenzentrum.de/geodaten/gdz_rahmen.gdz_div?gdz_spr=deu&gdz_akt_zeile=5&gdz_anz_zeile=1&gdz_unt_zeile=14&gdz_user_id=0`.

Bundesamt für Seeschifffahrt und Hydrographie (2017a). Nordsee Offshore-Windparks Pilotgebiete. Online available at: `https://www.bsh.de/DE/THEMEN/Offshore/Nutzungskarten/_Anlagen/Downloads/Nordsse-OffshoreWindparksPilotgebiete.pdf?__blob=publicationFile&v=2`.

Bundesamt für Seeschifffahrt und Hydrographie (2017b). Ostsee Offshore-Windparks Poilotgebiete. Online available at: `https://www.bsh.de/DE/THEMEN/Offshore/Nutzungskarten/_Anlagen/Downloads/Ostsee-OffshoreWindparksPilotgebiete.pdf?__blob=publicationFile&v=2`.

Bundesministerium der Justiz und für Verbraucherschutz (2005). Verordnung über die Entgelte für den Zugang zu Elektrizitätsversorgungsnetzen (Stromnetzentgeltverordnung - §27). Online available at: http://www.gesetze-im-internet.de/bundesrecht/stromnev/gesamt.pdf.

Bundesnetzagentur and Bundeskartellamt (2016). Monitoringbericht 2016. Online available at: https://www.bundesnetzagentur.de/DE/Sachgebiete/ElektrizitaetundGas/Unternehmen_Institutionen/DatenaustauschundMonitoring/Monitoring/Monitoringberichte/Monitoring_Berichte_node.html.

Bunke, W.-D. (2016). Open Power System Data - Data Package Renewable power plants, version 2016-02-10. Primary data from BNetzA, BNetzA_PV, TransnetBW, TenneT, Amprion, 50Hertz, Netztransparenz.de, Postleitzahlen Deutschland, Energinet.dk, Energistyrelsen, GeoNames, French Ministery of the Environment, Energy and the Sea, OpenDataSoft, Urzad Regulacji Energetyki (URE). Online available at: http://open-power-system-data.org/.

Bunke, W. D., Söthe, M., Christ, M., and Kaldemeyer, C. (2017). Flensburg Energy Scenarios - open_eGo Scenarios for 2014/2035/2050. Online available at: https://osf.io/bpf36/.

Bussar, C., Moos, M., Alvarez, R., Wolf, P., Thien, T., Chen, H., Cai, Z., Leuthold, M., Sauer, D. U., and Moser, A. (2014). Optimal allocation and capacity of energy storage systems in a future European power system with 100% renewable energy generation. *Energy Procedia*, 46:40 – 47. 8th International Renewable Energy Storage Conference and Exhibition (IRES 2013).

Bussar, C., Stöcker, P., Cai, Z., Jr., L. M., Magnor, D., Wiernes, P., van Bracht, N., Moser, A., and Sauer, D. U. (2016). Large-scale integration of renewable energies and impact on storage demand in a european renewable power system of 2050—sensitivity study. *Journal of Energy Storage*, 6:1 – 10.

Bussar, C., Stöcker, P., Cai, Z., Moraes, L., Alvarez, R., Chen, H., Breuer, C., Moser, A., Leuthold, M., and Sauer, D. (2015). Large-scale integration of renewable energies and impact on storage demand in a European renewable power system of 2050. *Energy Procedia*, 73:145 – 153. 9th International Renewable Energy Storage Conference, IRES 2015.

Bussar, C., Stöcker, P., Moraes, L., Jacqué, K., Axelsen, H., and Sauer, D. (2017). The long-term power system evolution – first optimisation results. *Energy Procedia*, 135:347 – 357. 11th International Renewable Energy Storage Conference, IRES 2017, 14-16 March 2017, Düsseldorf, Germany.

Carlini, E. M., Schroeder, R., Birkebæk, J. M., and Massaro, F. (2019). EU transition in power sector: How RES affects the design and operations of transmission power systems. *Electric Power Systems Research*, 169:74 – 91.

Cebulla, F., Naegler, T., and Pohl, M. (2017). Electrical energy storage in highly renewable European energy systems: Capacity requirements, spatial distribution, and storage dispatch. *Journal of Energy Storage*, 14:211 – 223.

Centre for Sustainable Energy Systems, DLR Institute for Networked Energy Systems, Reiner Lemoine Institut (2018). open_eGo DataProcessing. Online available at: `https://github.com/openego/data_processing`.

Centre for Sustainable Energy Systems Flensburg and DLR Institute for Networked Energy Systems (2019). eTraGo - electrical Transmission Grid optimization. Online available at: `https://github.com/openego/eTraGo/tree/upmdis`.

Child, M., Bogdanov, D., and Breyer, C. (2018). The role of storage technologies for the transition to a 100% renewable energy system in Europe. *Energy Procedia*, 155:44 – 60. 12th International Renewable Energy Storage Conference, IRES 2018, 13-15 March 2018, Düsseldorf, Germany.

Child, M., Kemfert, C., Bogdanov, D., and Breyer, C. (2019). Flexible electricity generation, grid exchange and storage for the transition to a 100% renewable energy system in Europe. *Renewable Energy*, 139:80 – 101.

Choi, J., Mount, T. D., and Thomas, R. J. (2007). Transmission expansion planning using contingency criteria. *IEEE Transactions on Power Systems*, 22(4):2249–2261.

Cotilla-Sanchez, E., Hines, P. D. H., Barrows, C., Blumsack, S., and Patel, M. (2013). Multi-attribute partitioning of power networks based on electrical distance. *IEEE Transactions on Power Systems*, 28(4):4979–4987.

Couckuyt, D., Orlic, D., Bruninx, K., Zani, A., Leger, A.-C., Momot, E., and Grisey, N. (2015). e-Highway - System simulations analysis and overlay-grid development–Digest. Online available at: `https://docs.entsoe.eu/baltic-conf/bites/www.e-highway2050.eu/fileadmin/documents/Results/D_2.3_System_simulations_analysis_and_overlay_grid_development_digest.pdf`.

Czisch, G. (2005). *Szenarien zur zukünftigen Stromversorgung - Kostenoptimierte Variationen zur Versorgung Europas und seiner Nachbarn mit Strom aus erneuerbaren Energien*. Dissertation, Universität Kassel.

Da Fonseca Manso, L. A., de Assis, F. A., da Silva, A. M. L., de Resende, L. C., and dos Santos, F. L. (2014). Constructive heuristic algorithm for sub-transmission system planning. In *2014 Power Systems Computation Conference*, pp. 1–7.

Denholm, P. and Hand, M. (2011). Grid flexibility and storage required to achieve very high penetration of variable renewable electricity. *Energy Policy*, 39(3):1817 – 1830.

Després, J., Hadjsaid, N., Criqui, P., and Noirot, I. (2015). Modelling the impacts of variable renewable sources on the power sector: Reconsidering the typology of energy modelling tools. *Energy*, 80:486 – 495.

Dvijotham, K., Chertkov, M., and Backhaus, S. (2014). Storage sizing and placement through operational and uncertainty-aware simulations. In *2014 47th Hawaii International Conference on System Sciences*, pp. 2408–2416.

Dvorkin, Y., Fernández-Blanco, R., Kirschen, D. S., Pandžić, H., Watson, J., and Silva-Monroy, C. A. (2017). Ensuring profitability of energy storage. *IEEE Transactions on Power Systems*, 32(1):611–623.

e-Highway 2050 project (2015a). Europe's future secure and sustainable electricity infrastructure. Online available at: https://docs.entsoe.eu/baltic-conf/bites/www.e-highway2050.eu/fileadmin/documents/e_highway2050_booklet.pdf.

e-Highway 2050 project (2015b). Modular development plan of the pan-European transmission system 2050 - database per country. Online available at: http://www.e-highway2050.eu/fileadmin/documents/Results/e-Highway_database_per_country-08022016.xlsx.

EEG (2014 (last changes 2019)). *Gesetz für den Ausbau erneuerbarer Energien (Erneuerbare-Energien-Gesetz - EEG 2017)*. Bundesgesetzblatt 1066. Online available at: https://www.bgbl.de/xaver/bgbl/start.xav#__bgbl__%2F%2F*%5B%40attr_id%3D%27bgbl114s1066.pdf%27%5D__1578835066303.

Egerer, J., Gerbaulet, C., and Lorenz, C. (2015). European electricity grid infrastructure expansion in a 2050 context: Berlin conference on energy and electricity economics. In *Berlin Conference on Energy and Electricity Economics*.

ENTSO-E (2012). Ten-Year Network Development Plan 2012. Online available at: https://www.entsoe.eu/fileadmin/user_upload/_library/SDC/TYNDP/2012/120705_Table_of_projects_TYNDP_2012_package_FINAL.zip.

ENTSO-E (2014). Scenario Outlook & Adequacy Forecast (SO&AF) 2014-2030 Dataset. Online available at: www.entsoe.eu/publications/system-development-reports/adequacy-forecasts/soaf-2014-2030/Pages/default.aspx.

ENTSO-E (2015). ENTSO-E Historical data (until December 2015). Online available at: https://www.entsoe.eu/data/data-portal/.

ENTSO-E (2016). Ten-Year Network Development Plan 2016 (TYNDP) - Data and Maps. Online available at: https://tyndp.entsoe.eu/.

ENTSO-E (2018a). 2nd ENTSO-E guideline for cost benefit analysis of grid development projects. Online available at: https://tyndp.entsoe.eu/Documents/TYNDP%20documents/Cost%20Benefit%20Analysis/2018-10-11-tyndp-cba-20.pdf.

ENTSO-E (2018b). ENTSO-E transmission system map. Online available at: https://www.entsoe.eu/data/map/.

ENTSO-E Data Expert Group (2016). *Specific national considerations*. ENTSO-E. Online available at: https://eepublicdownloads.entsoe.eu/clean-documents/Publications/Statistics/Specific_national_considerations.pdf.

EnWG (2005 (last changes 2019)). *Gesetz über die Elektrizitäts- und Gasversorgung (Energiewirtschaftsgesetz - EnWG)*. Bundesgesetzblatt 1970. Online available at: https://www.bgbl.de/xaver/bgbl/start.xav#__bgbl__%2F%2F*%5B%40attr_id%3D%27bgbl105s1970.pdf%27%5D__1578834862094.

Erlach, B., Lunz, B., and Merzkirch, M. (2015). *Energiespeicher Technologiesteckbrief zur Analyse Flexibilitaetskonzepte für die Stromversorgung 2050*. Acatech – Deutsche Akademie der Technikwissenschaften e.V. Online available at: https://www.acatech.de/wp-content/uploads/2018/03/ESYS_Technologiesteckbrief_Energiespeicher.pdf.

European Climate Foundation (2010). *Roadmap 2050: a practical guide to a prosperous, low-carbon, Europe. Volume I: technical and economic assessment: A report by the European Climate Foundation*. European Climate Foundation. Online available at: http://www.roadmap2050.eu/attachments/files/Volume1_fullreport_PressPack.pdf.

EWE Netz (2013). Standard Lastprofile. Online available at: http://www.ewe-netz.de/strom/1988.php.

Faulstich, M., Foth, H., Calliess, C., Hohmeyer, O., Holm-Müller, K., Niekisch, M., and Schreurs, M. (2011). Wege zur 100% erneuerbaren Stromversorgung - Sondergutachten. Online available at: https://www.umweltrat.de/SharedDocs/Downloads/DE/02_Sondergutachten/2008_2012/2011_07_SG_Wege_zur_100_Prozent_erneuerbaren_Stromversorgung.pdf?__blob=publicationFile.

Fernández-Blanco, R., Dvorkin, Y., Xu, B., Wang, Y., and Kirschen, D. S. (2017). Optimal energy storage siting and sizing: A WECC case study. *IEEE Transactions on Sustainable Energy*, 8(2):733–743.

Flosdorff, R. and Hilgarth, G. (2005). *Elektrische Energieverteilung (Leitfaden der Elektrotechnik)*, volume 9. B. B. Teubner Verlag.

Forschungsstelle für Energiewirtschaft e.V. (2014). Kurzgutachten zum Kostenvergleich Stromtransport - Hybridnetz (Power-to-Gas) vs. HGÜ-Leitung. Online available at: https://www.ffe.de/attachments/article/527/Kurzgutachten_Kostenvergleich%20Stromtransport.pdf.

Franco, J. F., Rider, M. J., and Romero, R. (2016). Robust multi-stage substation expansion planning considering stochastic demand. *IEEE Transactions on Power Systems*, 31(3):2125–2134.

Fraunhofer IEE (2018). *Windmonitor (IEE): Marktanteile der wichtigsten Offshore-Windenergieanlagenhersteller weltweit nach Zahl der Anlagen im Jahr 2016*. Fraunhofer Institut für Energiewirtschaft und Energiesystemtechnik (IEE), Kassel. Online available at: http://windmonitor.iee.fraunhofer.de/windmonitor_de/4_Offshore/2_technik/4_anlagenhersteller_weltweit/.

Gan, W., Ai, X., Fang, J., Yan, M., Yao, W., Zuo, W., and Wen, J. (2019). Security constrained co-planning of transmission expansion and energy storage. *Applied Energy*, 239:383 – 394.

Gerbaulet, C. and Kunz, F. (2016). Open Power System Data - Data Package Conventional power plants, version 2016-02-08. Primary data from BNetzA Kraftwerksliste, Umweltbundesamt Datenbank Kraftwerke in Deutschland. Online available at: http://open-power-system-data.org/.

Geyer, B. (2014). High-resolution atmospheric reconstruction for Europe 1948-2012: coastDat2. *Earth System Science Data*, 6(1):147.

Geyer, B. and Rockel, B. (2013). coastDat-2 COSMO-CLM atmospheric reconstruction. World Data Center for Climate (WDCC) at DKRZ. Online available at: https://doi.org/10.1594/WDCC/coastDat-2_COSMO-CLM.

Ghofrani, M., Arabali, A., Etezadi-Amoli, M., and Fadali, M. S. (2013). A framework for optimal placement of energy storage units within a power system with high wind penetration. *IEEE Transactions on Sustainable Energy*, 4(2):434–442.

Gils, H. C. (2015). *Balancing of intermittent renewable power generation by demand response and thermal energy storage*. Dissertation, Universität Stuttgart.

Gils, H. C., Scholz, Y., Pregger, T., de Tena, D. L., and Heide, D. (2017). Integrated modelling of variable renewable energy-based power supply in Europe. *Energy*, 123:173 – 188.

Gimeno-Gutierrez, M. and Lacal-Arantegui, R. (2013). *Assessment of the European potential for pumped hydropower energy storage*. European Commission Joint Research Centre. Online available at: https://ec.europa.eu/jrc/sites/jrcsh/files/jrc_20130503_assessment_european_phs_potential.pdf.

Gomes, P. V. and Saraiva, J. T. (2019). State-of-the-art of transmission expansion planning: A survey from restructuring to renewable and distributed electricity markets. *International Journal of Electrical Power & Energy Systems*, 111:411 – 424.

Gonzalez-Romero, I.-C., Wogrin, S., and Gomez, T. (2019). Proactive transmission expansion planning with storage considerations. *Energy Strategy Reviews*, 24:154 – 165.

Gotzens, F., Gillessen, B., Burges, S., Hennings, W., Müller-Kirchenbauer, J., Seim, S., Verwiebe, P., Schmid, T., Jetter, F., and Limmer, T. (2020). *DemandRegio - Harmonisierung und Entwicklung von Verfahren zur regionalen und zeitlichen Auflösung von Energienachfragen - Abschlussbericht* . Forschungszentrum Jülich, Technische Universität Berlin, Forschungsstelle für Energiewirtschaft. Online available at: `https://www.ffe.de/attachments/article/1037/DemandRegio_Abschlussbericht.pdf`.

Greenpeace International, Global Wind Energy Council, SolarPowerEurope (2015). energy revolution - A sustainable world - Energy Outlook 2015 - 100% Renewable Energy for all. Online available at: `https://www.greenpeace.org/archive-international/Global/international/publications/climate/2015/Energy-Revolution-2015-Full.pdf`.

Groiss, C., Schaffer, W., and Gawlik, W. (2017). Interaction between short-term and seasonal storages in a predominantly renewable power system. *CIRED - Open Access Proceedings Journal*, 2017(1):1858–1861.

Guney, M. S. and Tepe, Y. (2017). Classification and assessment of energy storage systems. *Renewable and Sustainable Energy Reviews*, 75:1187 – 1197.

Hagspiel, S., Jägemann, C., Lindenberger, D., Brown, T., Cherevatskiy, S., and Tröster, E. (2014). Cost-optimal power system extension under flow-based market coupling. *Energy*, 66:654 – 666.

Haller, M., Ludig, S., and Bauer, N. (2012a). Bridging the scales: A conceptual model for coordinated expansion of renewable power generation, transmission and storage. *Renewable and Sustainable Energy Reviews*, 16(5):2687 – 2695.

Haller, M., Ludig, S., and Bauer, N. (2012b). Decarbonization scenarios for the EU and MENA power system: Considering spatial distribution and short term dynamics of renewable generation. *Energy Policy*, 47:282 – 290.

Hansen, M. (2018). *Simulation von Einspeisemanagementeinsätzen in Schleswig-Holstein*. Master's thesis, Europa-Universität Flensburg.

Harsha, P. and Dahleh, M. (2011). Optimal sizing of energy storage for efficient integration of renewable energy. In *2011 50th IEEE Conference on Decision and Control and European Control Conference*, pp. 5813–5819.

Harsha, P. and Dahleh, M. (2015). Optimal management and sizing of energy storage under dynamic pricing for the efficient integration of renewable energy. *IEEE Transactions on Power Systems*, 30(3):1164–1181.

Heard, B., Brook, B., Wigley, T., and Bradshaw, C. (2017). Burden of proof: A comprehensive review of the feasibility of 100% renewable-electricity systems. *Renewable and Sustainable Energy Reviews*, 76:1122 – 1133.

Hedayati, M., Zhang, J., and Hedman, K. W. (2014). Joint transmission expansion planning and energy storage placement in smart grid towards efficient integration of renewable energy. In *2014 IEEE PES T D Conference and Exposition*, pp. 1–5.

Heide, D., von Bremen, L., Greiner, M., Hoffmann, C., Speckmann, M., and Bofinger, S. (2010). Seasonal optimal mix of wind and solar power in a future, highly renewable Europe. *Renewable Energy*, 35(11):2483 – 2489.

Held, A., Ragwitz, M., Sensfuß, F., Resch, G., Olmos, L., Ramos, A., and Rivier, M. (2018). How can the renewables targets be reached cost-effectively? Policy options for the development of renewables and the transmission grid. *Energy Policy*, 116:112 – 126.

Hemmati, R., Hooshmand, R., and Khodabakhshian, A. (2013a). Comprehensive review of generation and transmission expansion planning. *IET Generation, Transmission Distribution*, 7(9):955–964.

Hemmati, R., Hooshmand, R., and Khodabakhshian, A. (2013b). State-of-the-art of transmission expansion planning: Comprehensive review. *Renewable and Sustainable Energy Reviews*, 23:312 – 319.

Hoffrichter, A., Barrios, H., Massmann, J., Venkataramanachar, B., and Schnettler, A. (2018). Impact of considering 110 kV grid structures on the congestion management in the German transmission grid. *Journal of Physics: Conference Series*, 977:012004. SciGRID International Conference on Power Grid Modelling, 30–31 March 2017, Oldenburg, Germany.

Holz, F. and von Hirschhausen, C. (2013). The infrastructure implications of the energy transformation in Europe until 2050 - lessons from the EMF28 modeling exercise. *Climate Change Economics*, 04(supp01):1340006.

Hosseini, S., Jalilzadeh, S., Jalilvand, A., and Bagheri, A. (2010). A new approach for sub-transmission system expansion planning using genetic algorithm. *International Review of Electrical Engineering*, 5(5):2343–2349.

Huber, M., Dimkova, D., and Hamacher, T. (2014). Integration of wind and solar power in Europe: Assessment of flexibility requirements. *Energy*, 69:236 – 246.

Hörsch, J. and Brown, T. (2017). The role of spatial scale in joint optimisations of generation and transmission for European highly renewable scenarios. In *2017 14th International Conference on the European Energy Market (EEM)*, pp. 1–7.

Hülk, L., Wienholt, L., Cußmann, I., Müller, U. P., Matke, C., and Koetter, E. (2017). Allocation of annual electricity consumption and power generation capacities across multi voltage levels in a high spatial resolution. *International Journal of Sustainable Energy Planning and Management*, 13:79–92.

IKS OvGU Mageburg, DLRVE Oldenburg, ZNES Flensburg and RLI Berlin (2020). OpenEnergyPlatform (OEP) - Schema 'grid' on the open energy data base. Online available at: https://openenergy-platform.org/dataedit/view/grid.

Jalali, M., Zare, K., and Hagh, M. T. (2014). A multi-stage MINLP-based model for sub-transmission system expansion planning considering the placement of DG units. *International Journal of Electrical Power & Energy Systems*, 63:8 – 16.

Kaldemeyer, C., Boysen, C., and Tuschy, I. (2016). Compressed air energy storage in the German energy system – status quo & perspectives. *Energy Procedia*, 99:298 – 313. 10th International Renewable Energy Storage Conference, IRES 2016, 15-17 March 2016, Düsseldorf, Germany.

Karimi, M. and Haghifam, M. R. (2017). Risk based multi-objective dynamic expansion planning of sub-transmission network in order to have eco-reliability, environmental friendly network with higher power quality. *IET Generation, Transmission Distribution*, 11(1):261–271.

Kellermann, J., Bredtmann, C., and Moser, A. (2018). Considering curtailment in 110 kV grid planning to mitigate uncertainties in the integration of renewables. In *2018 IEEE PES Asia-Pacific Power and Energy Engineering Conference (APPEEC)*, pp. 262–267.

Kishore, T. and Singal, S. (2014). Optimal economic planning of power transmission lines: A review. *Renewable and Sustainable Energy Reviews*, 39:949 – 974.

Knorr, K., Zimmermann, B., Kirchner, D., Speckmann, M., Spieckermann, R., Widdel, M., Wunderlich, M., Mackensen, R., Rohrig, K., Steinke, F., Wolfrum, P., Leveringhaus, T., Lager, T., Hofmann, L., Filzek, D., Göbel, T., Kusserow, B., Nicklaus, L., and Ritter, P. (2014). Kombikraftwerk 2 – Abschlussbericht. Online available at: https://www.iee.fraunhofer.de/content/dam/iee/energiesystemtechnik/de/Dokumente/Veroeffentlichungen/2014/2014_Abschlussbericht_Kombikraftwerk2.pdf.

Knörr, W., Heidt, C., Gores, S., and Bergk, F. (2016). *Aktualisierung "Daten- und Rechenmodell: Energieverbrauch und Schadstoffemissionen des motorisierten Verkehrs in Deutschland 1960-2035" (TREMOD) für die Emissionsberichterstattung 2016*. IFEU. Online available at: https://www.ifeu.de/wp-content/uploads/Endbericht_TREMOD_2016_160701.pdf.

Konstantelos, I. and Strbac, G. (2015). Valuation of flexible transmission investment options under uncertainty. *IEEE Transactions on Power Systems*, 30(2):1047–1055.

Konstantin, P. (2009). *Praxisbuch Energiewirtschaft: Energieumwandlung, -transport und -beschaffung im liberalisierten Markt*. Springer Science & Business Media.

Korpaas, M., Holen, A. T., and Hildrum, R. (2003). Operation and sizing of energy storage for wind power plants in a market system. *International Journal of Electrical Power & Energy Systems*, 25(8):599 – 606. 14th Power Systems Computation Conference.

Kotzur, L., Markewitz, P., Robinius, M., and Stolten, D. (2018). Impact of different time series aggregation methods on optimal energy system design. *Renewable Energy*, 117:474 – 487.

Krien, U. and oemof developing group (2016). feedinlib – time series of PV or wind power plants. `https://github.com/oemof/feedinlib`.

Krishnan, V. and Das, T. (2015). Optimal allocation of energy storage in a co-optimized electricity market: Benefits assessment and deriving indicators for economic storage ventures. *Energy*, 81:175 – 188.

Krishnan, V., Ho, J., Hobbs, B. F., Liu, A. L., McCalley, J. D., Shahidehpour, M., and Zheng, Q. P. (2016). Co-optimization of electricity transmission and generation resources for planning and policy analysis: review of concepts and modeling approaches. *Energy Systems*, 7(2):297–332.

Kähler, J. (2018). *Evaluation einer Abstimmungskaskade zwischen Übertragungs- und Hochspannungsnetzbetreiber*. Master's thesis, Fachhochschule Bielefeld.

Länderarbeitskreis Energiebilanzen (2015). Energiebilanzen der Länder. Online available at: `http://www.lak-energiebilanzen.de/seiten/energiebilanzenLaender.cfm`.

Latorre, G., Cruz, R. D., Areiza, J. M., and Villegas, A. (2003). Classification of publications and models on transmission expansion planning. *IEEE Transactions on Power Systems*, 18(2):938–946.

Lavorato, M., Rider, M. J., Garcia, A. V., and Romero, R. (2010). A constructive heuristic algorithm for distribution system planning. *IEEE Transactions on Power Systems*, 25(3):1734–1742.

Lee, C. w., Ng, S. K. k., Zhong, J., and Wu, F. F. (2006). Transmission expansion planning from past to future. In *2006 IEEE PES Power Systems Conference and Exposition*, pp. 257–265.

Li, C., Dong, Z., Chen, G., Luo, F., and Liu, J. (2015). Flexible transmission expansion planning associated with large-scale wind farms integration considering demand response. *IET Generation, Transmission Distribution*, 9(15):2276–2283.

Lorente, J. L., Liu, X. A., Best, R., and Morrow, D. J. (2018). Energy storage allocation in power networks – a state-of-the-art review. In *2018 53rd International Universities Power Engineering Conference (UPEC)*, pp. 1–6.

Lotero, R. C. and Contreras, J. (2011). Distribution system planning with reliability. *IEEE Transactions on Power Delivery*, 26(4):2552–2562.

Luca de Tena, D. (2014). *Large scale renewable power integration with electric vehicles: long term analysis for Germany with a renewable based power supply*. Dissertation, Universität Stuttgart.

Lumbreras, S. and Ramos, A. (2016). The new challenges to transmission expansion planning. survey of recent practice and literature review. *Electric Power Systems Research*, 134:19 – 29.

Mahdavi, M., Sabillon Antunez, C., Ajalli, M., and Romero, R. (2018). Transmission expansion planning: Literature review and classification. *IEEE Systems Journal*, pp. 1–12.

Makarov, Y. V., Du, P., Kintner-Meyer, M. C. W., Jin, C., and Illian, H. F. (2012). Sizing energy storage to accommodate high penetration of variable energy resources. *IEEE Transactions on Sustainable Energy*, 3(1):34–40.

Mazhari, S. M. and Monsef, H. (2013). Dynamic sub-transmission substation expansion planning using learning automata. *Electric Power Systems Research*, 96:255 – 266.

Medjroubi, W., Müller, U. P., Scharf, M., Matke, C., and Kleinhans, D. (2017). Open-Data in power grid modelling: New approaches towards transparent grid models. *Energy Reports*, 3:14–21.

Meier, H., Fünfgeld, C., Adam, T., and Schiefdecker, B. (1999). *Repräsentative VDEW-Lastprofile*. Brandenburgische Technische Universität Cottbus.

Muehlenpfordt, J. (2016). Data provided by Open Power System Data - Data Package Time series, version 2016-07-14. Primary data from TenneT, ENTSO-E, Elia, TransnetBW, Svenska Kraftnaet, 50Hertz, own calculation, Amprion, 50Hertz, TenneT, TransnetBW, Amprion, own calculation. Online available at: `http://open-power-system-data.org/`.

Müller, U., Cussmann, I., Wingenbach, C., and Wendiggensen, J. (2016). AC power flow simulations within an open data model of a high voltage grid. In Wohlgemuth, V., Fuchs-Kittowski, F., and Wittmann, J., ed., *Advances and New Trends in Envrionmental Informatics*, pp. 181–191. Springer International Publishing Switzerland.

Müller, U., Schachler, B., Bunke, W.-D., Bartels, J., Glauer, M., Büttner, C., Günther, S., Kötter, E., Cußmann, I., Hülk, L., Scharf, M., Mossakowski, T., and

Wendiggensen, J. (2019a). *Netzebenenübergreifendes Planungsinstrument — zur Bestimmung des optimalen Netz- und Speicherausbaus in Deutschland — integriert in einer OpenEnergyPlatform*. ZNES - Flensburg University of Applied Sciences, ZNES - Europa-Universität Flensburg, Reiner Lemoine Institute, Otto-von-Guericke-Universität Magdeburg, DLR Institute of Networked Energy Systems. Online available at: `https://www.uni-flensburg.de/fileadmin/content/abteilungen/industrial/dokumente/downloads/veroeffentlichungen/forschungsergebnisse/20190426endbericht-openego-fkz0325881-final.pdf`.

Müller, U., Schachler, B., Scharf, M., Bunke, W.-D., Günther, S., Bartels, J., and Plessmann, G. (2019b). Integrated techno-economic power system planning of transmission and distribution grids. *Energies*, 12(11):2091.

Müller, U., Wienholt, L., and Cussmann, I. (2018a). The role of the high voltage power level in future power systems and their modelling. In *2018 International Conference on Smart Energy Systems and Technologies (SEST)*, pp. 1–6.

Müller, U., Wienholt, L., Kleinhans, D., Cussmann, I., Bunke, W.-D., Pleßmann, G., and Wendiggensen, J. (2018b). The eGo grid model: An open source approach towards a model of German high and extra-high voltage power grids. *Journal of Physics: Conference Series*, 977:012003. SciGRID International Conference on Power Grid Modelling, 30–31 March 2017, Oldenburg, Germany.

Niharika, Verma, S., and Mukherjee, V. (2016). Transmission expansion planning: A review. In *2016 International Conference on Energy Efficient Technologies for Sustainability (ICEETS)*, pp. 350–355.

Nitsch, J. and Pregger, T. and et al. (2012). *Langfristszenarien und Strategien für den Ausbau der erneuerbaren Energien in Deutschland bei Berücksichtigung der Entwicklung in Europa und global*. DLR, IWES, IFNE. Online available at: `http://www.dlr.de/dlr/Portaldata/1/Resources/bilder/portal/portal_2012_1/leitstudie2011_bf.pdf`.

Oeding, D. and Oswald, B. R. (2011). *Elektrische Kraftwerke und Netze*. Springer.

oemof developer group (2016). The oemof demandlib (oemof.demandlib). Online available at: `https://doi.org/10.5281/zenodo.438786`.

OpenStreetMap (2017). OSM Landuse. Online available at: `http://wiki.openstreetmap.org/wiki/Key:landuse`.

Palmintier, B., Hale, E., Hansen, T. M., Jones, W., Biagioni, D., Sorensen, H., Wu, H., and Hodge, B. (2017). IGMS: An integrated ISO-to-appliance scale grid modeling system. *IEEE Transactions on Smart Grid*, 8(3):1525–1534.

Palmintier, B. S. and Webster, M. D. (2016). Impact of operational flexibility on electricity generation planning with renewable and carbon targets. *IEEE Transactions on Sustainable Energy*, 7(2):672–684.

Papaemmanouil, A., Tuan, L. A., Andersson, G., Bertling, L., and Johnsson, F. (2010). A cost-benefit analysis of transmission network reinforcement driven by generation capacity expansion. In *IEEE PES General Meeting*, pp. 1–8.

Pedregosa, F., Varoquaux, G., Gramfort, A., Michel, V., Thirion, B., Grisel, O., Blondel, M., Prettenhofer, P., Weiss, R., Dubourg, V., et al. (2011). Scikit-learn: Machine learning in python. *Journal of machine learning research*, 12(Oct):2825–2830.

Pfenninger, S., DeCarolis, J., Hirth, L., Quoilin, S., and Staffell, I. (2017). The importance of open data and software: Is energy research lagging behind? *Energy Policy*, 101:211 – 215.

Pfenninger, S., Hawkes, A., and Keirstead, J. (2014). Energy systems modeling for twenty-first century energy challenges. *Renewable and Sustainable Energy Reviews*, 33:74 – 86.

Pleßmann, G. and Blechinger, P. (2017). How to meet EU GHG emission reduction targets? A model based decarbonization pathway for Europe's electricity supply system until 2050. *Energy Strategy Reviews*, 15:19 – 32.

Pudjianto, D., Aunedi, M., Djapic, P., and Strbac, G. (2014). Whole-systems assessment of the value of energy storage in low-carbon electricity systems. *IEEE Transactions on Smart Grid*, 5(2):1098–1109.

Purchala, K., Meeus, L., Van Dommelen, D., and Belmans, R. (2005). Usefulness of DC power flow for active power flow analysis. *Power Engineering Society General Meeting, 2005. IEEE*, pp. 454–459.

Qiong Zhou and Bialek, J. W. (2005). Approximate model of European interconnected system as a benchmark system to study effects of cross-border trades. *IEEE Transactions on Power Systems*, 20(2):782–788.

Qiu, T., Xu, B., Wang, Y., Dvorkin, Y., and Kirschen, D. S. (2017). Stochastic multistage coplanning of transmission expansion and energy storage. *IEEE Transactions on Power Systems*, 32(1):643–651.

Rad, H. K. and Moravej, Z. (2017). An approach for simultaneous distribution, subtransmission, and transmission networks expansion planning. *International Journal of Electrical Power & Energy Systems*, 91:166 – 182.

Rehtanz, C., Greve, M., Häger, U., Hagemann, Z., Kippelt, S., Kittl, C., Kloubert, M.-L., Pohl, O., Rewald, F., and Wagner, C. (2017). *Verteilnetzstudie für das Land Baden-Württemberg*. ef.Ruhr GmbH, Technische Universität Dortmund. Online available at: `https://um.baden-wuerttemberg.de/fileadmin/redaktion/m-um/intern/Dateien/Dokumente/5_Energie/Versorgungssicherheit/170413_Verteilnetzstudie_BW.pdf`.

Rendel, T. (2015). *Erweiterung und Plausibilisierung eines Modells für die integrierte Simulation des europäischen Verbundnetzes und Strommarktes*. Dissertation, Gottfried Wilhelm Leibniz Universität Hannover.

Ringkjøb, H.-K., Haugan, P. M., and Solbrekke, I. M. (2018). A review of modelling tools for energy and electricity systems with large shares of variable renewables. *Renewable and Sustainable Energy Reviews*, 96:440 – 459.

Rodríguez, R. A., Becker, S., Andresen, G. B., Heide, D., and Greiner, M. (2014). Transmission needs across a fully renewable european power system. *Renewable Energy*, 63:467 – 476.

Romero, R., Monticelli, A., Garcia, A., and Haffner, S. (2002). Test systems and mathematical models for transmission network expansion planning. *IEE Proceedings - Generation, Transmission and Distribution*, 149(1):27–36.

Schaber, K. (2013). *Integration of Variable Renewable Energies in the European power system: a model-based analysis of transmission grid extensions and energy sector coupling*. Dissertation, Technische Universität München.

Schaber, K., Steinke, F., and Hamacher, T. (2012a). Transmission grid extensions for the integration of variable renewable energies in Europe: Who benefits where? *Energy Policy*, 43:123 – 135.

Schaber, K., Steinke, F., Mühlich, P., and Hamacher, T. (2012b). Parametric study of variable renewable energy integration in Europe: Advantages and costs of transmission grid extensions. *Energy Policy*, 42:498 – 508.

Schachler, B. (2014). *Bewertung des Einsatzes von Kraft-Wärme-Kopplungsanlagen hinsichtlich der CO2-Emissionen bei wachsendem Anteil Erneuerbarer Energien*. Master's thesis, Technische Universität Berlin.

Scharf, M. (2015). *Entwicklung eines Modells des deutschen Übertragungsnetzes auf Basis der offenen Geodatenbank OpenStreetMap*. Bachelor's thesis, Fachhochschule Flensburg.

Schill, W.-P. (2014). Residual load, renewable surplus generation and storage requirements in Germany. *Energy Policy*, 73:65–79.

Schlachtberger, D., Brown, T., Schramm, S., and Greiner, M. (2017). The benefits of cooperation in a highly renewable European electricity network. *Energy*, 134:469 – 481.

Schlemminger, M. (2018). *Modellierung von Redispatch-Maßnahmen im deutschen Hoch- und Höchstspannungsnetz*. Master's thesis, Europa-Universität Flensburg.

Schlott, M., Kies, A., Brown, T., Schramm, S., and Greiner, M. (2018). The impact of climate change on a cost-optimal highly renewable European electricity network. *Applied Energy*, 230:1645 – 1659.

Scholz, Y. (2012). *Renewable energy based electricity supply at low costs - Development of the REMix model and application for Europe*. Dissertation, Universität Stuttgart.

Scholz, Y., Gils, H. C., and Pietzcker, R. C. (2017). Application of a high-detail energy system model to derive power sector characteristics at high wind and solar shares. *Energy Economics*, 64:568 – 582.

Schröder, A., Kunz, F., Meiss, J., Mendelevitch, R., and Von Hirschhausen, C. (2013). *Current and prospective costs of electricity generation until 2050*. Data Documentation, DIW. Online available at: https://www.diw.de/documents/publikationen/73/diw_01.c.424566.de/diw_datadoc_2013-068.pdf.

Schumacher, M. and Hirth, L. (2015). How much electricity do we consume? A guide to German and European electricity consumption and generation data. *FEEM Working Paper*, 88.2015.

Schwab, A. (2012). *Elektroenergiesysteme: Erzeugung, Transport, Übertragung und Verteilung elektrischer Energie*. Springer-Verlag, 3rd edition.

Shayeghi, H. and Bagheri, A. (2013). Dynamic sub-transmission system expansion planning incorporating distributed generation using hybrid DCGA and LP technique. *International Journal of Electrical Power & Energy Systems*, 48:111 – 122.

Singh, A., Willi, D., Chokani, N., and Abhari, R. S. (2014). Optimal power flow analysis of a Switzerland's transmission system for long-term capacity planning. *Renewable and Sustainable Energy Reviews*, 34:596 – 607.

Statistisches Bundesamt (2016). VGR der Länder - Bruttoinlandsprodukt / Bruttowertschöpfung in den Kreisen. Online available at: https://www.destatis.de/DE/Publikationen/Thematisch/VolkswirtschaftlicheGesamtrechnungen/AlteAusgaben/VGR_KreisergebnisseBand1Alt.html.

Statistisches Bundesamt (Destatis) (2016). Ergebnisse des Zensus 2011 - Bevölkerung im 100 Meter-Gitter. Online available at: https://www.zensus2011.de/SharedDocs/Aktuelles/Ergebnisse/DemografischeGrunddaten.html.

Stetter, D. (2014). *Enhancement of the REMix energy system model : global renewable energy potentials, optimized power plant siting and scenario validation*. Dissertation, Universität Stuttgart.

Stott, B., Jardim, J., and Alsac, O. (2009). DC Power Flow Revisited. *IEEE Transactions on Power Systems*, 24(3):1290–1300.

The European Parliament and the council of the European Union (2009). Directive 2009/28/EC of the European Parliament and of the Council. Online available at: https://eur-lex.europa.eu/LexUriServ/LexUriServ.do?uri=OJ:L:2009:140:0016:0062:EN:PDF.

Thien, T., Moos, M., Alvarez, R., Chen, H., Cai, Z., Leuthold, D. M., Moser, U.-P. D.-I. A., and rer. nat. Dirk Uwe Sauer, U.-P. D. (2013). Storage demand in a 100%-RES-power system for Europe with different PV-installation levels. In *28th European Photovoltaic Solar Energy Conference and Exhibition*, pp. 4261 – 4265.

Tranberg, B., Schäfer, M., Brown, T., Hörsch, J., and Greiner, M. (2018). Flow-based analysis of storage usage in a low-carbon European electricity scenario. In *2018 15th International Conference on the European Energy Market (EEM)*, pp. 1–5.

Ueckerdt, F., Hirth, L., Luderer, G., and Edenhofer, O. (2013). System LCOE: What are the costs of variable renewables? *Energy*, 63:61 – 75.

Van den Bergh, K., Boury, J., and Delarue, E. (2016). The Flow-Based Market Coupling in Central Western Europe: Concepts and definitions. *The Electricity Journal*, 29(1):24 – 29.

van Leeuwen, T., Dierkes, S., Verheggen, L., Schuster, H., Köhne, F., and Moser, A. (2014). Ermittlung von Transitflüssen im Hochspannungsnetz durch mehrere Verknüpfungspunkte mit dem Übertragungsnetz. In *13. Symposium Energieinnovation, 12.-14.2.2014, Graz/Austria*.

VanderPlas, J. (2016). *Python Data Science Handbook: Essential Tools for Working with Data*. O'Reilly Media, Inc., 1st edition.

Vespermann, M. (2017). *Entwicklung einer Methodik zur Betriebsmittel-Parametrisierung im Rahmen eines offenen Stromnetzmodells der Höchst- und Hochspannungsebene Deutschlands*. Master's thesis, Europa-Universität Flensburg.

von Schemde, A., Tennbakk, B., Gravdehaug, G., and Grøndahl, R. (2013). Loop flows – final advice. Online available at: `https://ec.europa.eu/energy/sites/ener/files/documents/201310_loop-flows_study.pdf`.

Weitemeyer, S., Kleinhans, D., Vogt, T., and Agert, C. (2015). Integration of renewable energy sources in future power systems: The role of storage. *Renewable Energy*, 75:14 – 20.

Wiegmans, B. (2016). Gridkit. Online available at: `https://github.com/bdw/GridKit`.

Wienholt, L., Müller, U., and Bartels, J. (2018). Optimal sizing and spatial allocation of storage units in a high-resolution power system model. *Energies*, 11(12):3365.

Wiese, F., Bökenkamp, G., Wingenbach, C., and Hohmeyer, O. (2014). An open source energy system simulation model as an instrument for public participation in the development of strategies for a sustainable future. *Wiley Interdisciplinary Reviews: Energy and Environment*, 3(5):490–504.

Willis, L. and Scott, W. (2000). *Distributed Power Generation: Planning and Evaluation*. Marcel Dekker, inc.

Wingenbach, M. (2018). *Integration sozial-ökologischer Faktoren in die Energiesystemmodellierung - am Beispiel von Entwicklungspfaden für den Windenergieausbau in Deutschland*. Dissertation, Europa-Universität Flensburg.

Wirth, H. (2018). Aktuelle Fakten zur Photovoltaik in Deutschland. Online available at: `www.pv-fakten.de`.

Wogrin, S. and Gayme, D. F. (2015). Optimizing storage siting, sizing, and technology portfolios in transmission-constrained networks. *IEEE Transactions on Power Systems*, 30(6):3304–3313.

Wuppertal Institute and DLR Institute of Networked Energy Systems (2018). osmTGmod - open_eGo github fork. `https://github.com/openego/osmTGmod`.

Zappa, W., Junginger, M., and van den Broek, M. (2019). Is a 100% renewable European power system feasible by 2050? *Applied Energy*, 233-234:1027 – 1050.

Zhang, F., Hu, Z., and Song, Y. (2013). Mixed-integer linear model for transmission expansion planning with line losses and energy storage systems. *IET Generation, Transmission Distribution*, 7(8):919–928.

Ziari, I., Ledwich, G., Ghosh, A., and Platt, G. (2012). Integrated distribution systems planning to improve reliability under load growth. *IEEE Transactions on Power Delivery*, 27(2):757–765.

Zidar, M., Georgilakis, P. S., Hatziargyriou, N. D., Capuder, T., and Škrlec, D. (2016). Review of energy storage allocation in power distribution networks: applications, methods and future research. *IET Generation, Transmission Distribution*, 10(3):645–652.